整數階與分數階統一渾沌系統之渾沌與渾沌同步

Chaos and Chaos Synchronization of Integral and Fractional Order Unified Chaotic System

研究生: 楊坤偉 Student: Kung-Wei Yang

指導教授: 戈正銘 Advisor: Zheng-Ming Ge

國 立 交 通 大 學

機 械 工 程 研 究 所

碩 士 論 文

A Thesis
Submitted to Department of Mechanical Engineering
College of Engineering
National Chiao Tung University
in Partial Fulfillment of the Requirement
for the Degree of Master
in
Mechanical Engineering
June 2005
Hsinchu, Taiwan, Republic of China

中華民國九十四年六月

Chapter 1

Introduction

Lorenz studied the strange changes in the atmosphere which is the first example to study chaos in 1963. In the past four decades, a large number of studies have shown that chaotic phenomena are observed in many physical systems that possess nonlinearity [1,2]. It was also reported that the chaotic motion occurred in many non-linear control systems [3].

Most of physical systems in nature are nonlinear and can be described by the nonlinear equations of motion which in general can not be linearized. So the studies of nonlinear systems spread quickly today. For the nonlinear system, the study of the types of system behavior, the effects to the behavior caused by different parameters and initial conditions, the behavior analysis of the system, consist of the major tasks. Besides, we are also interested in the understanding of the complicated phenomena arised from nonlinearity. The central characteristics are that a process like randomization happens in the deterministic system and small differences in the system parameters or initial conditions produce great ones in the final phenomena. The unpredictable and irregular motions of many nonlinear systems have been labeled “chaotic”. Chaotic behavior is irregular, complex and generally undesirable. In other words, a fundamental characteristic of chaotic system is its extreme sensitivity to initial conditions which prevent long term forecasting. Chaos has been found to be useful in analyzing many problems such as information processing [4-8], collapse prevention of power systems, high-performance circuits and device, etc. By applying various numerical results, such as bifurcation, phase portraits, time history analysis, the behavior of the chaotic motion are presented. A large number of studies on the chaotic behavior have been reached up to now.

In recent years, synchronization in chaotic dynamic system is very interesting problem and has been widely studied [9-13]. Over the last decade, chaos synchronization has received interesting attention due to its potential application in many areas such as secure communication, information process, biological systems, and chemical reactions [14-16]. In the synchronized systems, one is called master and another is called slave. Synchronization means that the state variables of a response system approach eventually to that of a drive system. There are many control techniques to synchronize chaotic systems, such as linear error feedback control, adaptive control, active control.

New chaotic systems have been constantly put forward in the last 30 years. In 1999, Chen found another chaotic attractor- the Chen system [17], which is the dual to the Lorenz system and has a similarly simple structure but displays even more sophisticated dynamical behavior. Very recently, Lü and Chen produced a new chaotic system—unified chaotic system [18-28], which contains the Lorenz and Chen systems as two extremes and the Lü system as a special case. In Chapter 3, we use two methods to achieve synchronization of two identical unified chaotic systems. The speed feedback synchronization is first proposed in this thesis. In Chapter 4, unified chaotic system is studied in detail. In Chapter 5, a unified chaotic system with various periodic switches are put forward. Four functions $\sin^2 \omega t, \sin \omega t$, triangular wave, sawtooth wave are used to replace α which is the original constant parameter of unified chaotic system and we find much interesting results. In Chapter 6, chaos, chaos control and synchronization of the fractional order [29,30] unified chaotic systems are studied.

Chapter 2

Differential Equations of Motion

and Description of the System

2.1 Unified Chaotic System

New chaotic systems have been constantly put forward in the last 30 years. In 1999, Chen found another chaotic attractor- the Chen system [17], which is the dual to the Lorenz system and has a similarly simple structure but displays even more sophisticated dynamical behavior. Here, the duality is in the sense defined by Vaněček and ČelikovskÝ [31]: for the linear part of the system, $A = \lfloor a_{ij} \rfloor_{3\times 3}$, the Lorenz system satisfies the condition $a_{12}a_{21}>0$ while the Chen system satisfies $a_{12}a_{21}<0$. In 2002, Lü found a new chaotic system, which satisfies the condition $a_{12}a_{21}=0$ [32]. Very recently, Lü and Chen produced a new chaotic system—unified chaotic system [18-28], which contains the Lorenz and Chen systems as two extremes and the Lü system as a special case. Recently, there are some results reported about the unified chaotic system [23-28]. The unified chaotic system is described as follows:

$$\begin{aligned}
\dot{x} &= (25\alpha + 10)(y - x) \\
\dot{y} &= (28 - 35\alpha)x + (29\alpha - 1)y - xz \qquad (2.1) \\
\dot{z} &= xy - \frac{8+\alpha}{3} z
\end{aligned}$$

where $\alpha \in [0,1]$. The system is told to be chaotic for any $\alpha \in [0,1]$. When $\alpha = 0$ the system can be seem as Lorenz system, when $\alpha = 1$ it becomes Chen system.

2.2 Lyapunov Exponent of Unified Chaotic System

In order to determine the chaos existing in a nonlinear system, the method of detecting the chaos becomes very important. The Lyapunov exponent may be used to measure the sensitive dependence upon initial condition. It is an index for chaotic behavior. Different solutions of the dynamical system, such as fixed point, periodic motions, quasiperiodic motion, and chaotic motion can be distinguished by it. In three-dimensional space, the Lyapunov exponent spectra for a strange attractor, a two-torus, a limit cycle and a fixed point are described by (+,0,-), (0,0,-), (0,-,-), (-,-,-), respectively. Fig.2.2.1 is shown that unified chaotic system is chaotic for $\alpha \in [0,1]$.

2.3 Phase Portrait

In Fig.2.3.1(a)-(d),we can see the phase portraits of unified chaotic system ,when $\alpha = 0$, and Fig.2.3.2(a)-(d),when $\alpha = 1$.

In Fig.2.3.3(a)-(d), we show the phase portraits of case (-,-,-). In Fig2.2.1, when $\alpha = -1$, the three Lyapunov exponents are all negative, and the phase portraits converge to a fixed point.

In Fig.2.3.4(a)-(d), we show the phase portraits of case (0,-,-). In Fig2.2.1, when $\alpha = 1.7$, the three Lyapunov exponents are described as (0,-,-), and the phase portraits show a limit cycle.

Chapter 3

Synchronization of Unified Chaotic System

First, we use unidirectional coupling to synchronize unified chaotic system, and the coupling includes two types - state coupling and speed coupling.

3.1 State Feedback Synchronization of Unified Chaotic System

We add a state coupling $k(x_1 - x_2)$ respectively to unified chaotic system, and the master and slave system is shown as below:

3.1.1 Case1: add state coupling $k_1(x_1 - x_2)$ to first equation of the slave system

Master system:

$$\begin{aligned}
\dot{x}_1 &= (25\alpha + 10)(y_1 - x_1) \\
\dot{y}_1 &= (28 - 35\alpha)x_1 + (29\alpha - 1)y_1 - x_1 z_1 \\
\dot{z}_1 &= x_1 y_1 - \frac{8+\alpha}{3} z_1
\end{aligned} \tag{3.1.1}$$

Slave system:

$$\begin{aligned}
\dot{x}_2 &= (25\alpha + 10)(y_2 - x_2) + k_1(x_1 - x_2) \\
\dot{y}_2 &= (28 - 35\alpha)x_2 + (29\alpha - 1)y_2 - x_2 z_2 \\
\dot{z}_2 &= x_2 y_2 - \frac{8+\alpha}{3} z_2
\end{aligned} \tag{3.1.2}$$

Let

$$e_1 = x_2 - x_1,\ \ e_2 = y_2 - y_1,\ \ e_3 = z_2 - z_1,$$

$$\dot{e}_1 = \dot{x}_2 - \dot{x}_1,\ \ \dot{e}_2 = \dot{y}_2 - \dot{y}_1,\ \ \dot{e}_3 = \dot{z}_2 - \dot{z}_1$$

Then the error dynamics is shown as follows:

$$\dot{e}_1 = (25\alpha + 10)(e_2 - e_1) - k_1 e_1$$
$$\dot{e}_2 = (28 - 35\alpha)e_1 + (29\alpha - 1)e_2 - x_2 z_2 + x_1 z_1 \qquad (3.1.3)$$
$$\dot{e}_3 = -\frac{8+\alpha}{3} e_3 + x_2 y_2 - x_1 y_1$$

According to Lyapunov first approximation theory, for sufficiently small $\boldsymbol{e}$, we can neglect high-order terms for stability study.

The coefficient matrix of the linear terms of the right hand side of Eq.(3.1.3) is

$$J = \begin{bmatrix} -(25\alpha + 10 + k_1) & 25\alpha + 10 & 0 \\ 28 - 35\alpha & 29\alpha - 1 & 0 \\ 0 & 0 & -\frac{8+\alpha}{3} \end{bmatrix} \qquad (3.1.4)$$

Then the characteristic equation $|J - \lambda I| = 0$:

$$\begin{bmatrix} -(25\alpha + 10 + k_1) - \lambda & 25\alpha + 10 & 0 \\ 28 - 35\alpha & 29\alpha - 1 - \lambda & 0 \\ 0 & 0 & -\frac{8+\alpha}{3} - \lambda \end{bmatrix} = 0 \qquad (3.1.5)$$

After computing, characteristic equation is expressed as follows:

$$\lambda^3 + \frac{1}{3}(-11\alpha + 3k_1 + 41)\lambda^2 + \frac{1}{3}\left(446\alpha^2 - 86\alpha k_1 - 2811\alpha + 11k_1 - 722\right)\lambda$$
$$+\frac{1}{3}\left(100\alpha^3 + 270\alpha^2 + 7710\alpha - 29\alpha^2 k_1 - 231\alpha + 8k_1 - 2160\right) = 0 \qquad (3.1.6)$$

Considering $\alpha = 0$,

$a_0 = 1$,

$a_1 = \frac{1}{3}(3k_1 + 41)$,

$a_2 = \frac{1}{3}(11k_1 - 722)$,

$a_3 = \frac{1}{3}(8k_1 - 2160)$, where a_0, a_1, a_2, a_3 are coefficients of characteristic equation

$$a_0\lambda^3 + a_1\lambda^2 + a_2\lambda + a_3 = 0 \qquad (3.1.7)$$

According to Routh- Hurwitz theorem, if all Hurwitz determinants are positive, all characteristic roots have negative real parts, e_1, e_2, e_3 will gradually converge to zero.

Hurwitz determinants are defined as follows:

$$\Delta_1 = a_1 ,$$

$$\Delta_2 = \begin{vmatrix} a_1 & a_0 \\ a_3 & a_2 \end{vmatrix}, \tag{3.1.8}$$

$$\Delta_3 = \begin{vmatrix} a_1 & a_0 & 0 \\ a_3 & a_2 & a_1 \\ 0 & 0 & a_3 \end{vmatrix},$$

In our case, $\Delta_1 = \frac{1}{3}(3k_1 + 41) > 0,\ \ k_1 > -\frac{41}{3}$,

$\Delta_2 > 0,\ \ k_1 > 63.697$ or $k_1 < -11$,

$\Delta_3 > 0,\ \ k_1 > 270$ or $63.697 > k_1 > -11$,

k_1 must greater than 270, then e_1, e_2, e_3 will gradually converge to zero. In Fig.3.1.1(a) we can see time history of errors. After a short period of time, $e \to 0$, then two systems are synchronized. Trying to use parameter $k_1 < 270$ to simulate the systems in computer, we find the systems also can be synchronized. This result indicates that Lyapunov first approximation theory gives only the sufficient condition by asymptotic stability of ***e***. Fig.3.1.1(b) shows time history of errors with $k_1 = 20$.

Next we consider $\alpha = 1$, characteristic equation :

$$\lambda^3 + (k_1 + 10)\lambda^2 + (-25k_1 - 714)\lambda + (-84k_1 - 2205) = 0,$$

$$\Delta_1 = a_1 > 0 \ \Rightarrow k_1 > -10,$$

$$\Delta_2 = \begin{vmatrix} a_1 & a_0 \\ a_3 & a_2 \end{vmatrix} > 0 \ \Rightarrow\ -28.2 < k_1 < -7,$$

$$\Delta_3 = \begin{vmatrix} a_1 & a_0 & 0 \\ a_3 & a_2 & a_1 \\ 0 & 0 & a_3 \end{vmatrix} > 0 \ \Rightarrow k_1 > -7 \text{ or } \ -28.2 < k_1 < -26.25,$$

where k_1 does not exist. Fig.3.1.2(a)(b) show that errors e_1, e_2, e_3 can not converge to zero, since the sufficient condition for asymptotical stability cannot be satisfied. Although we increase time to 1000 seconds, the systems are not synchronized.

3.1.2 Case2: add state coupling $k_2(x_1 - x_2)$ to second equation of the slave system

Master system:

$$\begin{aligned}
\dot{x}_1 &= (25\alpha + 10)(y_1 - x_1) \\
\dot{y}_1 &= (28 - 35\alpha)x_1 + (29\alpha - 1)y_1 - x_1 z_1 \\
\dot{z}_1 &= x_1 y_1 - \frac{8+\alpha}{3} z_1
\end{aligned} \tag{3.1.9}$$

Slave system:

$$\begin{aligned}
\dot{x}_2 &= (25\alpha + 10)(y_2 - x_2) \\
\dot{y}_2 &= (28 - 35\alpha)x_2 + (29\alpha - 1)y_2 - x_2 z_2 + k_2(x_1 - x_2) \\
\dot{z}_2 &= x_2 y_2 - \frac{8+\alpha}{3} z_2
\end{aligned} \tag{3.1.10}$$

The error dynamics (3.1.10) - (3.1.9) is shown as follows:

$$\dot{e}_1 = (25\alpha + 10)(e_2 - e_1)$$

$$\dot{e}_2 = (28 - 35\alpha)e_1 + (29\alpha - 1)e_2 - x_2 z_2 + x_1 z_1 - k_2 e_1$$

(3.1.11)

$$\dot{e}_3 = -\frac{8+\alpha}{3} e_3 + x_2 y_2 - x_1 y_1$$

According to Lyapunov first approximation theory, for sufficiently small $\boldsymbol{e}$, we can neglect high-order terms for stability study. The coefficient matrix of the linear terms of the right hand side of Eq.(3.1.11) is

$$J = \begin{bmatrix} -(25\alpha + 10) & 25\alpha + 10 & 0 \\ 28 - 35\alpha - k_2 & 29\alpha - 1 & 0 \\ 0 & 0 & -\frac{8+\alpha}{3} \end{bmatrix} \tag{3.1.12}$$

We consider $\alpha = 0$, matrix(3.1.12) can be simplified as:

$$J = \begin{bmatrix} -10 & 10 & 0 \\ 28 - k_2 & -1 & 0 \\ 0 & 0 & -\frac{8}{3} \end{bmatrix} \tag{3.1.13}$$

We can get characteristic equation $|J - \lambda I| = 0$:

$$3\lambda^3 + 41\lambda^2 + (30k_2 - 722)\lambda + (80k_2 - 2160) = 0 \tag{3.1.14}$$

According to Routh- Hurwitz theorem, if all Hurwitz determinants(see 3.1.8) are positive, all characteristic roots have negative real parts, e_1, e_2, e_3 will gradually converge to zero. After computing, we obtain that when k_2 greater than 27 the systems will be synchronized. Fig.3.1.3(a) shows the time history of errors. After a short period of time, $e \to 0$, then two systems are synchronized. Trying to use parameter k_2 < 27 to simulate the systems in computer, we find the systems also can be synchronized. This result indicates that Lyapunov first approximation theory gives only the sufficient condition by asymptotic stability of ***e***. Fig.3.1.3(b) shows time history of errors with $k_2 = 10$

Next we consider $\alpha = 1$, to omit previous computing, matrix (3.1.12) becomes:

$$J = \begin{bmatrix} -35 & 35 & 0 \\ -7 - k_2 & 28 & 0 \\ 0 & 0 & -3 \end{bmatrix}$$

The characteristic equation $|J - \lambda I| = 0$:

$$\lambda^3 + 10\lambda^2 + (35k_2 - 714)\lambda + (105k_2 - 2205) = 0 \tag{3.1.15}$$

According to Routh- Hurwitz theorem, all Hurwitz determinants must be positive, we obtain: when k_2 greater than 21 the systems will be synchronized. Fig.3.1.4(a) shows the time history of errors. After a short period of time, $e \to 0$, then two systems are synchronized. Trying to use parameter k_2 < 21 to simulate the systems in computer, we find the systems also can be synchronized. This result indicates that Lyapunov first approximation theory gives only the sufficient condition by asymptotic stability of $\boldsymbol{e}$. Fig.3.1.4(b) shows time history of errors with $k_2 = 18$.

3.1.3 Case3 : add state coupling $k_3(x_1 - x_2)$ to third equation of the slave system

Master system:

$$\begin{aligned}
\dot{x}_1 &= (25\alpha + 10)(y_1 - x_1) \\
\dot{y}_1 &= (28 - 35\alpha)x_1 + (29\alpha - 1)y_1 - x_1 z_1 \\
\dot{z}_1 &= x_1 y_1 - \frac{8+\alpha}{3} z_1
\end{aligned} \tag{3.1.16}$$

Slave system:

$$\begin{aligned}
\dot{x}_2 &= (25\alpha + 10)(y_2 - x_2) \\
\dot{y}_2 &= (28 - 35\alpha)x_2 + (29\alpha - 1)y_2 - x_2 z_2 \\
\dot{z}_2 &= x_2 y_2 - \frac{8+\alpha}{3} z_2 + k_3(x_1 - x_2)
\end{aligned} \tag{3.1.17}$$

The error dynamics (3.1.17)- (3.1.16) is shown as follows:

$$\begin{aligned}
\dot{e}_1 &= (25\alpha + 10)(e_2 - e_1) \\
\dot{e}_2 &= (28 - 35\alpha)e_1 + (29\alpha - 1)e_2 - x_2 z_2 + x_1 z_1 \\
\dot{e}_3 &= -\frac{8+\alpha}{3} e_3 + x_2 y_2 - x_1 y_1 - k_3 e_1
\end{aligned} \tag{3.1.18}$$

According to Lyapunov first approximation theory, for sufficiently small $\boldsymbol{e}$, we can neglect high-order terms for stability study. The coefficient matrix of the linear terms of the right hand side of Eq.(3.1.18):

$$J = \begin{bmatrix} -(25\alpha + 10) & 25\alpha + 10 & 0 \\ 28 - 35\alpha & 29\alpha - 1 & 0 \\ -k_3 & 0 & -\dfrac{8+\alpha}{3} \end{bmatrix} \tag{3.1.19}$$

we consider $\alpha = 0$ directly, matrix (3.1.19) can be simplified as:

$$J = \begin{bmatrix} -10 & 10 & 0 \\ 28 & -1 & 0 \\ -k_3 & 0 & -\frac{8}{3} \end{bmatrix} \tag{3.1.20}$$

We can get characteristic equation $|J - \lambda I| = 0$:

$$3\lambda^3 + 41\lambda^2 + (-722)\lambda + (-2160) = 0 \tag{3.1.21}$$

According to Routh- Hurwitz theorem, all coefficients of characteristic equation must be all positive or all negative, in this case $a_0 = 3$, $a_2 = 41$, $a_3 = -722$, $a_4 = -2160$, we can directly obtain $\lambda = -22.8277, 11.8277, -2.6667$. Since k_3 is absent in the coefficients of characteristic equation, the state feedback synchronization fails in this case. The positive characteristic root causes unsynchronization as shown in Fig.3.1.5(a)(b).

Fig3.1.5(c)(d) show the computer simulation results of case $\alpha = 1$.

3.2 Speed Feedback Synchronization of Unified Chaotic System

Now, we try another method to synchronize two systems, we use speed coupling $G(\dot{x}_1 - \dot{x}_2)$.

3.2.1 Case1: add speed coupling $G(\dot{x}_1 - \dot{x}_2)$ to second equation of the slave system, the systems is described as below:

Master system:

$$\begin{aligned} \dot{x}_1 &= (25\alpha + 10)(y_1 - x_1) \\ \dot{y}_1 &= (28 - 35\alpha)x_1 + (29\alpha - 1)y_1 - x_1 z_1 \\ \dot{z}_1 &= x_1 y_1 - \frac{8+\alpha}{3} z_1 \end{aligned} \tag{3.2.1}$$

Slave system:

$$\begin{aligned} \dot{x}_2 &= (25\alpha + 10)(y_2 - x_2) \\ \dot{y}_2 &= (28 - 35\alpha)x_2 + (29\alpha - 1)y_2 - x_2 z_2 + G(\dot{x}_1 - \dot{x}_2) \\ \dot{z}_2 &= x_2 y_2 - \frac{8+\alpha}{3} z_2 \end{aligned} \tag{3.2.2}$$

Let

$$e_1 = x_2 - x_1,\ \ e_2 = y_2 - y_1,\ \ e_3 = z_2 - z_1,$$

$$\dot{e}_1 = \dot{x}_2 - \dot{x}_1,\ \ \dot{e}_2 = \dot{y}_2 - \dot{y}_1,\ \ \dot{e}_3 = \dot{z}_2 - \dot{z}_1$$

The error dynamics is shown as follows:

$$\begin{aligned} \dot{e}_1 &= (25\alpha + 10)(e_2 - e_1) \\ \dot{e}_2 &= (28 - 35\alpha)e_1 + (29\alpha - 1)e_2 - G\dot{e}_1 - x_2 z_2 + x_1 z_1 \\ \dot{e}_3 &= -\frac{8+\alpha}{3} e_3 + x_2 y_2 - x_1 y_1 \end{aligned} \tag{3.2.3}$$

According to Lyapunov first approximation theory, for sufficiently small $\boldsymbol{e}$, we can neglect high-order terms for stability study. The coefficient matrix of the linear terms of the right hand side of Eq.(3.2.3):

$$J=\begin{bmatrix} -(25\alpha+10) & 25\alpha+10 & 0 \\ (28-35\alpha)+(25\alpha+10)G & (29\alpha-1)-(25\alpha+10)G & 0 \\ 0 & 0 & -\dfrac{8+\alpha}{3} \end{bmatrix} \tag{3.2.4}$$

We consider $\alpha=0$, matrix (3.2.4) can be simplified as:

$$J=\begin{bmatrix} -10 & 10 & 0 \\ 28+10G & -1-10G & 0 \\ 0 & 0 & -\dfrac{8}{3} \end{bmatrix} \tag{3.2.5}$$

We can get characteristic equation $|J-\lambda I|=0$:

$$3\lambda^3+(30G+41)\lambda^2+(80G-722)\lambda+(-2160)=0 \tag{3.2.6}$$

According to Routh- Hurwitz theorem, if all Hurwitz determinants(see 3.1.8) are positive, all characteristic roots have negative real parts, e_1,e_2,e_3 will gradually converge to zero. After computing, we find G does not exist, so e_1,e_2,e_3 will not gradually converge to zero, the systems are not synchronized by Lyapunov first approximation theory which gives only the sufficient condition by asymptotic stability of $\boldsymbol{e}$. But Fig.3.2.1 shows the time history of errors. After a short period of time, $e\to 0$, two systems are synchronized, which indicates that for the synchronization conditions obtained by Lyapunov first approximation theory, there exists potential of improvement.

Next we consider $\alpha=1$, to omit previous computing, matrix (3.2.4) becomes:

$$J=\begin{bmatrix} -35 & 35 & 0 \\ -7+35G & 28-35G & 0 \\ 0 & 0 & -3 \end{bmatrix}$$

The characteristic equation $|J-\lambda I|=0$:

$$\lambda^3+(35G+10)\lambda^2+(105G-714)\lambda+(-2205)=0 \tag{3.2.7}$$

According to Routh- Hurwitz theorem, if all Hurwitz determinants(see 3.1.8) are positive, all characteristic roots have negative real parts, e_1,e_2,e_3 will gradually converge to zero. After computing, we find G does not exist, so e_1, e_2, e_3 can not gradually converge to zero, the systems are not synchronized by Lyapunov first approximation theory which gives only the sufficient condition by asymptotic stability of $\boldsymbol{e}$. But Fig.3.2.2 shows the time history of errors. After a short period of time, $e \to 0$, two systems are synchronized, which indicates that for the synchronization conditions obtained by Lyapunov first approximation theory, there exists potential of improvement.

3.2.2 Case2: add state coupling $G(\dot{x}_1 - \dot{x}_2)$ to third equation of the slave system, the systems is described as below:

Master system:

$$\begin{aligned}
\dot{x}_1 &= (25\alpha + 10)(y_1 - x_1) \\
\dot{y}_1 &= (28 - 35\alpha)x_1 + (29\alpha - 1)y_1 - x_1 z_1 \\
\dot{z}_1 &= x_1 y_1 - \frac{8+\alpha}{3} z_1
\end{aligned} \tag{3.2.8}$$

Slave system:

$$\begin{aligned}
\dot{x}_2 &= (25\alpha + 10)(y_2 - x_2) \\
\dot{y}_2 &= (28 - 35\alpha)x_2 + (29\alpha - 1)y_2 - x_2 z_2 \\
\dot{z}_2 &= x_2 y_2 - \frac{8+\alpha}{3} z_2 + G(\dot{x}_1 - \dot{x}_2)
\end{aligned} \tag{3.2.9}$$

(3.2.9)- (3.2.8) error dynamics is shown as follows:

$$\begin{aligned}
\dot{e}_1 &= (25\alpha + 10)(e_2 - e_1) \\
\dot{e}_2 &= (28 - 35\alpha)e_1 + (29\alpha - 1)e_2 - x_2 z_2 + x_1 z_1 \\
\dot{e}_3 &= -\frac{8+\alpha}{3} e_3 + x_2 y_2 - x_1 y_1 - G\dot{e}_1
\end{aligned} \tag{3.2.10}$$

According to Lyapunov first approximative theory, for sufficiently small $\boldsymbol{e}$, we can neglect high-order terms for stability study. The coefficient matrix of the linear terms of the right hand side of Eq.(3.2.10):

$$J=\begin{bmatrix} -(25\alpha+10) & 25\alpha+10 & 0 \\ (28-35\alpha) & (29\alpha-1) & 0 \\ (25\alpha+10)G & -(25\alpha+10)G & -\dfrac{8+\alpha}{3} \end{bmatrix} \tag{3.2.11}$$

Considering $\alpha=0$ directly, matrix (3.2.11)can be simplified as:

$$J=\begin{bmatrix} -10 & 10 & 0 \\ 28 & -1 & 0 \\ 10G & 10G & -\dfrac{8}{3} \end{bmatrix} \tag{3.2.12}$$

we can get characteristic equation $|J-\lambda I|=0$:

$$3\lambda^3+41\lambda^2+(-722)\lambda+(-2160)=0 \tag{3.2.13}$$

According to Routh- Hurwitz theorem, all coefficients must be all positive or all negative, in this case $a_0=3$, $a_2=41$, $a_3=-722$, $a_4=-2160$, we can directly obtain $\lambda=$ -22.8277 ,11.8277, - 2.6667 . Since G is absent in the coefficients of characteristic equation, the state feedback synchronization fails in this case. The positive characteristic root causes unsynchronization as shown in Fig.3.2.3.

Fig3.2.4 show the computer simulation results of case $\alpha=1$.

3.3 $\alpha \sim G$ Diagram of Speed Coupling Adding to Second Equation of the slave System

In this section, we specially discuss relation of parameter α and G about case(1) of section 3.2. In the range $\alpha \in [0, 1.05]$, computer simulation is used to find the threshold limit value (TLV) of G which can synchronize two systems. α is taken equally spaced 22 values between $\alpha = 0$ and $\alpha = 1.05$. For example we first fixed $\alpha = 0$, then computer simulations are used to find the minima of G which give synchronization of the systems. Above steps are repeated until $\alpha = 1.05$. Some data are obtained in Table. 3.3.1.

Then we use regression analysis method to find the approximate curve which is described as below:

$$\begin{aligned} G = &-40942\alpha^{11} + 253860\alpha^{10} - 689450\alpha^{9} + 1077200\alpha^{8} - 1069200\alpha^{7} \\ &+ 702670\alpha^{6} - 309200\alpha^{5} + 90184\alpha^{4} - 16909\alpha^{3} + 1924.5\alpha^{2} - 119.3\alpha + 3.4688 \end{aligned} \tag{3.3.1}$$

Fig.3.3.1 shows that when G satisfies inequality described below

$$\begin{aligned} G \geq &-40942\alpha^{11} + 253860\alpha^{10} - 689450\alpha^{9} + 1077200\alpha^{8} - 1069200\alpha^{7} \\ &+ 702670\alpha^{6} - 309200\alpha^{5} + 90184\alpha^{4} - 16909\alpha^{3} + 1924.5\alpha^{2} - 119.3\alpha + 3.4688 \end{aligned} \tag{3.3.2}$$

two systems are synchronized.

Chapter 4

Detailed Study of the Chaos of Unified Chaotic System

Unified chaotic system was told to be chaotic for any $\alpha \in [0,1]$ [21,33]. But we find that there exists some non-chaotic ranges within $\alpha \in [0,1]$. In order to confirm these ranges, three checking methods are used: Lyapunov exponents, phase portraits and power spectrums. The Lyapunov exponent may be used to measure the sensitive dependence upon initial condition. It is the most reliable index for chaotic behavior. Different solutions of the dynamical system, such as fixed point, periodic motions, quasiperiodic motion, and chaotic motion can be distinguished by it. In three-dimensional space, the Lyapunov exponent spectra for a strange attractor, a two-torus, a limit cycle and a fixed point are described by (+,0,-), (0,0,-), (0,-,-), (-,-,-), respectively. Another valuable technique for the characterization of the system is the power spectrum. It is often used to distinguish between periodic, quasi-periodic and chaotic behaviors of a dynamical system. When a chaotic motion appears, the power spectrum is continuous and broadband. In Fig.4.1.1, a power spectrum of a chaotic motion, Chen system, is shown. Although a broadband spectrum does not guarantee sensitivity to initial conditions, it is still a reliable indicator of the chaos.

4.1 Non-chaotic Ranges within $\alpha \in [0,1]$ for Unified Chaotic System

Unified chaotic system was told to be chaotic for any $\alpha \in [0,1]$ [21,33]. But we find that there exists some non-chaotic ranges within $\alpha \in [0,1]$. In Fig.4.1.2(a)(b), some non-chaotic ranges for $\alpha \in [0,1]$ are observed. For example, we can easily observe between $\alpha = 0.575$ and $\alpha = 0.598$, the corresponding Lyapunov exponents are less than 0. The three corresponding Lyapunov exponents are (0,-,-) and the dynamic behavior must be a periodic motion. In Fig.4.1.3(a)(b), a phase portrait and a power spectrum of a non-chaotic motion($\alpha = 0.583$) is shown. Using these three different methods, Fig. 4.1.4 is presented to show many non-chaotic ranges of unified chaotic system within $\alpha \in [0,1]$.

4.2 Chaotic Ranges besides $\alpha \in [0,1]$

Next, we try to find the chaotic ranges besides $\alpha \in [0,1]$. In Fig.2.2.1, it is shown that besides $\alpha \in [0,1]$, there still exists some small ranges whose corresponding Largest Lyaponov exponent are greater than 0. In Fig.4.2.1 and Fig.4.2.2, the part larger than 1 and smaller than 0 are specially magnified respectively. To observe these two figures and use the three checking methods, we finally obtain the chaotic range of α as $\alpha \in [-0.015, 1.152]$. An extended unified chaotic system is produced.

4.3 An Extended Unified Chaotic System for Parameter $\beta \in [0,1]$

We introduce a new parameter $\beta = f(\alpha)$ so that the extended unified chaotic system is chaotic when $\beta \in [0,1]$. Let $\alpha = a\beta + b$, when $\alpha = -0.015$, $\beta = 0$ and when $\alpha = 1.152$, $\beta = 1$. Then constants a and b are obtained as $a = 1.167$ and $b = -0.015$. We obtain $\alpha = 1.167\beta - 0.015$, an extended unified chaotic system is described as follows:

$$\begin{aligned} \dot{x} &= (29.175\beta + 9.625)(y - x) \\ \dot{y} &= (27.475 - 40.845\beta)x + (33.843\beta - 1.435)y - xz \\ \dot{z} &= xy - \frac{7.985 + 1.167\beta}{3} z \end{aligned} \tag{4.3.1}$$

where $\beta \in [0,1]$. The system is chaotic only for $\beta \in [0,1]$. In Fig. 4.3.1, a Lyapunov exponent is shown, we can easily observe that only for $\beta \in [0,1]$, the extended unified chaotic system exists chaos.

4.4 An Extended Unified Chaotic System with Two Continuous Periodic Switches

In this section, we put forward a non-autonomous unified chaotic system with continuous periodic switch. Because there exists a largest range $\alpha \in [0.575, 0.598]$ where the unified chaotic system does not exist chaos, we delete this non-chaotic range. We separate the range $\alpha \in [-0.015, 1.152]$ into two parts to simulate the system described as follows:

$$\begin{aligned} \dot{x} &= (25\sin^2 \omega t + 10)(y - x) \\ \dot{y} &= (28 - 35\sin^2 \omega t)x + (29\sin^2 \omega t - 1)y - xz \\ \dot{z} &= xy - \frac{8 + \sin^2 \omega t}{3} z \end{aligned} \tag{4.4.1}$$

Let $\sin^2 \omega t = -0.015 + 0.59\sin^2 \omega t$ for the first range, $\sin^2 \omega t = 0.598 + 0.554\sin^2 \omega t$ for the second range. And Eq.(4.4.1) become what is described as follows:

$$\begin{aligned} \dot{x} &= (14.75\sin^2 \omega t + 9.625)(y - x) \\ \dot{y} &= (28.525 - 20.65\sin^2 \omega t)x + (17.11\sin^2 \omega t - 1.435)y - xz \\ \dot{z} &= xy - \frac{7.985 + 0.59\sin^2 \omega t}{3} z \end{aligned} \tag{4.4.2}$$

Therefore, the non-chaotic range($\alpha \in [0.575, 0.598]$) is jumped. Fig.4.4.1(a) shows the Lyapunov exponent. Then, the second range is continued, and the system becomes

$$\begin{aligned} \dot{x} &= (13.85\sin^2 \omega t + 24.95)(y - x) \\ \dot{y} &= (7.07 - 19.39\sin^2 \omega t)x + (16.066\sin^2 \omega t - 16.342)y - xz \\ \dot{z} &= xy - \frac{8.598 + 0.554\sin^2 \omega t}{3} z \end{aligned} \tag{4.4.3}$$

Fig.4.4.1(b) shows the Lyapunov exponent. Next, $\sin^2 \omega t$ is substituted by $\sin^4 \omega t$ and $\sin^6 \omega t$ respectively. Four Lyapunov exponents are obtained— Fig4.4.2(a)、Fig4.4.2(b)、Fig4.4.3(a)、Fig4.4.3(b). Comparing Fig.4.4.1(a)、Fig.4.4.2(a)、Fig.4.4.3(a) with each other, the larger degree n of $\sin^n \omega t$ is, the smaller the largest Lyaponov exponent is; while for the second range, the larger degree n of $\sin^n \omega t$ is, the larger the largest Lyaponov exponent is. Furthermore, for the same degree n of $\sin^n \omega t$, the largest Lyapunov exponent of the second range is always greater than that of the first range. And this phenomenon is more and more obvious as degree n of $\sin^n \omega t$ increases.

Chapter 5

A Unified Chaotic System with

Four Different Periodic Switches

In reference [33], a non-autonomous unified chaotic system continuous periodic switch between the Lorenz and Chen system is given, which is described as (4.4.1). In this Chapter, we extend the periodic switch to various forms. Four different periodic switches $\sin^2 \omega t$, $\sin \omega t$, triangular wave, sawtooth wave are used to replace α which is the original constant parameter of unified chaotic system and we find many interesting results.

5.1 A Unified Chaotic System with $\sin^2 \omega t$ Continuous Periodic Switch

According to references [33], a non-autonomous unified chaotic system continuous periodic switch between the Lorenz and Chen system is given, which is described as (4.4.1). In that system, $\sin^2 \omega t$ was used in place of α which is the original parameter of unified chaotic system so that α is a continuous periodic switch between 0 and 1. In this section, we take α as a continuous periodic switch between 0 and 2, 0 and 4, respectively. Considering the system described as follows:

$$\begin{aligned} \dot{x} &= (25(k\sin^2 \omega t) + 10)(y - x) \\ \dot{y} &= (28 - 35(k\sin^2 \omega t))x + (29(k\sin^2 \omega t) - 1)y - xz \\ \dot{z} &= xy - \frac{8 + (k\sin^2 \omega t)}{3} z \end{aligned} \qquad (5.1.1)$$

where k is the amplitude of $\sin^2 \omega t$. When $k = 1$, the system is the same as (4.4.1). The Lyapunov exponent is shown in Fig. 5.1.1. It is easily observed that there exists chaos in this system for almost all $\omega \in [0, 1000]$. Next, we increase the amplitude of $\sin^2 \omega t$. Fig. 5.1.2 and Fig. 5.1.3 are Lyapunov exponent diagrams of $k = 2$ and $k = 4$ respectively. In Fig.5.1.2, there exists chaos for a large part of $\omega \in [0, 1000]$. But when k increases to 4, theres exists chaos for only a small part of $\omega \in [0, 1000]$ (see Fig. 5.1.3). The chaotic phenomenon decreases as amplitude k increases.

5.2 A Unified Chaotic System with $\sin \omega t$ Continuous Periodic Switch

In this section, we extended α to negative. A continuous periodic switch(-1~1) will be used. Considering the following system:

$$\begin{aligned}
\dot{x} &= (25(m\sin\omega t)+10)(y-x) \\
\dot{y} &= (28-35(m\sin\omega t))x+(29(m\sin\omega t)-1)y-xz \\
\dot{z} &= xy-\frac{8+(m\sin\omega t)}{3}z
\end{aligned} \tag{5.2.1}$$

$m\sin\omega t$ is used in place of α which is the original parameter of unified chaotic system so that α is a continuous periodic switch between -1 and 1. And m is the amplitude of $\sin\omega t$. First, we consider $m = 1$, and the system switches between -1~ 1. Then we gradually increase amplitude m to 2, 4, 6, 8, 10. In Fig.5.2.1, we can easily observe that in this system there exists chaos for almost all $\omega \in [0, 1000]$. Observing Fig.5.2.2~ Fig. 5.2.6, the larger amplitude m is, the less unobvious chaotic phenomenon is.

5.3 A Unified Chaotic System with 0~1 Triangular Wave Switch

In this section, a triangular wave is used to substitute for α which is the original parameter of unified chaotic system so that α is a periodic switch between 0 and 1 by two linear functions of time. Considering the following function:

$$f(t)=\begin{cases}\dfrac{2k}{L}t & if\ 0<t<\dfrac{L}{2}\\[2ex] \dfrac{2k}{L}(L-t) & if\ \dfrac{L}{2}<t<L\end{cases} \tag{5.3.1}$$

where t, k and L are time, amplitude and period of triangular wave respectively. Two methods are used—fixed period (fixed L) and fixed amplitude (fixed k). $f(t)$ is used in place of α which is the original parameter of unified chaotic system and the system is shown as follows:

$$\begin{aligned} &\dot{x} = (25f(t)+10)(y-x) \\ &\dot{y} = (28-35f(t))x + (29f(t)-1)y - xz \\ &\dot{z} = xy - \frac{8+f(t)}{3}z \end{aligned} \tag{5.3.2}$$

First, the period is fixed, and the amplitude gradually increases from 1 to 10. Fig. 5.3.1 shows the Lyapunov exponent of unified chaotic system with $\alpha = f(t)$, period $L = \pi$. We can easily find that the larger amplitude k is, the smaller the largest Lyapunov exponent is. So we can say, the chaotic phenomenon decreases as amplitude k increases. Fig. 5.3.2 and Fig. 5.3.3 show Lyapunov exponent of unified chaotic system with $\alpha = f(t)$, $L = 2\pi$ and $\alpha = f(t)$, $L = 3\pi$ respectively.

Second, the amplitude is fixed, and the period gradually increases from 1 to 100. Fig.5.3.4 shows the Lyapunov exponent of unified chaotic system with $\alpha = f(t)$, amplitude $k = 1$. Its largest value of Lyapunov exponent is around 2, which is very steady no matter what the period is. Fig. 5.3.5, Fig. 5.3.6 and Fig. 5.3.7 show the Lyapunov exponent of unified chaotic system for $\alpha = f(t)$, amplitude k = 2, 3, 10 respectively. The largest Lyapunov exponent is smaller and smaller as fixed amplitude k increases. Fig. 5.3.8 shows the bifurcation diagram of unified chaotic system with $\alpha = f(t)$, amplitude $k = 1$. It displays that the system is chaotic for all $\omega \in [0, 1000]$.

5.4 A Unified Chaotic System with -1~1 Triangular Wave Switch

In this section, we extend α to negative. A periodic switch(-1~1) by triangular wave mode will be used. Considering the following function:

$$g(t)=\begin{cases}\frac{2k}{L}t & if\ 0<t<\frac{L}{2}\\ \frac{2k}{L}(L-t) & if\ \frac{L}{2}<t<\frac{3}{2}L\\ \frac{2k}{L}(t-2L) & if\ \frac{3}{2}L<t<2L\end{cases} \tag{5.4.1}$$

where t,k and L are time, amplitude and period of triangular wave respectively. $g(t)$ is used in place of α which is the original parameter of unified chaotic system and the system is shown as follows:

$$\begin{aligned}\dot{x}&=(25g(t)+10)(y-x)\\ \dot{y}&=(28-35g(t))x+(29g(t)-1)y-xz\\ \dot{z}&=xy-\frac{8+g(t)}{3}z\end{aligned} \tag{5.4.2}$$

Amplitude is fixed at 1, 2, 4, 6, 8, 10, and period gradually increases from 1 to 1000. Fig. 5.4.1 shows Lyapunov exponent of unified chaotic system with $\alpha=g(x)$, amplitude $k=1$. It is easily seen that when period L is small than 300, the Lyapunov exponent shakes seriously. But it becomes smooth when period L is larger than 300. Fig. 5.4.2~ Fig. 5.4.6 show Lyapunov exponent of unified chaotic system with $\alpha=g(t)$, amplitude $k=2$, 4, 6, 8, 10 respectively. The largest Lyapunov exponent is smaller and smaller as fixed amplitude k increases. And we can find that when fixed amplitude k is greater than 4, the front section Lyapunov exponent doesn't shake so seriously any more.

5.5 A Unified Chaotic System with 0~1 Sawtooth Wave Switch

In this section, a sawtooth wave was used to substitute for α which is the original parameter of unified chaotic system so that α is in a periodic switch between 0 and 1 by a linear function as follows:

$$q(t)=\frac{k}{L}t \quad 0<t<L \quad \text{and} \quad q(t+L)=q(t) \tag{5.5.1}$$

where t,k and L are time, amplitude and period of sawtooth wave respectively. $q(t)$ is used in place of α which is the original parameter of unified chaotic system and the system is shown as follows:

$$\begin{aligned}
\dot{x} &= (25q(t)+10)(y-x) \\
\dot{y} &= (28-35q(t))x+(29q(t)-1)y-xz \\
\dot{z} &= xy-\frac{8+q(t)}{3}z
\end{aligned} \tag{5.5.2}$$

Amplitude is fixed at 1, 2, 4, 6, 8, 10, and period gradually increases from 1 to 1000. Fig. 5.5.1 shows Lyapunov exponent of unified chaotic system with $\alpha = q(x)$, amplitude $k = 1$. Its largest value of Lyapunov exponent is around 2, which is very steady no matter what the period is. Fig. 5.5.2~ Fig.5.5.6 show Lyapunov exponent of unified chaotic system with $\alpha = q(t)$, amplitude $k = 2, 4, 6, 8, 10$ respectively. The largest Lyapunov exponent is smaller and smaller as fixed amplitude k increases. And comparing Fig. 5.5.1~ Fig.5.5.6, the largest Lyapunov exponent is always greater than 0 when fixed amplitude k increases to10. It means that no matter the amplitude k of switch is, there exists chaos in the system.

Chapter 6

Chaos Control and Synchronization of the Fractional Order Unified Chaotic System

6.1 Introduction of Fractional Order System

Fractional calculus is a 300-year-old mathematical topic. Although it has a long history, the applications of fractional calculus to physics and engineering are just a recent focus of interest. It was well known that chaos cannot occur in continuous-time systems of order less than three. Many systems are known to display fractional order dynamics, such as viscoelastic systems, dielectric polarization, electrode–electrolyte polarization, and electromagnetic waves. More recently, there is a new trend to investigate the control [34-39] and dynamics [40-48] of fractional order dynamical systems.

6.2. Fractional Derivative and Its Approximation

There are several definitions of fractional derivatives. The well known is the Riemann–Liouville definition, which is given by

$$\frac{d^{\alpha} f(t)}{dt^{\alpha}} = \frac{1}{\Gamma(n-\alpha)} \frac{d^{n}}{dt^{n}} \int_{0}^{t} \frac{f(\tau)}{(t-\tau)^{\alpha-n+1}} d\tau \qquad (6.2.1)$$

where Γ is the gamma function and $n-1 \leq \alpha < n$. This definition is significantly different from the classical definition of derivative.

The Laplace transform is applicable and works. Upon considering all the initial conditions to be zero, the Laplace transform of the Riemann–Liouville fractional derivative satisfies

$$L\left\{\frac{d^{\alpha} f(t)}{dt^{\alpha}}\right\} = s^{\alpha} L\{f(t)\} \qquad (6.2.2)$$

An efficient method is to approximate fractional operators by using standard integer order operators. In [49], an effective algorithm is developed to approximate fractional order transfer functions. Basically, the idea is to approximate the system behavior in the frequency domain. By utilizing frequency domain techniques based on Bode diagrams, one can obtain a linear approximation of the fractional order integrator, the order of which depends on the desired bandwidth and discrepancy between the actual and the approximate magnitude Bode diagrams. In Table 1 of [50], approximations for $1/s^q$ with $q = 0.1 \sim 0.9$ in steps 0.1 are given, with errors of approximately 2 dB. We also use these approximations in the following simulations.

6.3 The Fractional Order Unified Chaotic System

In this section, the fractional order unified chaotic system is considered. The standard derivative is replaced by a fractional derivative as follows:

$$\begin{aligned} \frac{d^a x}{dt^a} &= (25\alpha + 10)(y - x) \\ \frac{d^a y}{dt^a} &= (28 - 35\alpha)x + (29\alpha - 1)y - xz \\ \frac{d^a z}{dt^a} &= xy - \frac{8+\alpha}{3}z \end{aligned} \tag{6.3.1}$$

where a is the fractional order. When $a = 1$, system (6.3.1) is the original integer order unified chaotic system in which chaos exists for any $\alpha \in [0,1]$ as described in Chapter 2.

First, let $a = 0.9$, Fig.6.3.1 shows the bifurcation diagram of $2.7(3 \times 0.9)$ order unified chaotic system. It is easily observed, for the major portion of $\alpha \in [0.7, 2.3]$ in the fractional order system there exists chaotic phenomenon. Only a small portion around $\alpha = 2.0$ and $\alpha = 2.3$, the dynamics of system becomes periodic motion. Fig. 6.3.2~ Fig. 6.3.5 are phase portraits of $2.7(3 \times 0.9)$ order unified chaotic system with $\alpha = 0.8$ (Lü system), 2.0, 2.2, 2.25 respectively.

Next, let $a = 0.8$, Fig.6.3.6 shows the bifurcation diagram of $2.4(3 \times 0.8)$ order unified chaotic system. It is easily observed, for the major portion of $\alpha \in [0.8, 2.2]$ in the fractional order system there exists chaotic phenomenon. Only a small portion around $\alpha = 1.8$, $\alpha = 2.1$ and some small ranges of α, dynamics of the system becomes periodic motion. Fig. 6.3.7~ Fig. 6.3.10 are phase portraits of 2.4(3×0.8) order unified chaotic system with $\alpha = 1.7$, 1.8, 1.9, 2.05 respectively.

For $a = 0.7$, some chaotic parameters of α are found. Fig. 6.3.11~Fig. 6.3.13 show phase portraits of 2.1(3×0.7) order unified chaotic system for $\alpha = 3.7$, 3.8, 4.0 respectively. Phase portraits are smaller and smaller (lower and lower at the same time) as α increases so that it is hard too draw a bifurcation diagram.

Fig.6.3.14 and Fig.6.3.15 show phase portraits of 1.8(3×0.6) order unified chaotic system for $\alpha = 2.5$, 3.0. Phase portraits are smaller and smaller (lower and lower at the same time) as α increases so that it is hard too draw a bifurcation diagram.

Fig.6.3.16 and Fig.6.3.17 show phase portraits of 1.5(3×0.5) order unified chaotic system for $\alpha = 2.0$, 2.5.

6.4 Chaos Control of Fractional Order Unified Chaotic System

Chaos control attracts more and more attention from various disciplines in science and engineering. In this section, we will try to control fractional order unified chaotic system to its equilibrium point. Recasting the fractional order unified chaotic system (6.3.1) in a compact vector form, we have

$$\frac{d^a X}{dt^a} = f(X) \tag{6.4.1}$$

with $X = [x, y, z]^T$. A simple linear state feedback controller is added as follows:

$$\frac{d^a X}{dt^a} = f(X) + u \tag{6.4.2}$$

where u is a linear state feedback controller of the form as follows:

$$u = \begin{bmatrix} k_1 & 0 & 0 \\ 0 & k_2 & 0 \\ 0 & 0 & k_3 \end{bmatrix} (X - \overline{X}) \tag{6.4.3}$$

where $\overline{X}$ is the control target, and k_1, k_2, k_3 are constant parameters. Clearly, (0, 0, 0) is always an equilibrium point of system(6.3.1). In the following simulation, we stabilize system (6.3.1) to this equilibrium point. Standard stability analysis easily shows that with (k_1, k_2, k_3) = (29, -23, 2), the equilibrium point is (0, 0, 0). Simulation results show that this controller can stabilize the fractional order unified chaotic systems with two values of α to this equilibrium point. Fig. 6.4.1(a)(b) show the time history of the controlled fractional order unified chaotic system with order $a = 0.9$ and system parameter $\alpha = 0.8, 1.8$ respectively. Fig. 6.4.2(a)(b) show the time history of the controlled fractional order unified chaotic system with order $a = 0.8$ and system parameter $\alpha = 1.4, 1.9$ respectively. Fig. 5.4.3 shows time history of the controlled fractional order unified chaotic system with order $a = 0.7$ and system parameter $\alpha = 3.7$. In all figures, the control signal is added at t = 40.

As we can see from these figures, the designed chaos controller can effectively control the fractional order unified chaotic system to its equilibrium $\overline{X} = (0,0,0)$

6.5 Chaos Synchronization of the Same Fractional Order Unified Chaotic Systems

In recent years, synchronization in chaotic dynamic system is very interesting problem and has been widely studied. In the synchronized systems, one is called master and another is called slave. Synchronization means that the state variables of a response system approach eventually to that of a drive system. There are many control techniques to synchronize chaotic systems, such as linear error feedback control, adaptive control, active control.

In this section, two unified chaotic systems of the same fractional order are tried to be synchronized. First, two 0.9 order master and slave systems are studied as follows:

Master system:

$$\begin{aligned}
\frac{d^a x_1}{dt^a} &= (25\alpha+10)(y_1-x_1) \\
\frac{d^a y_1}{dt^a} &= (28-35\alpha)x_1+(29\alpha-1)y_1-x_1z_1 \\
\frac{d^a z_1}{dt^a} &= x_1y_1-\frac{8+\alpha}{3}z_1
\end{aligned} \tag{6.5.1}$$

Slave system:

$$\begin{aligned}
\frac{d^a x_2}{dt^a} &= (25\alpha+10)(y_2-x_2)+k_1(x_1-x_2) \\
\frac{d^a y_2}{dt^a} &= (28-35\alpha)x_2+(29\alpha-1)y_2-x_2z_2+k_2(y_1-y_2) \\
\frac{d^a z_2}{dt^a} &= x_2y_2-\frac{8+\alpha}{3}z_2+k_3(z_1-z_2)
\end{aligned} \tag{6.5.2}$$

where order $a=0.9$. Fig.6.5.1(a)(b) show time history of errors with system parameter $\alpha=0.8, 2.2$ respectively, and the coupling strength $k_1=k_2=k_3=1$. We let two systems start to synchronize at $t=200$, and errors quickly converge to 0. Synchronization of the same fractional order unified chaotic systems had been achieved.

Second, another case as order $a=0.8$ is studied. Fig. 6.5.2(a)(b) show time history of errors with system parameter $\alpha=0.8, 1.9$ respectively, and the coupling strength $k_1=k_2=k_3=2$. Last, case order $a=0.7$ is studied. Fig. 6.5.3 shows time history of errors with system parameter $\alpha=3.7$ and the coupling strength $k_1=k_2=k_3=4$. The lower fractional order is, the stronger coupling strength k which can synchronize the two identical systems is.

6.6 Chaos Synchronization of Different Fractional Order Unified Chaotic Systems

In previous section, two unified chaotic systems of the same fractional order had tried to be synchronized and synchronization had been achieved successfully. In this section, we will try to synchronized two different fractional order unified chaotic systems. First, we try to use 0.9 order master system and 0.8 order slave system described as follows:

Master system:

$$\frac{d^{0.9}x_1}{dt^{0.9}} = (25\alpha+10)(y_1 - x_1)$$
$$\frac{d^{0.9}y_1}{dt^{0.9}} = (28-35\alpha)x_1 + (29\alpha-1)y_1 - x_1 z_1 \tag{6.6.1}$$
$$\frac{d^{0.9}z_1}{dt^{0.9}} = x_1 y_1 - \frac{8+\alpha}{3} z_1$$

Slave system:

$$\frac{d^{0.8}x_2}{dt^{0.8}} = (25\alpha+10)(y_2 - x_2) + k_1(x_1 - x_2)$$
$$\frac{d^{0.8}y_2}{dt^{0.8}} = (28-35\alpha)x_2 + (29\alpha-1)y_2 - x_2 z_2 + k_2(y_1 - y_2) \tag{6.6.2}$$
$$\frac{d^{0.8}z_2}{dt^{0.8}} = x_2 y_2 - \frac{8+\alpha}{3} z_2 + k_3(z_1 - z_2)$$

Fig.6.6.1 shows time history of errors with system parameter $\alpha = 1.2$. The coupling strength k_1, k_2, k_3 must be large enough as 3000, two systems will be practically synchronized, the errors are around 10^{-3}

Second, we try to use 0.8 order master system(with $\alpha = 1.2$) and 0.7 order slave system(with $\alpha = 3.7$) described as follows:

Master system:

$$\frac{d^{0.8}x_1}{dt^{0.8}} = (25\alpha+10)(y_1 - x_1)$$
$$\frac{d^{0.8}y_1}{dt^{0.8}} = (28-35\alpha)x_1 + (29\alpha-1)y_1 - x_1 z_1 \tag{6.6.3}$$
$$\frac{d^{0.8}z_1}{dt^{0.8}} = x_1 y_1 - \frac{8+\alpha}{3} z_1$$

Slave system:

$$\frac{d^{0.7}x_2}{dt^{0.7}} = (25\alpha+10)(y_2 - x_2) + k_1(x_1 - x_2)$$
$$\frac{d^{0.7}y_2}{dt^{0.7}} = (28-35\alpha)x_2 + (29\alpha-1)y_2 - x_2 z_2 + k_2(y_1 - y_2) \tag{6.6.4}$$
$$\frac{d^{0.7}z_2}{dt^{0.7}} = x_2 y_2 - \frac{8+\alpha}{3} z_2 + k_3(z_1 - z_2)$$

Fig. 6.6.2 shows time history of errors. The coupling strength k_1, k_2, k_3 must be large enough as 5000, two systems will be practically synchronized, the errors are around 10^{-3}.

Last, we try to use 0.7 order master system(with $\alpha = 3.7$) and 0.9 order slave system(with $\alpha = 2.2$) described as follows:

Master system:

$$\begin{aligned}
\frac{d^{0.7}x_1}{dt^{0.7}} &= (25\alpha + 10)(y_1 - x_1) \\
\frac{d^{0.7}y_1}{dt^{0.7}} &= (28 - 35\alpha)x_1 + (29\alpha - 1)y_1 - x_1 z_1 \\
\frac{d^{0.7}z_1}{dt^{0.7}} &= x_1 y_1 - \frac{8+\alpha}{3} z_1
\end{aligned} \tag{6.6.5}$$

Slave system:

$$\begin{aligned}
\frac{d^{0.9}x_2}{dt^{0.9}} &= (25\alpha + 10)(y_2 - x_2) + k_1(x_1 - x_2) \\
\frac{d^{0.9}y_2}{dt^{0.9}} &= (28 - 35\alpha)x_2 + (29\alpha - 1)y_2 - x_2 z_2 + k_2(y_1 - y_2) \\
\frac{d^{0.9}z_2}{dt^{0.9}} &= x_2 y_2 - \frac{8+\alpha}{3} z_2 + k_3(z_1 - z_2)
\end{aligned} \tag{6.6.6}$$

Fig.6.6.3 shows time history of errors. The coupling strength k_1, k_2, k_3 must be large enough as 5000, two systems will be practically synchronized, the errors are around 10^{-3}.

Chapter 7

Conclusions

In this thesis, chaos and chaos synchronization of integral and fractional order unified chaotic system are studied.

In Chapter 2, description of the system and differential equations of motion are introduced. Lyapunov exponents and phase portraits of unified chaotic system are drawn.

In Chapter 3, we use two methods, state and speed coupling, to achieve synchronization of two identical unified chaotic systems. First, state couplings $k(x_1 - x_2)$ are added to different equations of slave system, respectively. We find the state coupling must be added at suitable equation of slave system, synchronization is achieved. Second, speed couplings $G(\dot{x}_1 - \dot{x}_2)$ are added to different equations of slave system, respectively. In this case, we find a phenomenon which indicates that for the synchronization conditions obtained by Lyapunov first approximation theory, there exists potential of improvement. Last, regression analysis methods are used. An approximate curve (3.3.1) about G and α is obtained. When G satisfies inequality (3.3.2), two systems are synchronized.

In Chapter 4, unified chaotic system is studied in detail. Not only non-chaotic ranges within $\alpha \in [0,1]$ but also chaotic ranges besides $\alpha \in [0,1]$ for unified chaotic system are found. We also introduce a new parameter $\beta = f(\alpha)$ so that the extended unified chaotic system is chaotic only when $\beta \in [0,1]$.

In Chapter 5, a unified chaotic system with various periodic switches are put forward. Four functions $\sin^2 \omega t$, $\sin \omega t$, triangular wave, sawtooth wave are used to replace α which is the original constant parameter of unified chaotic system and we find much interesting results. We find that different switching functions cause different behaviors of system. A common trend is that the larger switching range is, the smaller the largest Lyapunov exponent is.

Finally, chaos, chaos control and synchronization of the fractional order unified chaotic systems are studied. In the beginning, conception of fractional order system is brought in. Some values of α which cause the system chaotic are found. Controlling the fractional order unified chaotic systems to its equilibrium point is accomplished. The same and different fractional orders unified chaotic systems are synchronized. In the case of the same fractional order unified chaotic systems, synchronizations are realized with small coupling strength. But in the different fractional order case, coupling strength must be over 2000, two systems are just practically synchronized.

References

[1] Ott,E., *Chaos in Dynamical Systems*, 2^{nd} Edition, Cambridge, England, 2002.

[2] Khailil, H. K., *Nonlinear Systems*, Prentice Hall, New Jersey, 2002.

[3] Holmes, P., "Bifurcation and chaos in a Simole feedback control system", Proceedings of the IEEE 22^{nd} Conference on Decision and Control, 1983, pp.365-370.

[4] Wu C. W. and Chua L. O., "A simple way to synchronize chaotic systems with applications to secure communication systems", Int. J. Bifurcation and Chaos 3, 1619 (1993).

[5] Short K. M., "Steps toward unmasking secure communications", Int. J. Bifurcation and Chaos 4, 959 (1994).

[6] Cuomo K. M., Oppenheim A. V. and Strogatz S. H., "Synchronization of Lorenz-based chaotic circuits with applications to communications", IEEE Trans. Circuits Syst. 40, 626 (1993).

[7] Williams C., "Chaotic communications over radio channels", IEEE Trans. Circuit Syst.- I 48, 1394 (2001).

[8] Rulkov N. F. *et. al.*, "Digital communication using Chaotic-pulse-position modulation", IEEE Trans. Circuits Syst.- I 48, 1436 (2001).

[9] Pecora L. M. and Carroll T. L., "Synchronization in chaotic systems", Phys. Rev. Lett. 64, 821-824(1990).

[10] Pecora L. M. and Carroll T. L., "Cascading synchronized chaotic systems", Physica D 67, 126 (1993).

[11] Carroll T. L. and Pecora L. M., "Synchronizing nonautonomous chaotic circuits", IEEE Trans. Circuits Syst. II 40, 646 (1993).

[12] Pyragas K., "Weak and strong synchronization of chaos", Phys. Rev. E 54, 4508 (1996).

[13] Kocarev L., Parlitz U. and Brown R., "A unifying definition of synchronization for dynamical systems", Phys. Rev. E 61, 3716 (2000).

[14] Chen G., Dong X., *From Chaos to Order: Perspectives, Methodologies and Applications*, World Scientific, Singapore, 1998.

[15] Lü J., Lu J., Chen S., *Chaotic Time Series Analysis and its Application*, Wuhan Univ. Press, China, 2002.

[16] Chen S., Lu J., *The Introduction to Chaotic Dynamics*, Wuhan Univ. Press, China, 1998.

[17] Chen G. R., Ueta T., "Yet another chaotic attractor", Int J Bifurcat Chaos 1999; 9: 1465-6.

[18] Tao C. H., Lu J. A., "Control of a unified chaotic system". Acta Phys Sinica 2003; 52(2): 0281-04(in Chinese).

[19] Tao C. H., Lu J. A., Lü J. H. "The feedback synchronization of a unified chaotic system". Acta Phys Sinica 2002; 51(7): 1497-505(in Chinese).

[20] Lu J., Chen G., Cheng D., ČelikovskЎ S. "Bridge the gap between the Lorenz system and the Chen system". Int J Bifurcat Chaos 2002; 12: 2917-26.

[21] Li D., Lu J., Wu X., "Linearly coupled synchronization of the unified chaotic systems and the Lorenz systems", Chaos, Solitons and Fractals 23 (2005) 79-85.

[22] Tao C. H., Yang C., Luo Y., Xiong H., Hu F., "Speed feedback control of chaotic system". Chaos, Solitons and Fractals 23 (2005) 259-263.

[23] Chen S., Lü J., "Synchronization of an uncertain unified chaotic system via adaptive control". Chaos, Solitons & Fractals 2002; 14: 643–7.

[24] Lu J., Wu X., Lü J., "Synchronization of a unified chaotic system and the application in secure communication". Phys Lett A 2002; 305: 365–70.

[25] Lu J., Tao C., Lü J., Liu M., "The parameter identification and tracking of a unified system". Chin Phys Lett 2002; 19(5): 632–5.

[26] Wu X., Lu J., "Parameter identification and backstepping control of uncertain Lü

system”. Chaos, Solitons & Fractals 2003; 18: 721–9.

[27] Lü J., Lu J., “Controlling uncertain Lü system using linear feedback”. Chaos, Solitons & Fractals 2002; 17: 127–33.

[28] Chen G., Lü J., “Dynamical analysis, control and synchronization of the Lorenz systems family”. China: Science Press; 2003.

[29] Li C. U., Chen G. R., “Chaos in the fractional order Chen system and its control”. Chaos, Solitons and Fractals 22(2004) 549-554.

[30] Oldham K. B. and Spanier J., *The Fractional Calculus*, San Diego, CA: Academic, 1974.

[31] Vaněček A., and ČelikovskÝ S., “Control systems: from linear analysis to synthesis of chaos”. London: Prentice-Hall; 1996.

[32] Lü J. H., Chen G. R., “A new chaotic attractor coined”. Int J Bifurcat Chaos 2002; 12: 659-61.

[33] Lu J. A., Wu X. Q., “A unified chaotic system with periodic switch”. Chaos, Solitons and Fractals 20(2004) 245-251.

[34] Oustaloup A., Sabatier J., Lanusse P., “From fractal robustness to CRONE control”. Fract Calculus Appl Anal 1999; 2: 1–30.

[35] Oustaloup A., Levron F., Nanot F., Mathieu B., “Frequency band complex non integer differentiator: characterization and synthesis”. IEEE Trans CAS-I 2000; 47: 25–40.

[36] Chen Y. Q., Moore K., “Discretization schemes for fractional-order differentiators and integrators”. IEEE Trans CAS-I 2002; 49: 363–7.

[37] Hartley T. T., Lorenzo C. F., “Dynamics and control of initialized fractional-order systems”. Nonlinear Dyn 2002; 29: 201–33.

[38] Hwang C., Leu J.-F., Tsay S.-Y., “A note on time-domain simulation of feedback fractional-order systems”. IEEE Trans Auto Contr 2002; 47: 625–31.

[39] Podlubny I., Petras I., Vinagre B. M., O’Leary P., Dorcak L., “Analogue realizations of fractional-order controllers”. Nonlinear Dyn 2002; 29: 281–96.

[40] Arena P., Caponetto R., Fortuna L., Porto D., “Chaos in a fractional order Duffing system”. In: Proc. ECCTD, Budapest 1997. p. 1259–62.

[41] Ahmad W., El-Khazali R., El-Wakil A., “Fractional-order Wien-bridge oscillator”. Electr Lett 2001; 37: 1110–2.

[42] Ahmad W. M., Sprott J. C., “Chaos in fractional-order autonomous nonlinear systems”. Chaos, Solitons & Fractals 2003; 16: 339–51.

[43] Ahmad W. M., Harb W. M., “On nonlinear control design for autonomous chaotic systems of integer and fractional orders”. Chaos, Solitons & Fractals 2003; 18: 693–701.

[44] Grigorenko I., Grigorenko E., “Chaotic dynamics of the fractional Lorenz system”. Phys Rev Lett 2003; 91: 034101.

[45] Arena P., Caponetto R., Fortuna L., Porto D., “Bifurcation and chaos in noninteger order cellular neural networks”. Int J Bifur Chaos 1998; 7: 1527–39.

[46] Arena P., Fortuna L., Porto D., “Chaotic behavior in noninteger-order cellular neural networks. Phys Rev E 2000; 61: 776–81.

[47] Li C., Chen G., “Chaos and hyperchaos in fractional order Rössler equations”. Physica A, 2004; 341: 55-61.

[48] Li C., Liao X., Yu J., “Synchronization of fractional order chaotic systems”. Phys Rev E 2003; 68: 067203.

[49] Charef A., Sun H. H., Tsao Y. Y., Onaral B., “Fractal system as represented by singularity function”. IEEE Trans Auto Control 1992; 37: 1465–70.

[50] Hartley T. T., Lorenzo C. F., Qammer H. K., “Chaos in a fractional order Chua’s system”. IEEE Trans CAS-I 1995; 42: 485–90.

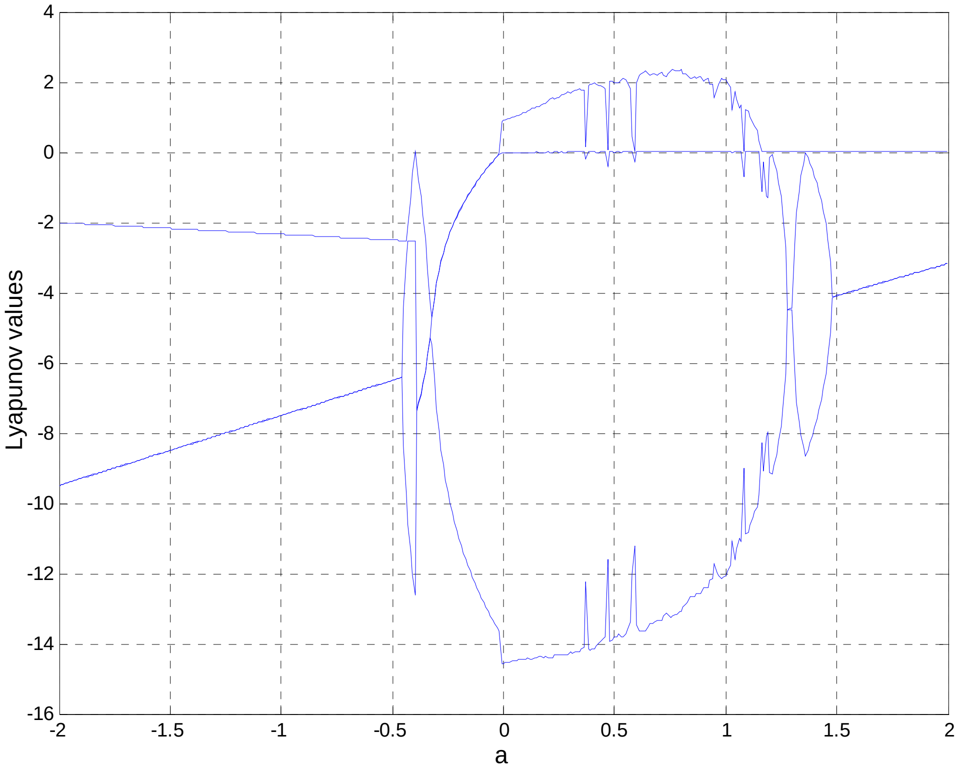

Fig 2.2.1 The Lyapunov exponents for a between -2 and 2

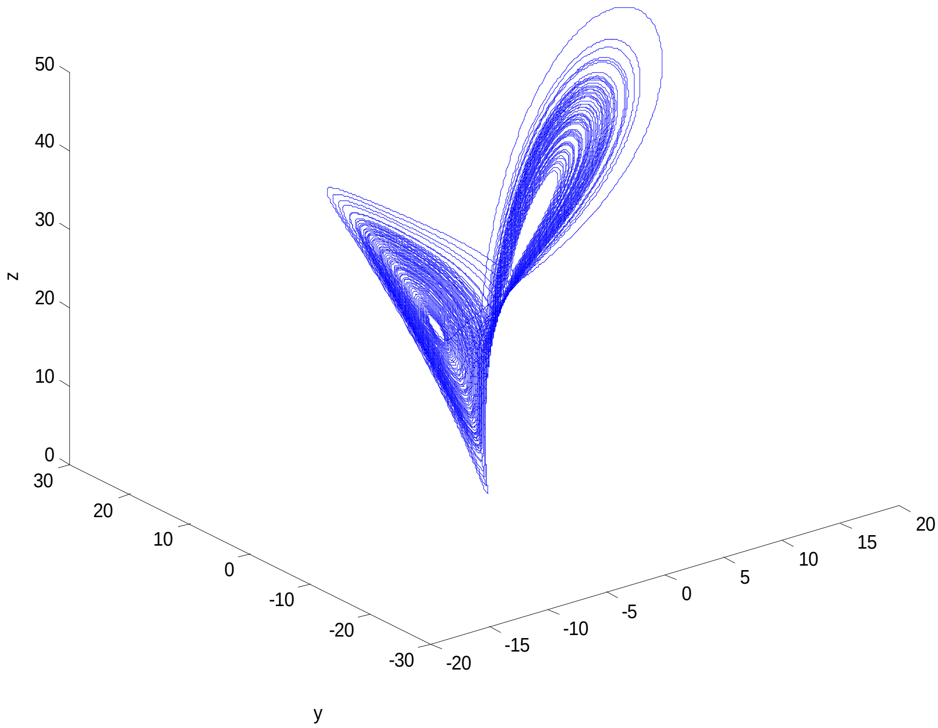

Fig.2.3.1(a) 3D phase portrait for unified chaotic system with $\alpha = 0$.

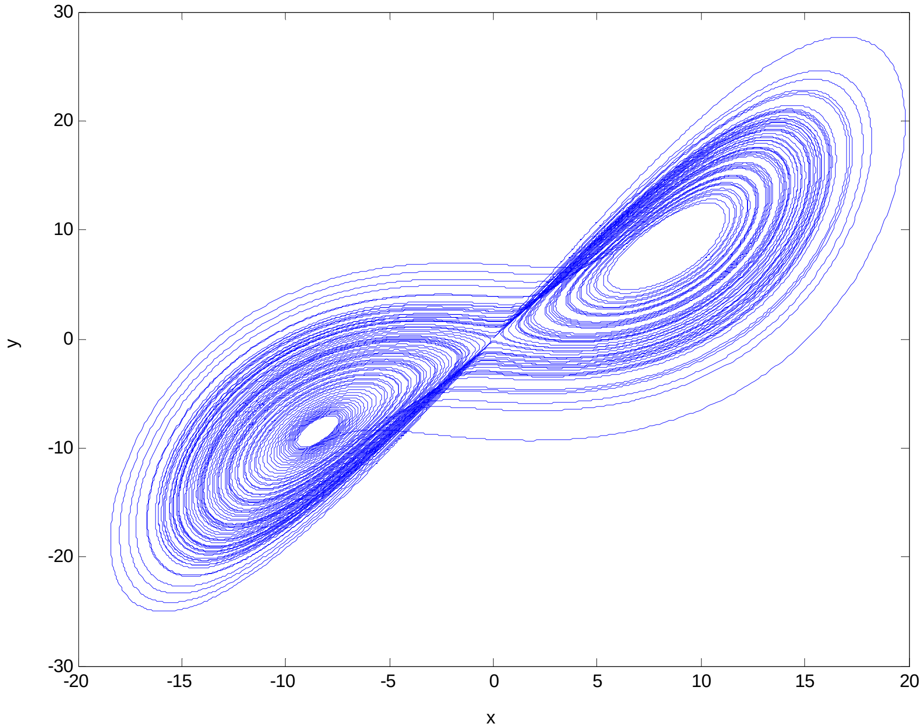

Fig.2.3.1(b) 2D(xy) phase portrait for unified chaotic system with $\alpha = 0$.

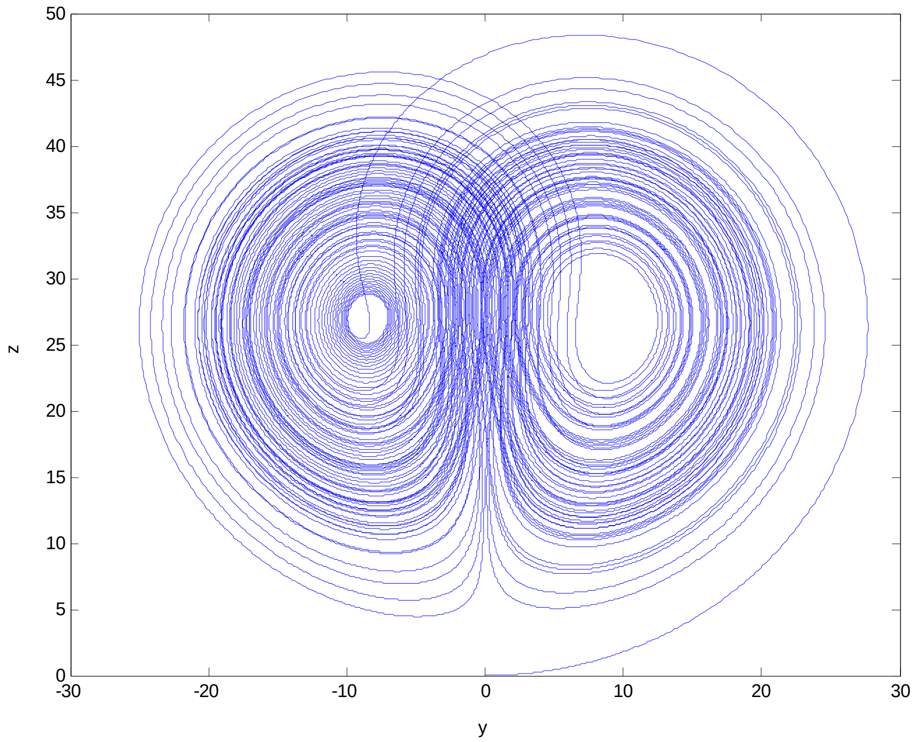

Fig.2.3.1(c) 2D(yz) phase portrait for unified chaotic system with $\alpha = 0$.

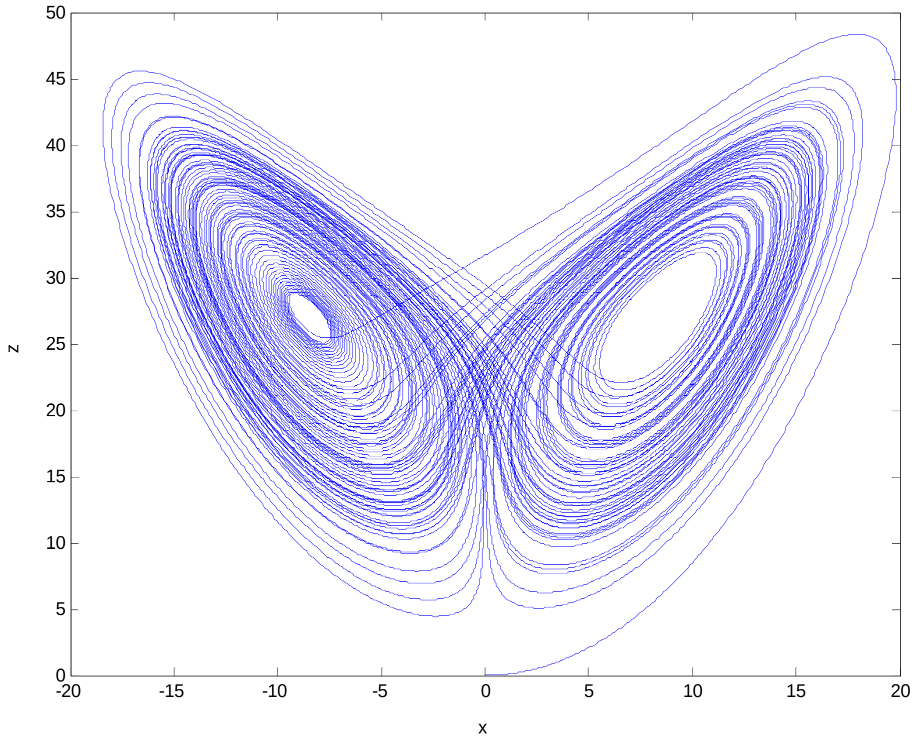

Fig.2.3.1(d) 2D(xz) phase portrait for unified chaotic system with $\alpha = 0$.

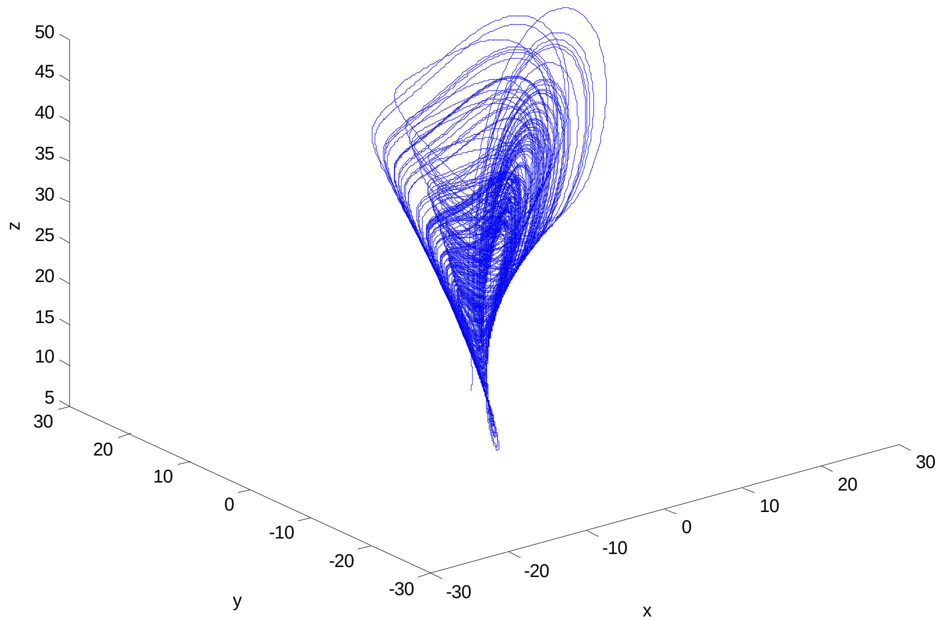

Fig.2.3.2(a) 3D phase portrait for unified chaotic system with $\alpha = 1$.

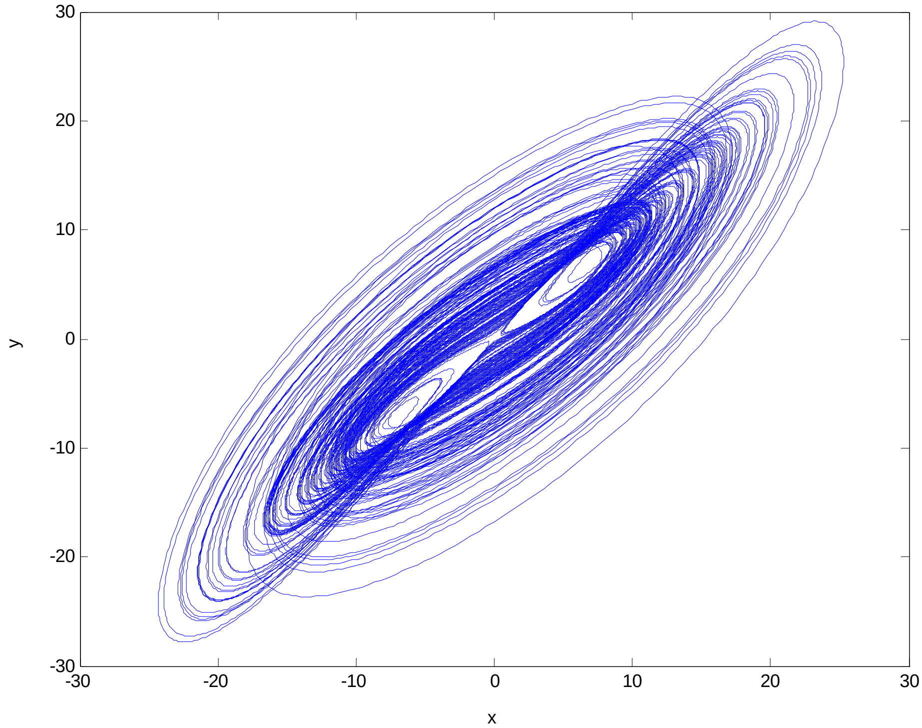

Fig.2.3.2(b) 2D(xy) phase portrait for unified chaotic system with $\alpha = 1$.

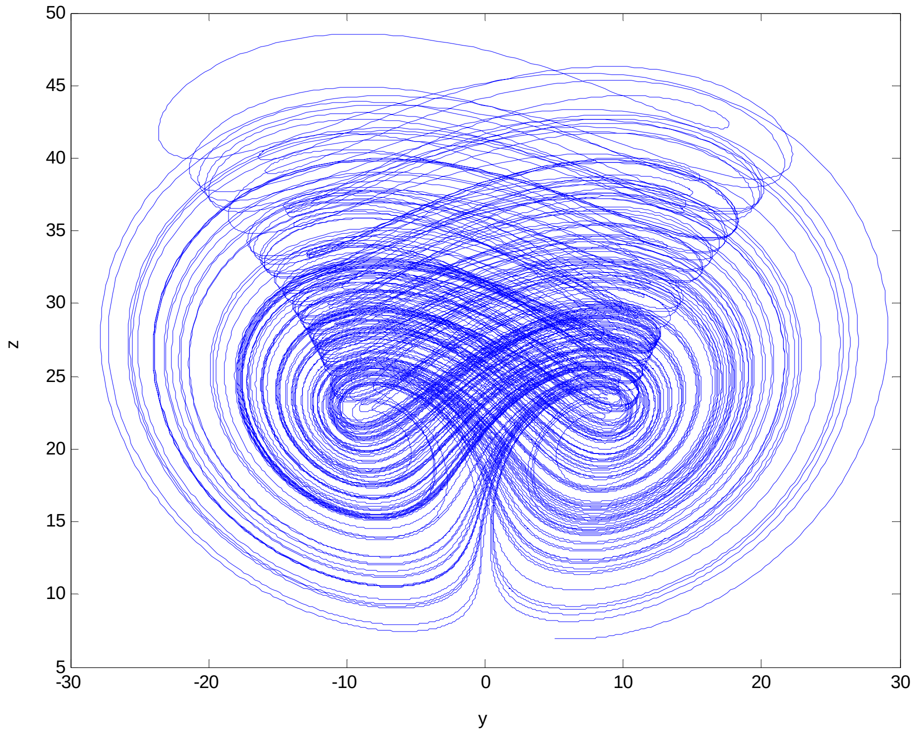

Fig.2.3.2(c) 2D(yz) phase portrait for unified chaotic system with $\alpha = 1$.

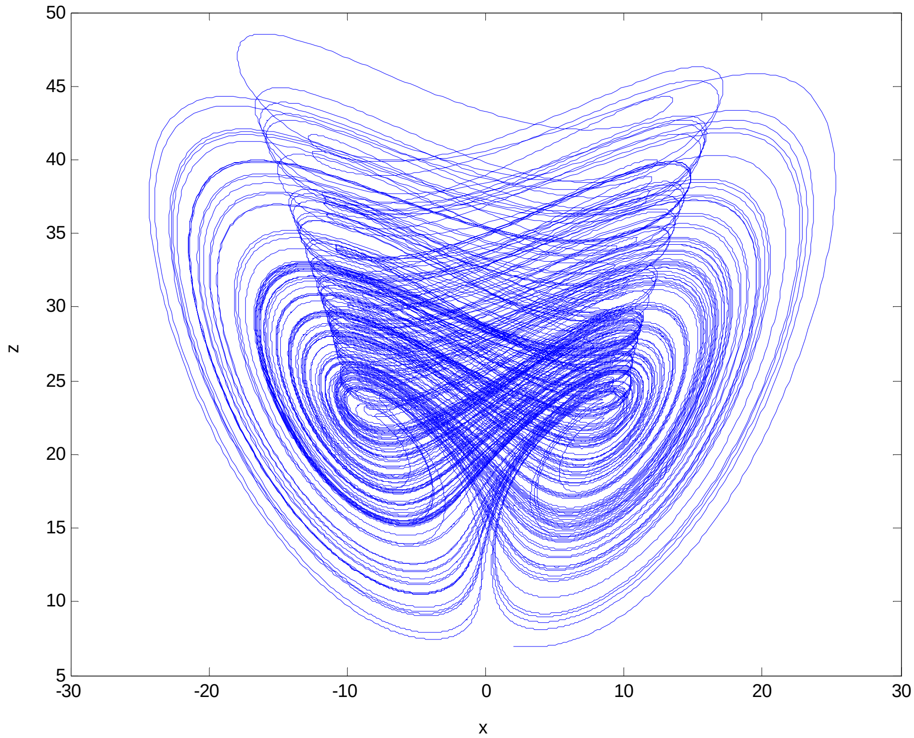

Fig.2.3.2(d) 2D(xz) phase portrait for unified chaotic system with $\alpha = 1$.

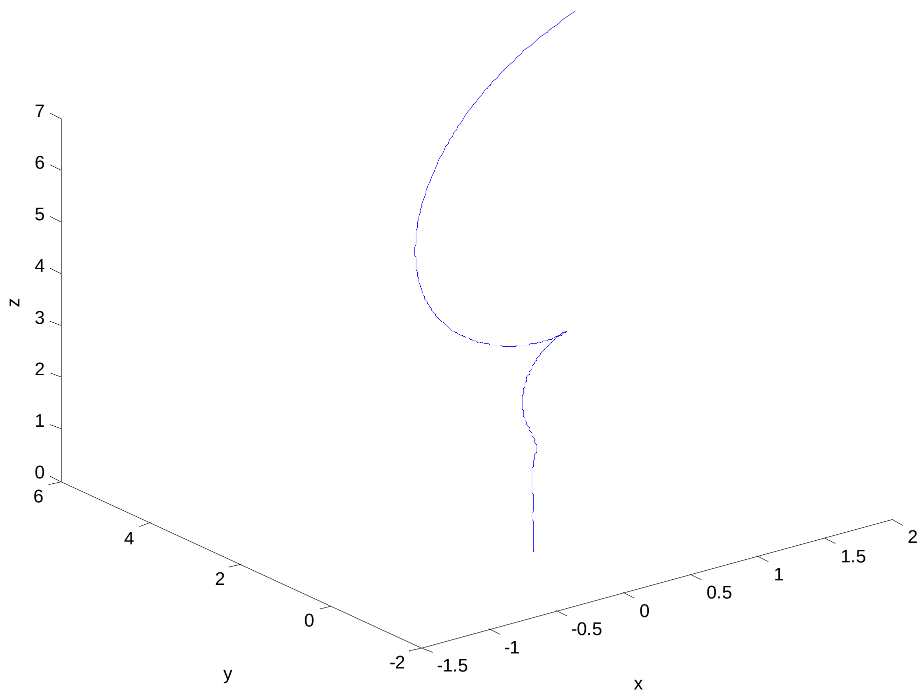

Fig.2.3.3(a) 3D phase portrait for unified chaotic system with $\alpha = -1$ and initial condition x=2, y=5, z=7.

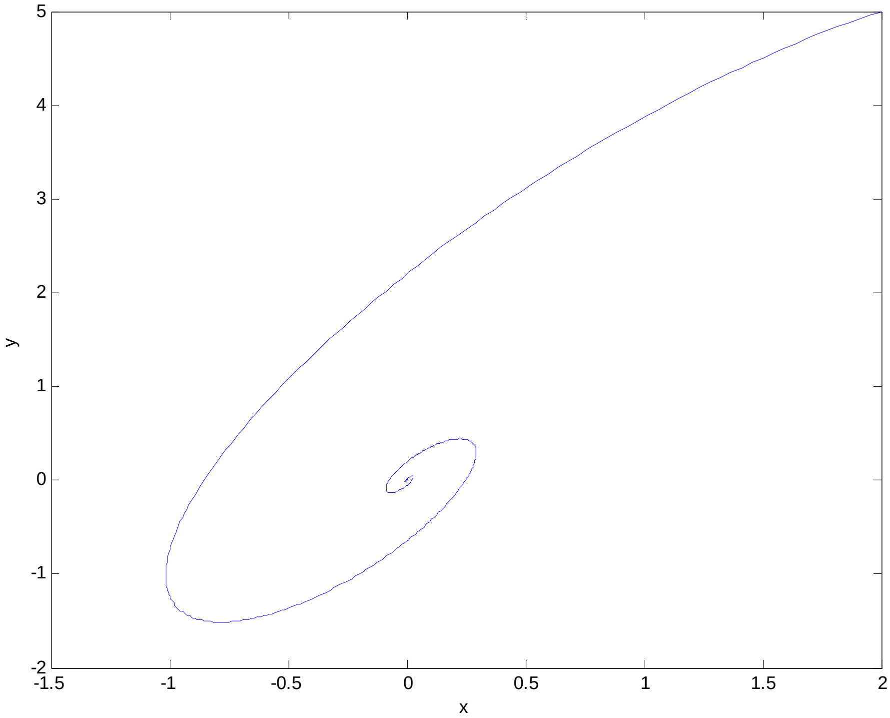

Fig.2.3.3(b) 2D(xy) phase portrait for unified chaotic system with $\alpha = -1$ and initial condition x=2, y=5, z=7.

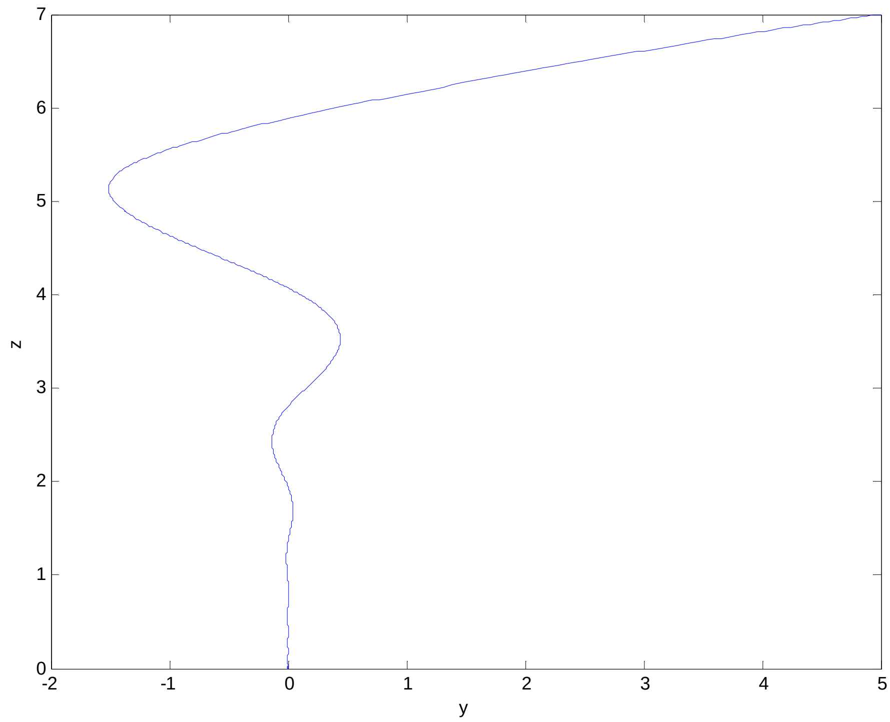

Fig.2.3.3(c) 2D(yz) phase portrait for unified chaotic system with $\alpha = -1$ and initial condition x=2, y=5, z=7.

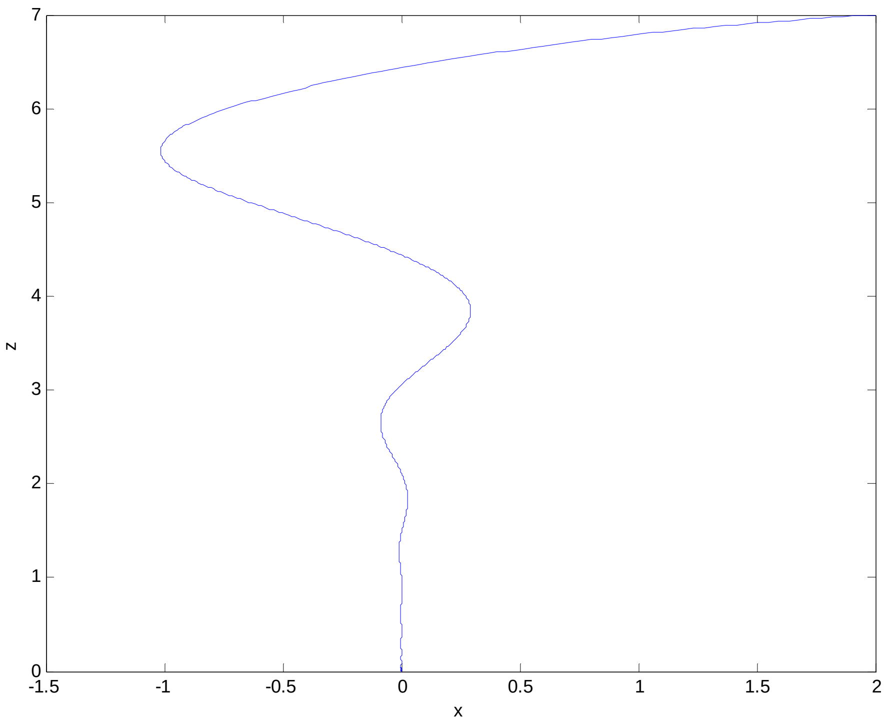

Fig.2.3.3(d) 2D(xz) phase portrait for unified chaotic system with $\alpha = -1$ and initial condition x=2, y=5, z=7.

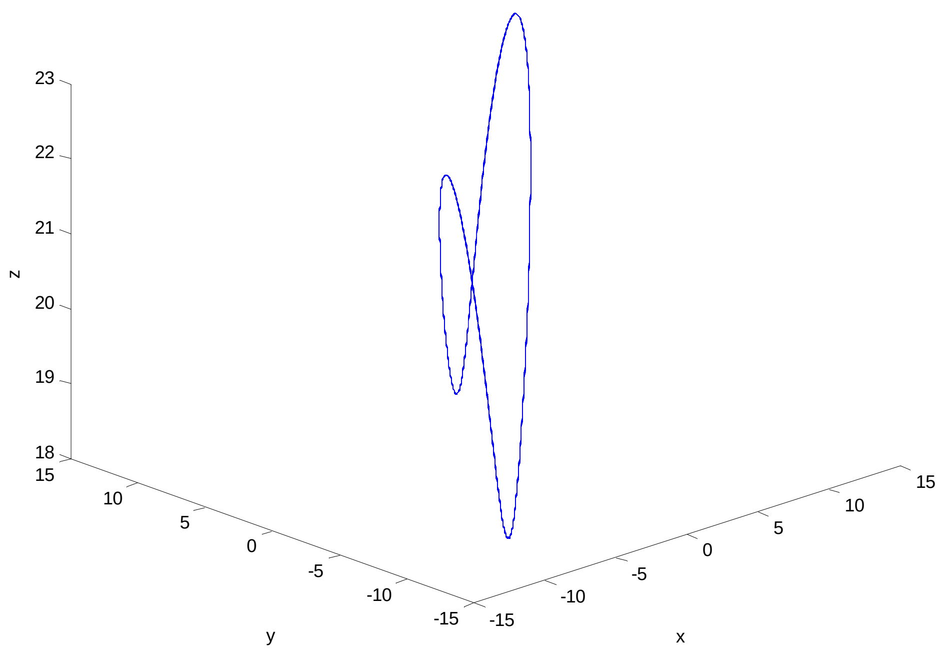

Fig.2.3.4(a) 3D phase portrait for unified chaotic system with $\alpha = 1.7$.

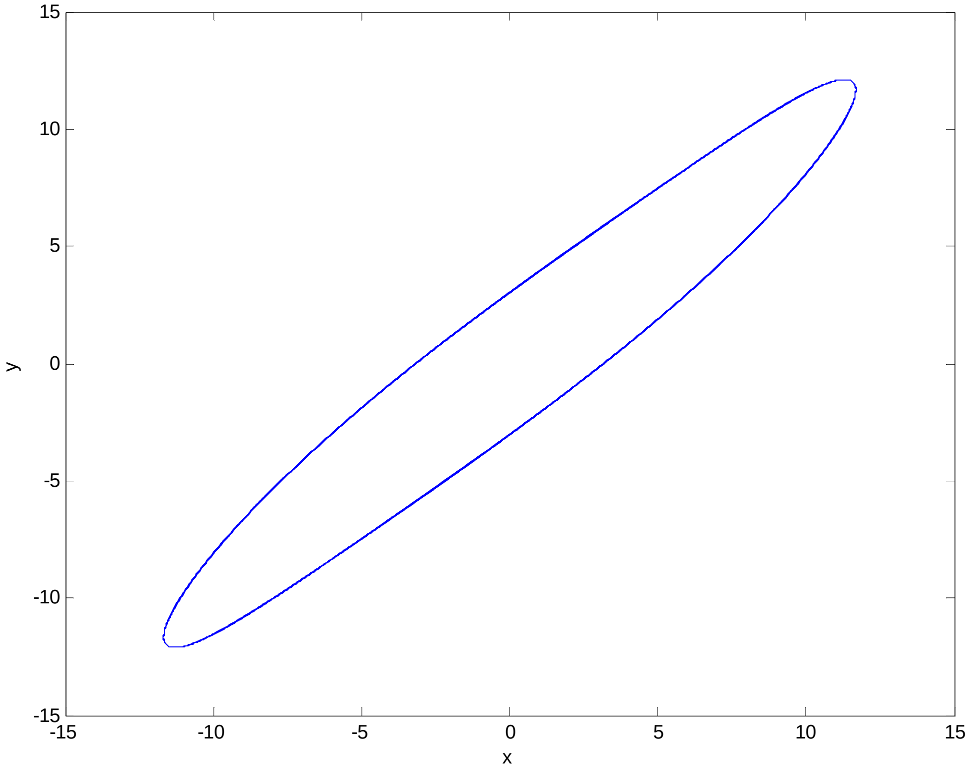

Fig.2.3.4(b) 2D(xy) phase portrait for unified chaotic system with $\alpha = 1.7$.

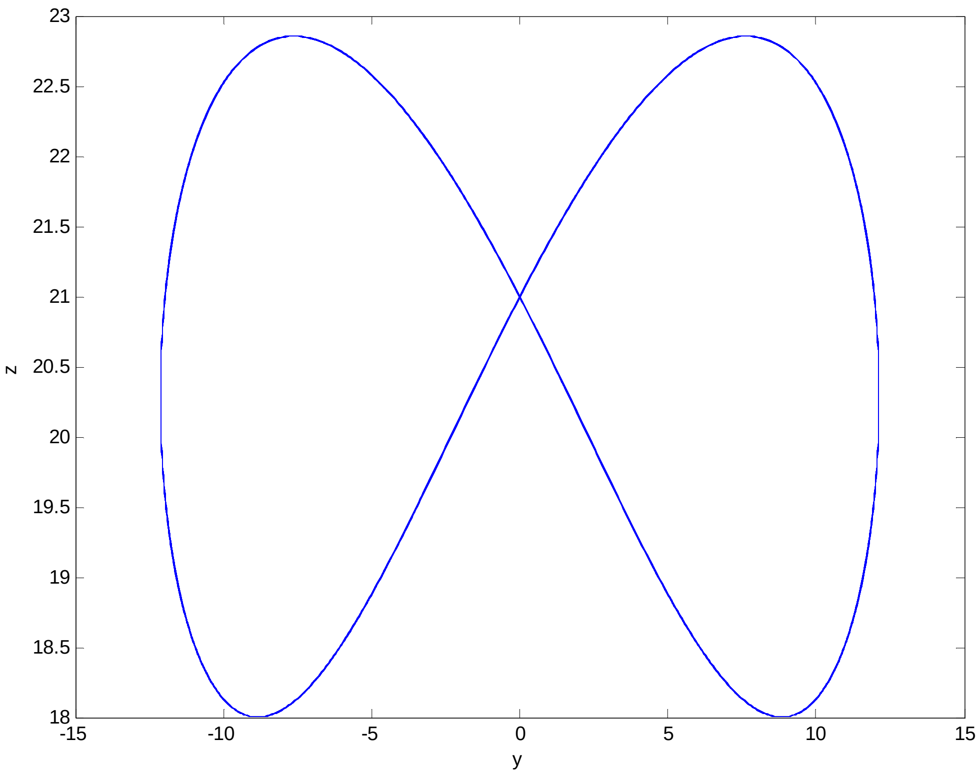

Fig.2.3.4(c) 2D(yz) phase portrait for unified chaotic system with $\alpha = 1.7$.

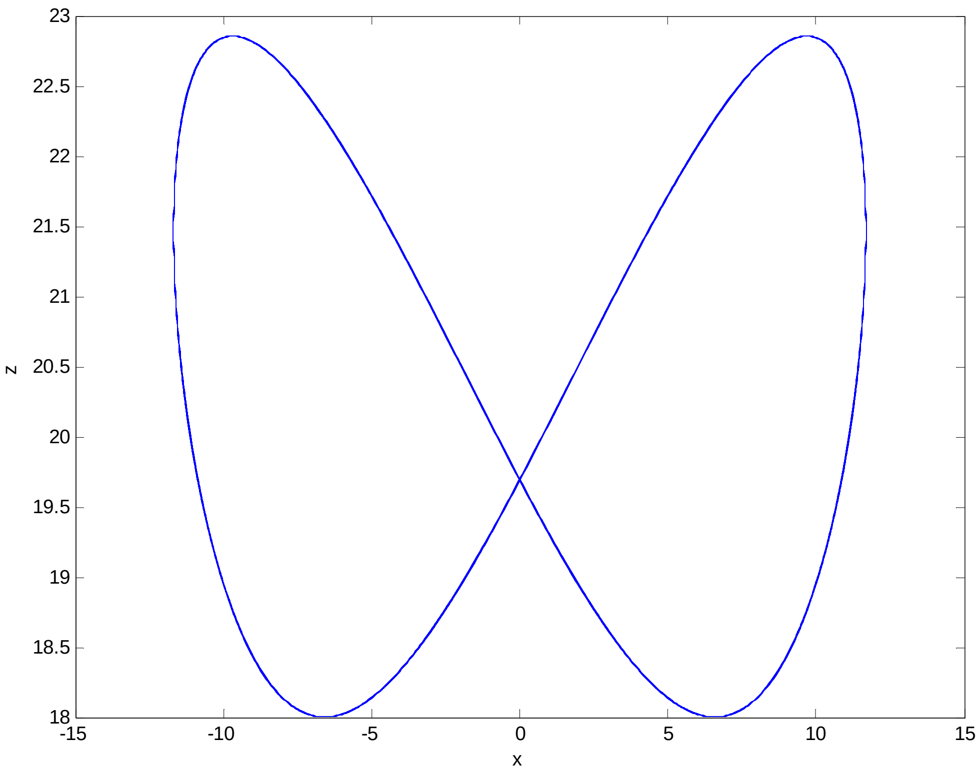

Fig.2.3.4(d) 2D(xz) phase portrait for unified chaotic system with $\alpha = 1.7$.

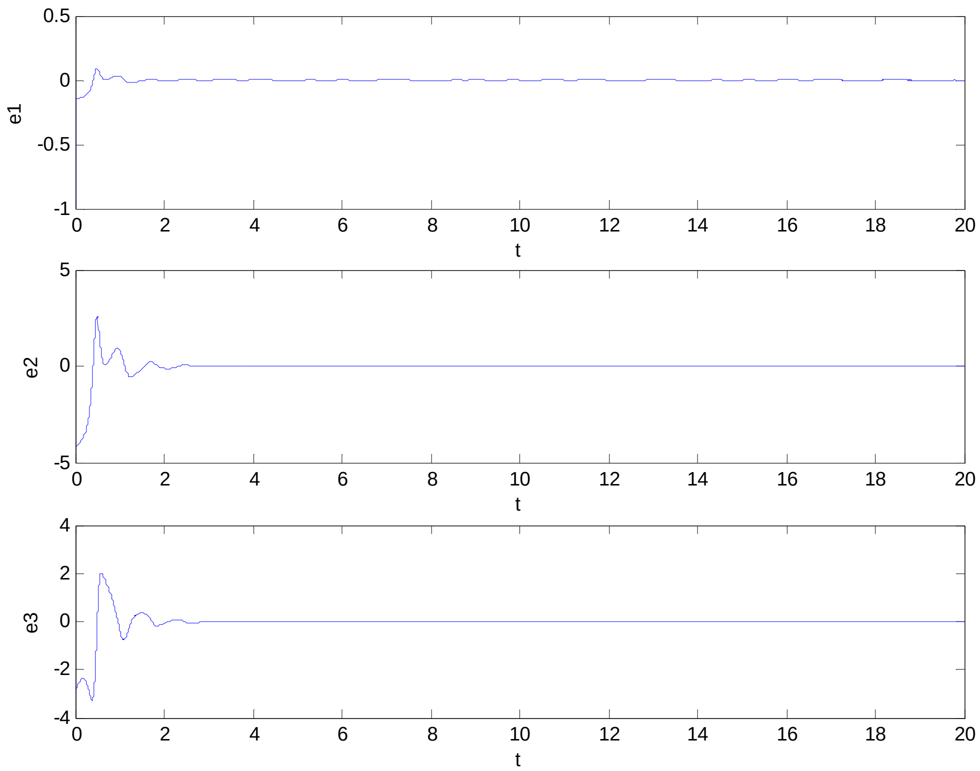

Fig.3.1.1(a) Time history of errors with $\alpha = 0 \quad k_1 = 270$.

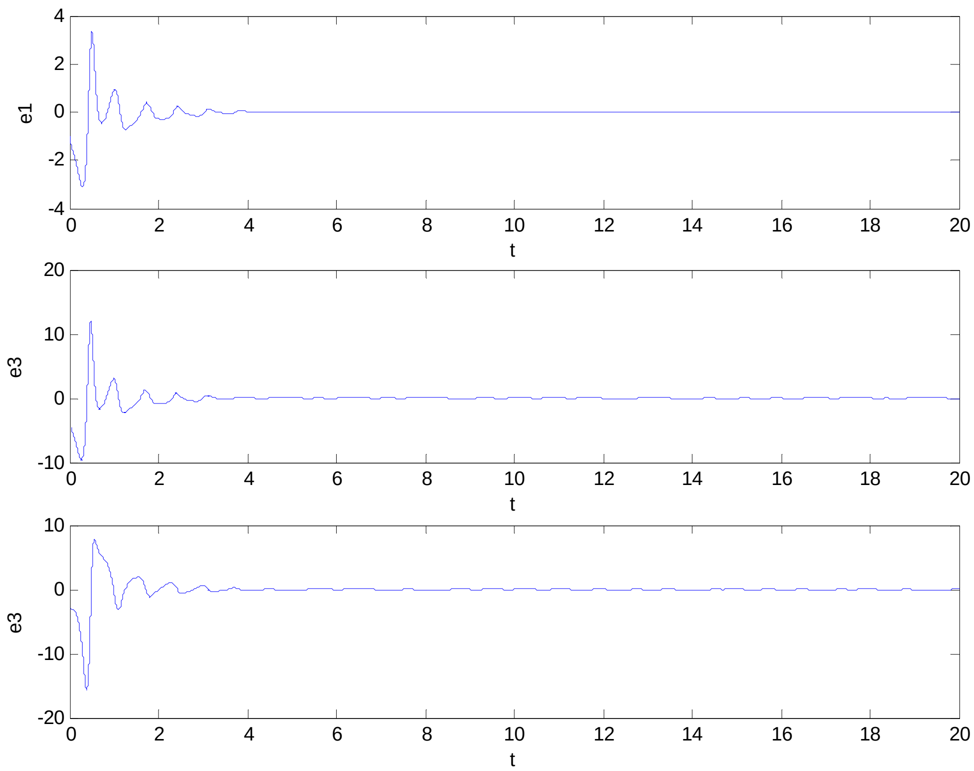

Fig.3.1.1(b) Time history of errors with $\alpha = 0$ $k_1 = 20$.

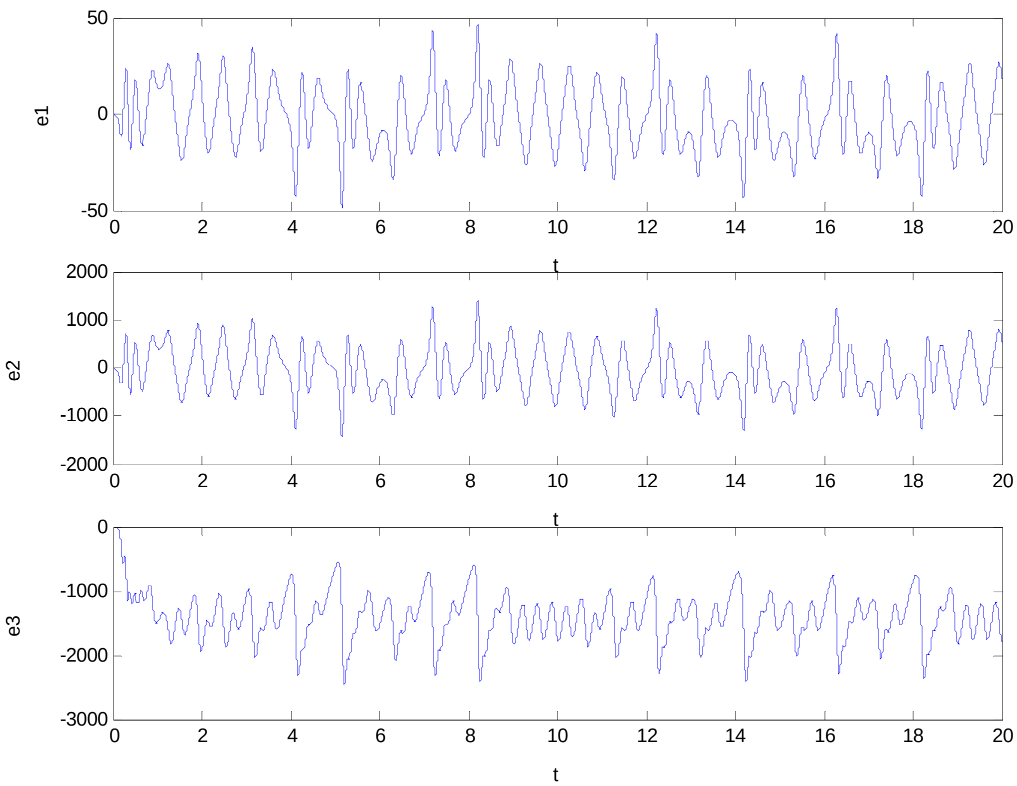

Fig.3.1.2(a) Time history of errors with $\alpha = 1$ $k_1 = 1000$ t=20.

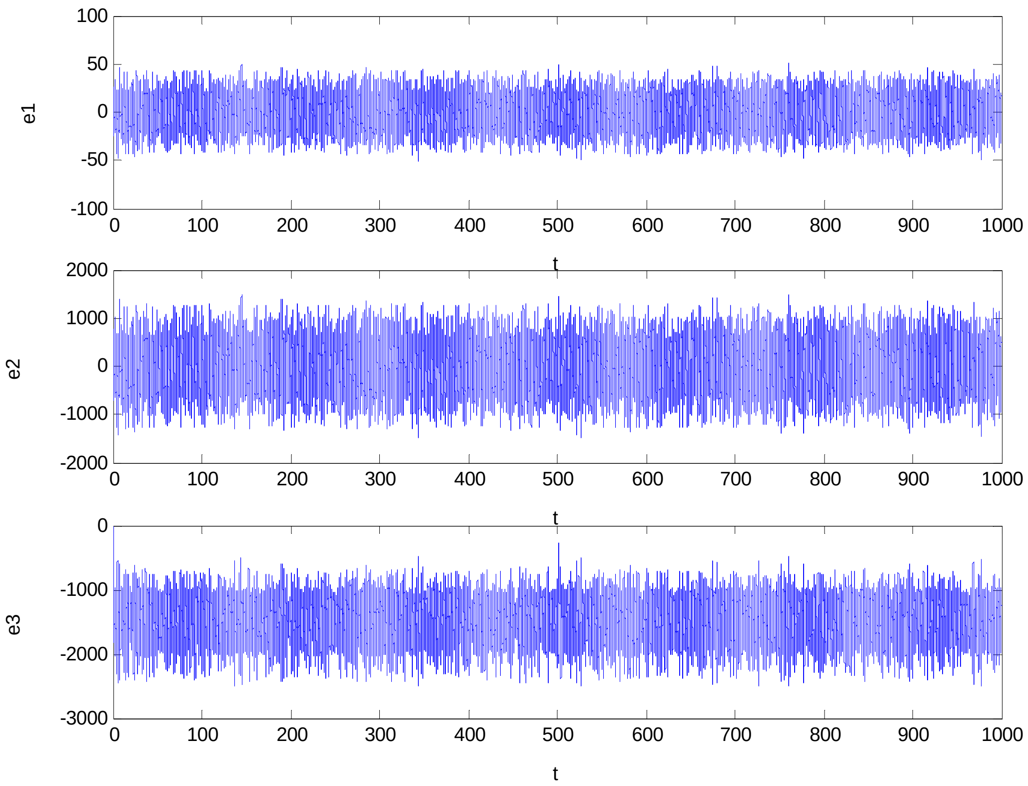

Fig.3.1.2(b) Time history of errors with $\alpha = 1$ $k_1 = 1000$ t=1000.

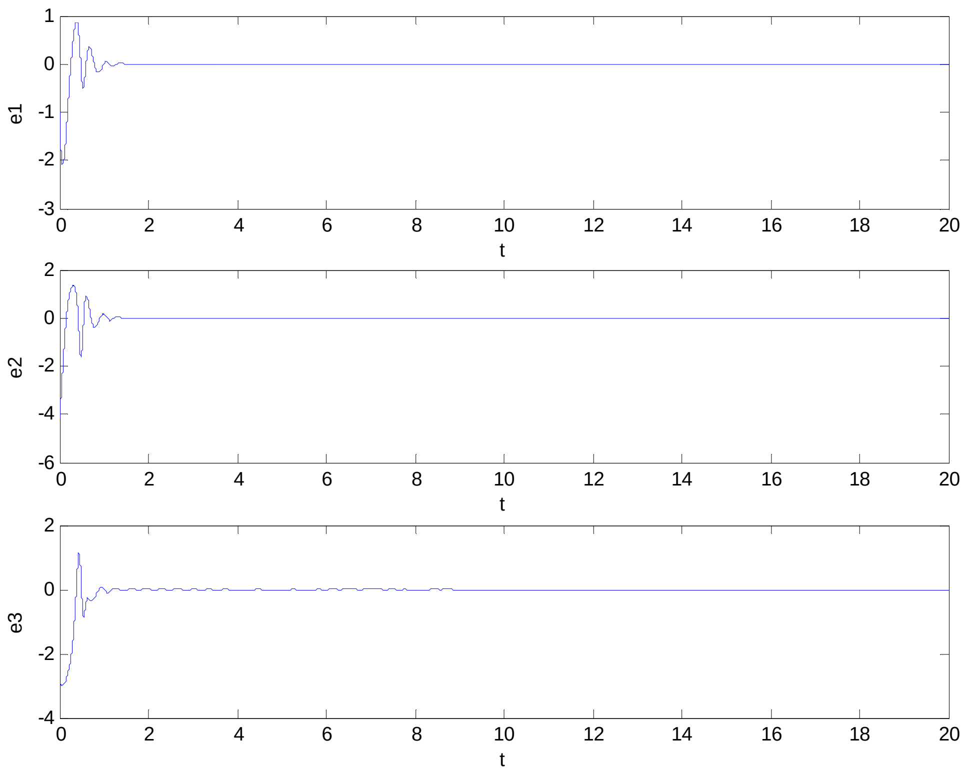

Fig.3.1.3(a) Time history of errors with $\alpha = 0$ $k_2 = 30$.

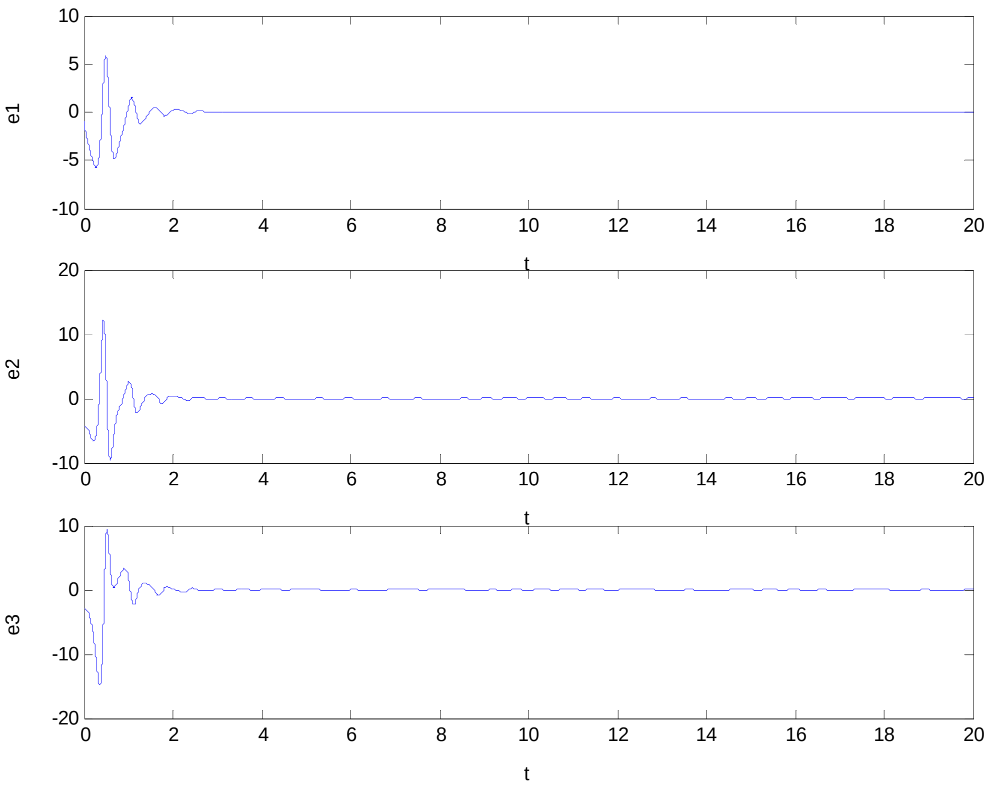

Fig.3.1.3(b) Time history of errors with $\alpha = 0 \quad k_2 = 10$.

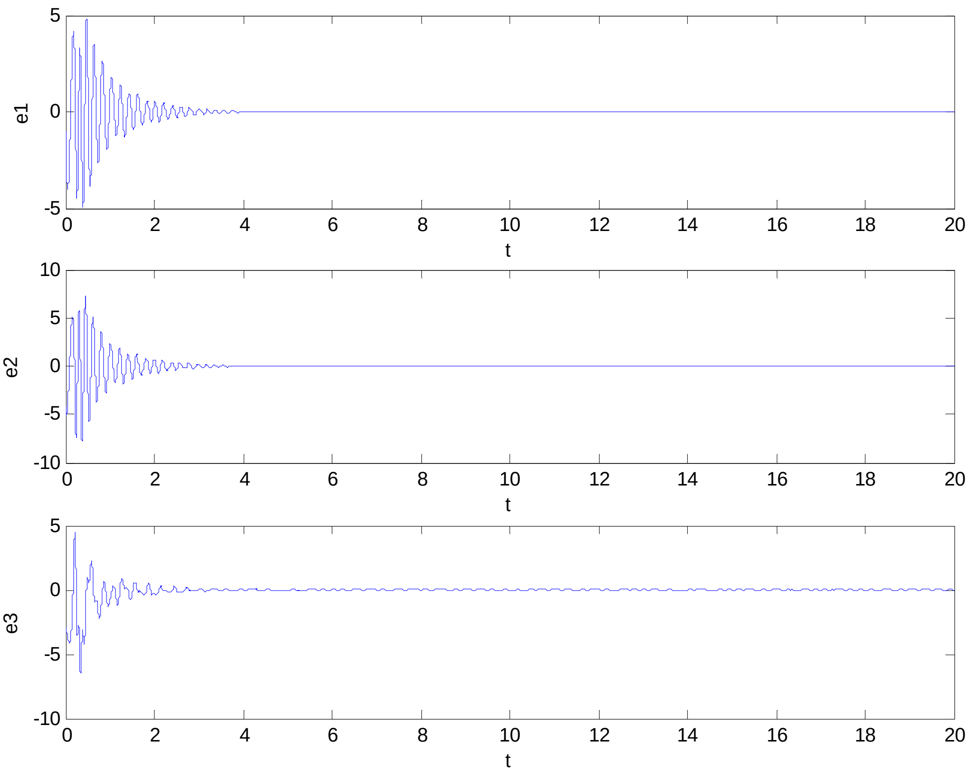

Fig.3.1.4(a) Time history of errors with $\alpha = 1 \quad k_2 = 25$.

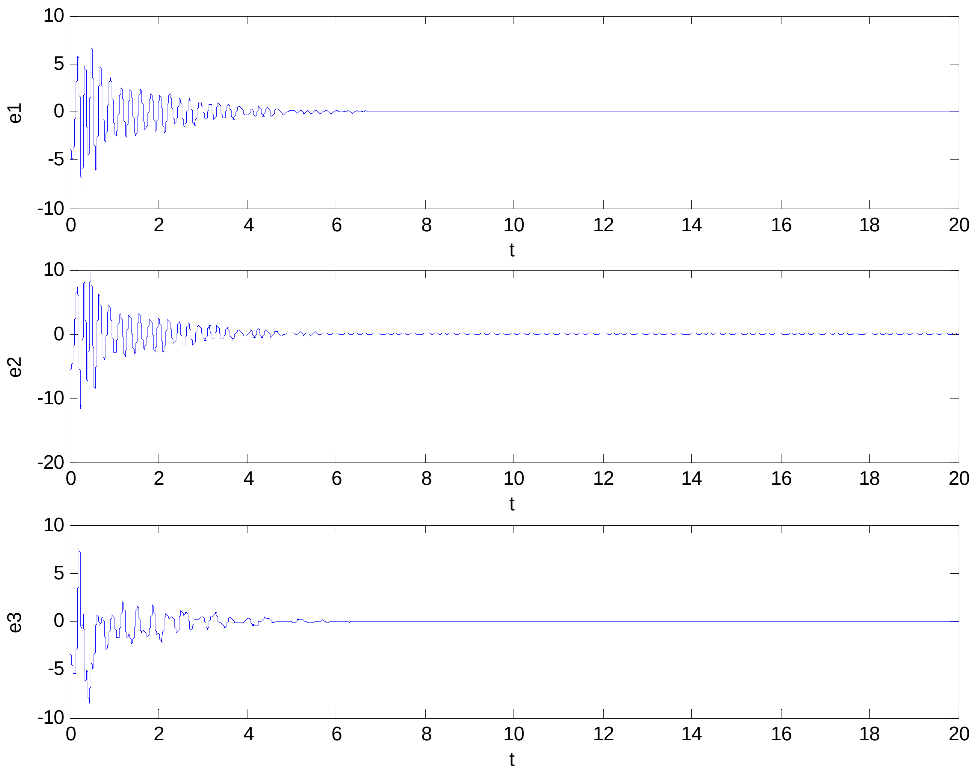

Fig.3.1.4(b) Time history of errors with $\alpha = 1$ $k_2 = 18$.

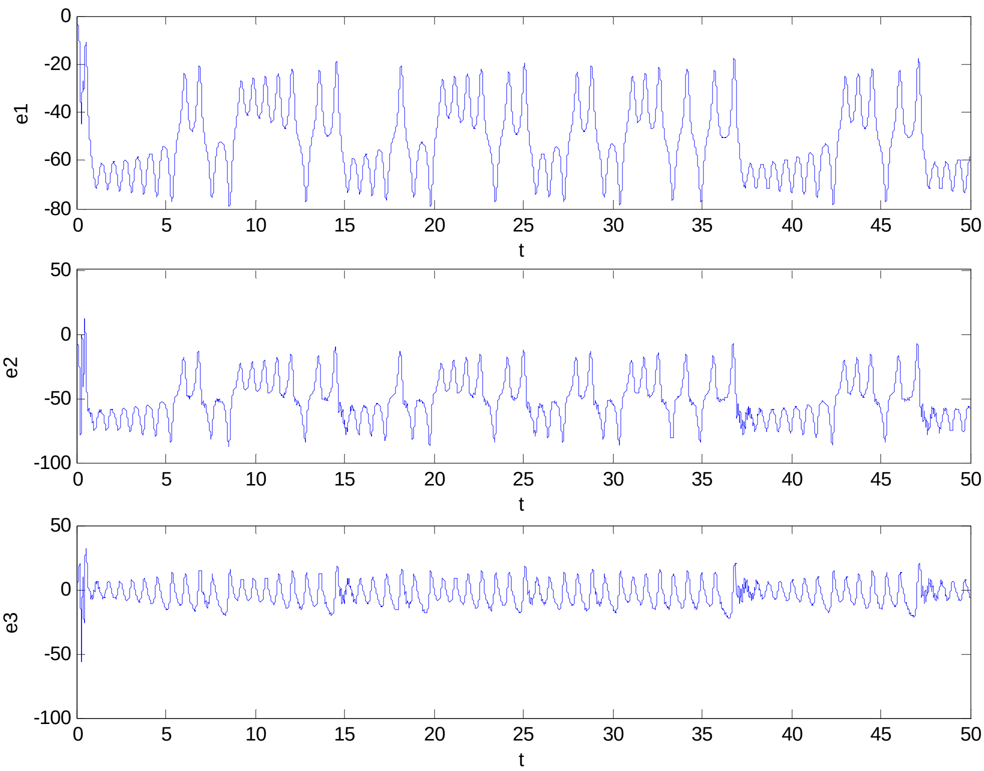

Fig.3.1.5(a) Time history of errors with $\alpha = 0$ $k_3 = 50$.

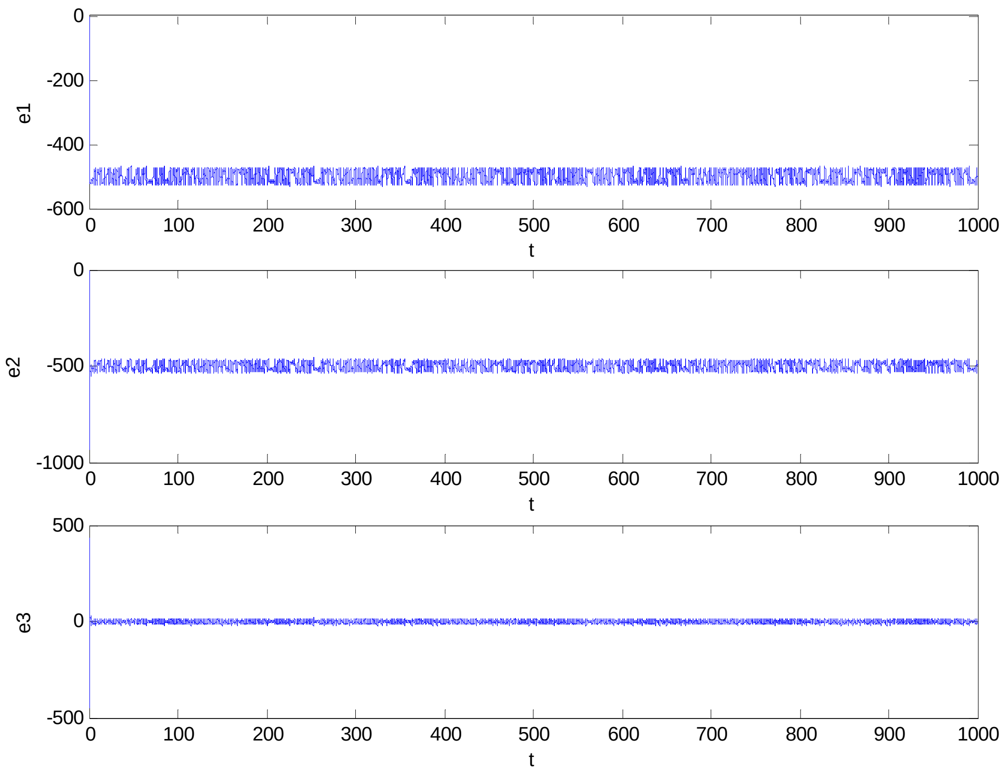

Fig.3.1.5(b) Time history of errors with $\alpha = 0 \quad k_3 = 500$.

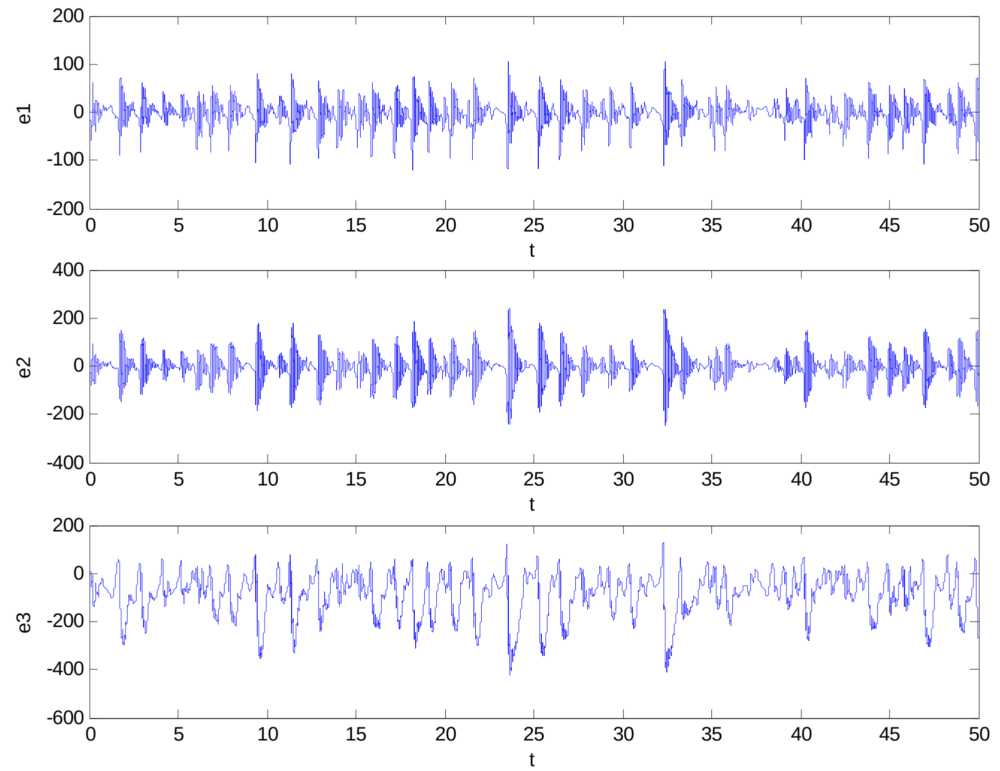

Fig.3.1.5(c) Time history of errors with $\alpha = 1 \quad k_3 = 50$.

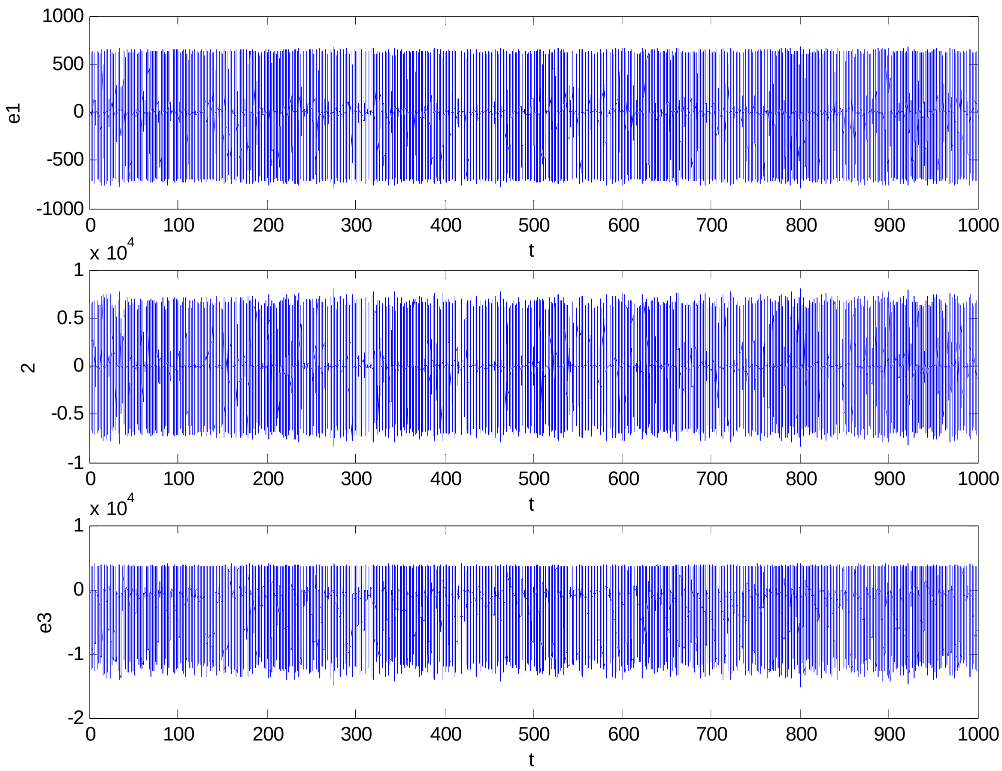

Fig.3.1.5(d) Time history of errors with $\alpha = 1$ $k_3 = 500$.

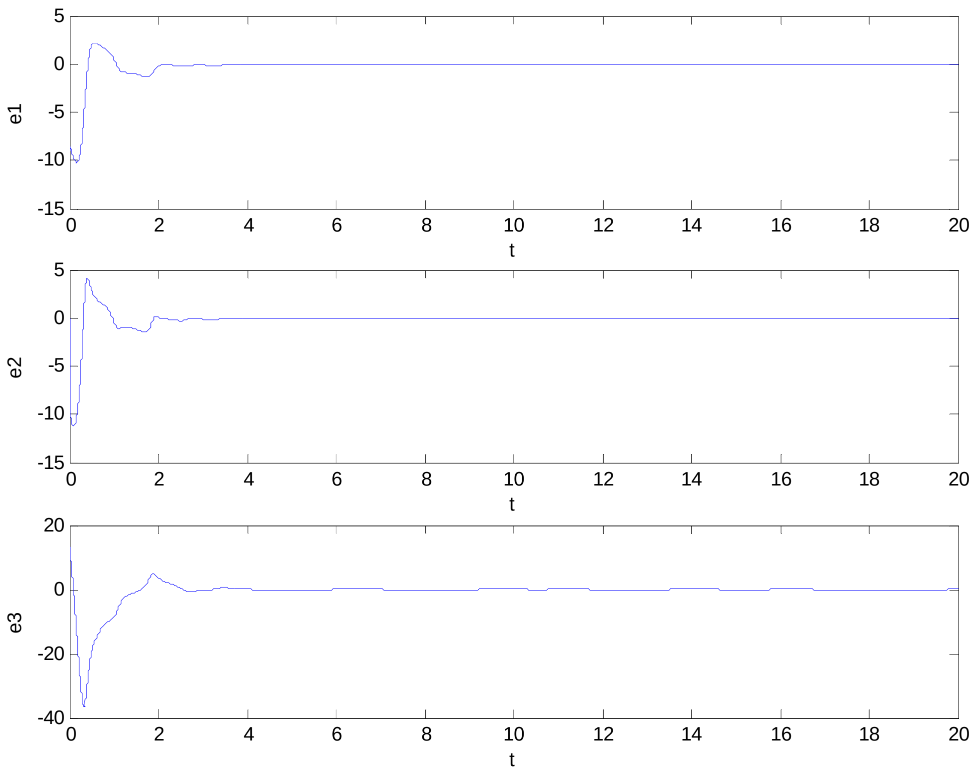

Fig.3.2.1 Time history of errors with $\alpha = 0$ $G = 10$.

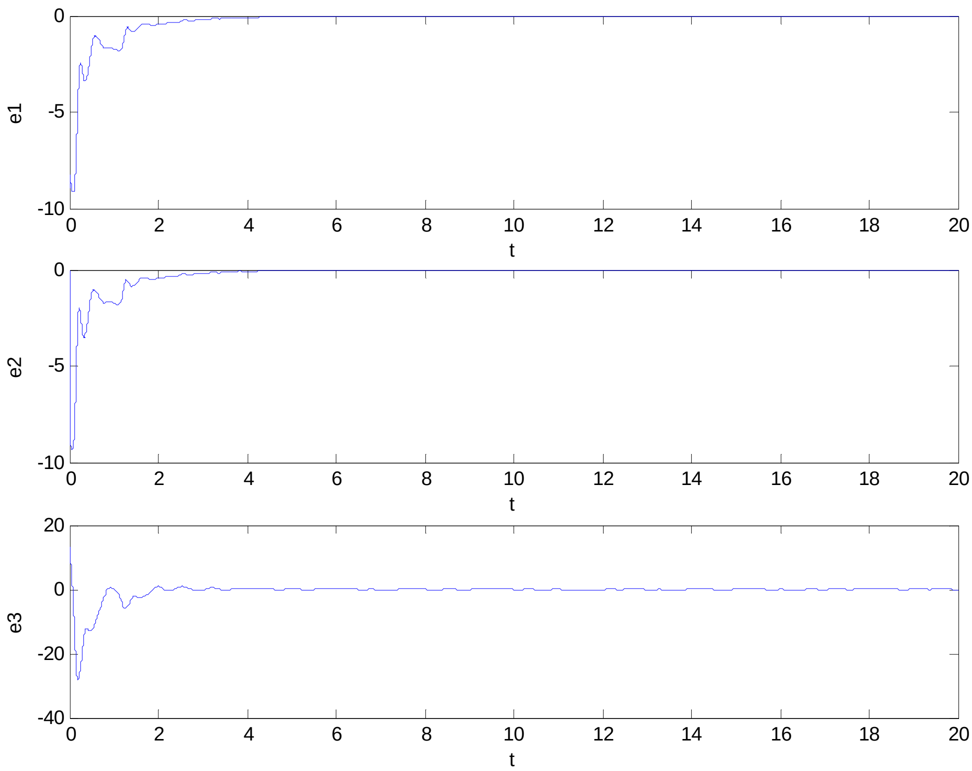

Fig.3.2.2 Time history of errors with $\alpha = 1 \quad G = 10$.

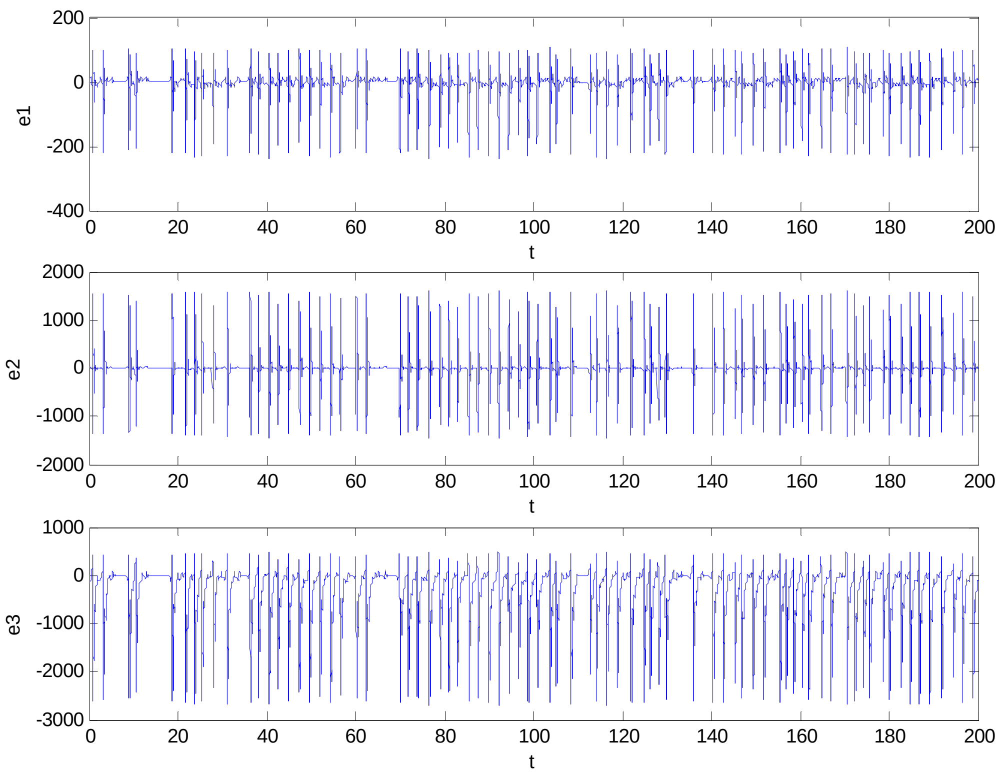

Fig.3.2.3 Time history of errors with $\alpha = 0 \quad G = 10$.

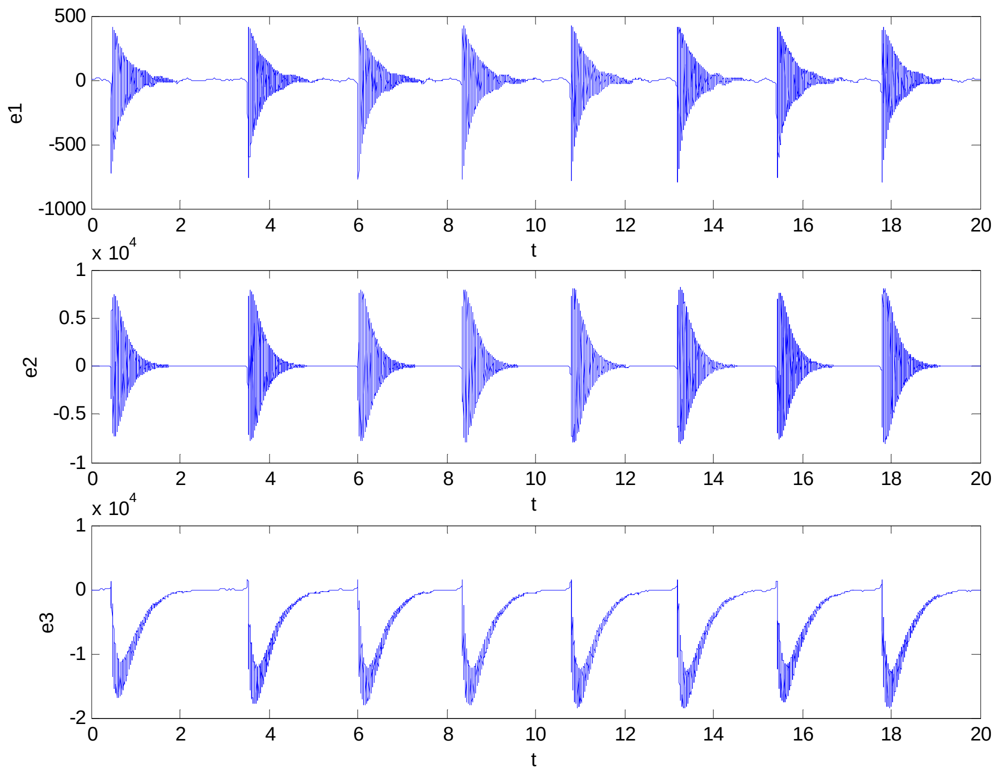

Fig.3.2.4 Time history of errors with $\alpha = 1$ $G = 10$.

α	0	0.05	0.10	0.15	0.20	0.25	0.30	0.35	0.40	0.45	0.50
G	3.47	0.67	0.43	0.38	0.39	0.39	0.38	0.43	0.44	0.33	0.30

α	0.55	0.60	0.65	0.70	0.75	0.80	0.85	0.90	0.95	1.00	1.05
G	0.33	0.31	0.26	0.28	0.26	0.35	0.19	0.23	0.19	0.17	0.13

Table3.3.1 α G value for $\alpha \in [0,1]$, where G is the TLV for synchronization.

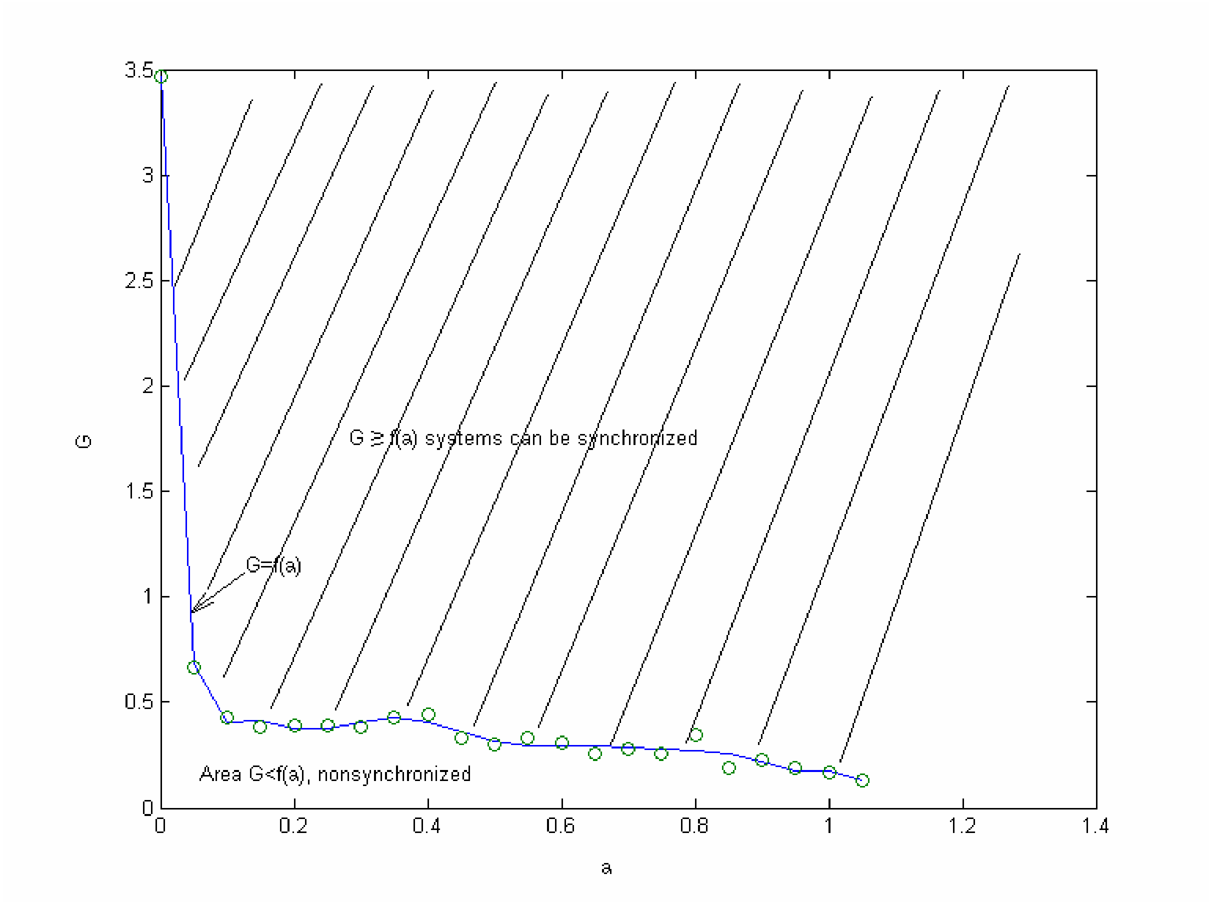

Fig.3.3.1 Curve fitting diagram for $\alpha \in [0,1]$.

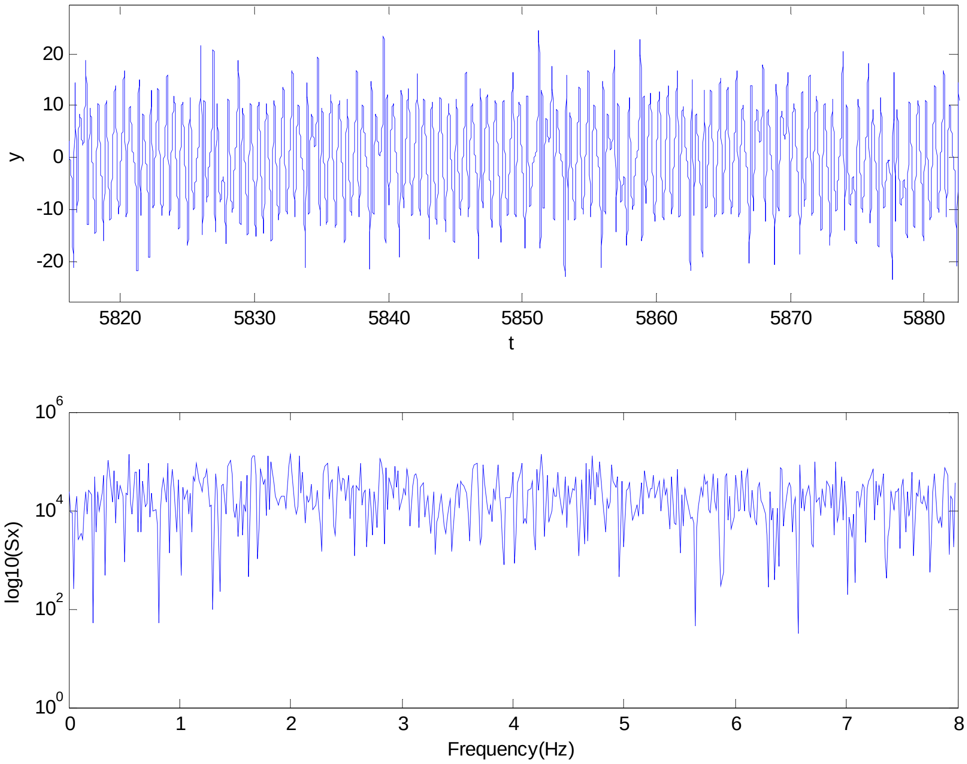

Fig.4.1.1 Power spectrum of unified chaotic system with $\alpha = 1$(Chen system).

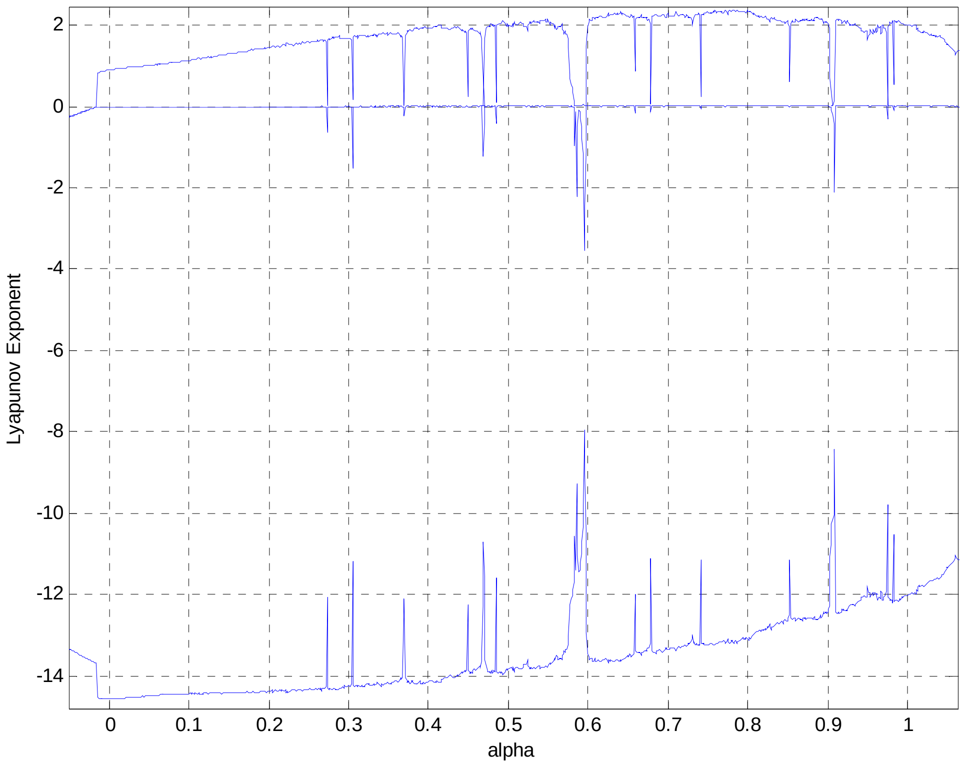

Fig.4.1.2(a) Lyapunov exponents of Unified Chaotic System for α between -1 and 1.

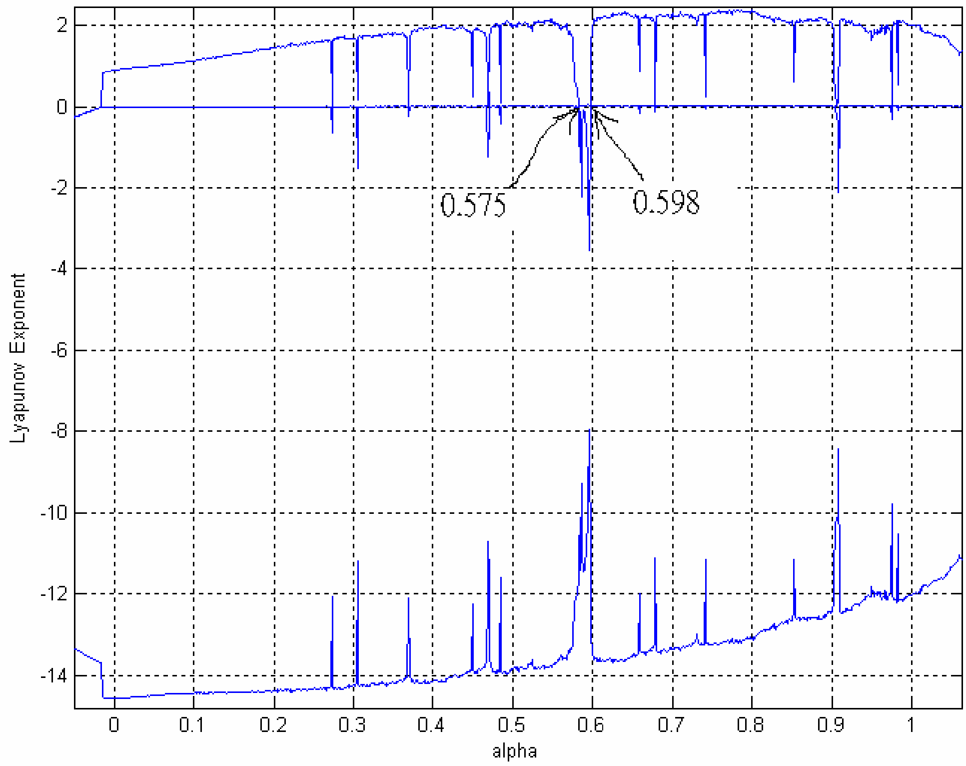

Fig.4.1.2(b) Lyapunov exponents of Unified Chaotic System for α between -1 and 1.

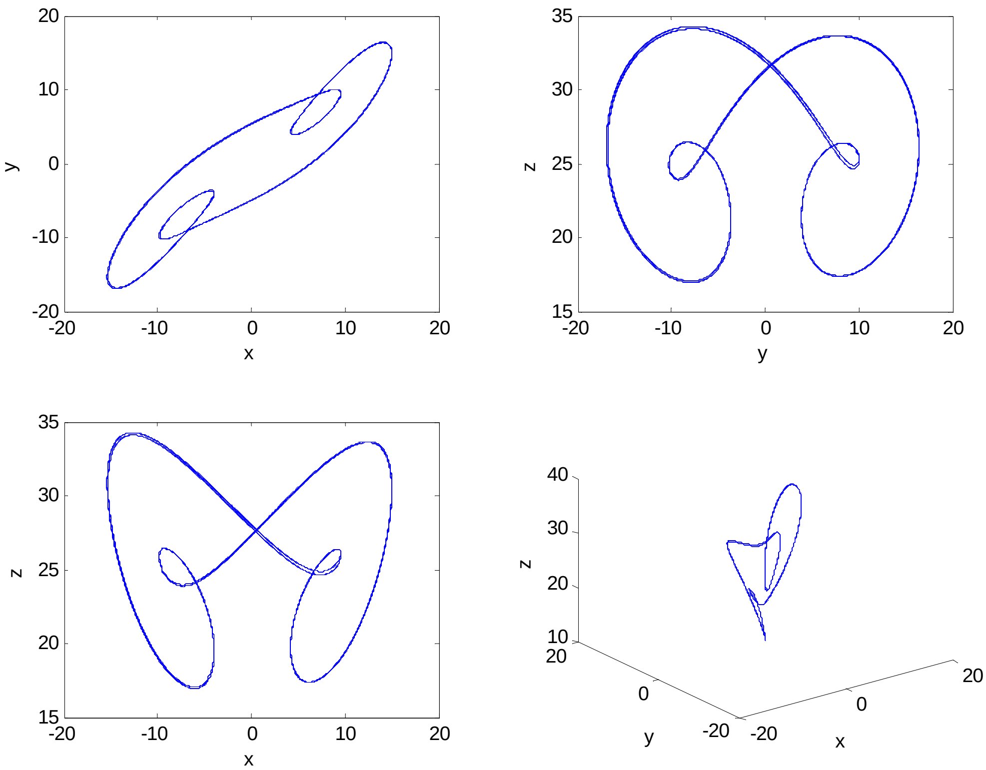

Fig.4.1.3(a) Phase portrait of unified chaotic system with $\alpha = 0.583$.

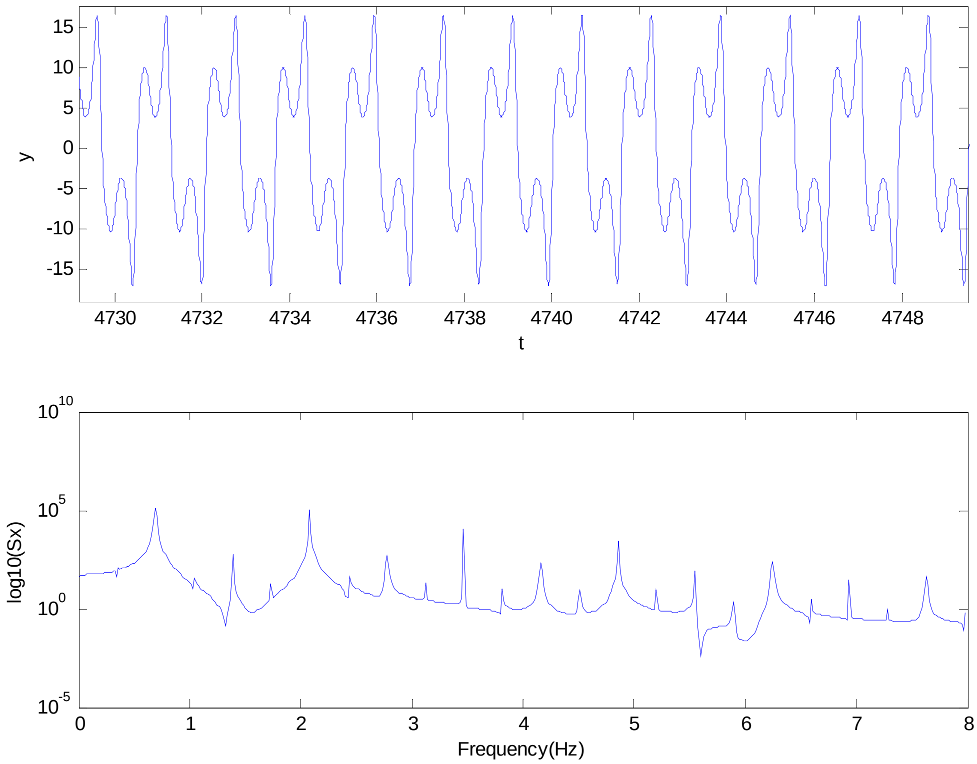

Fig.4.1.3(b) Power spectrum of unified chaotic system with $\alpha = 0.583$.

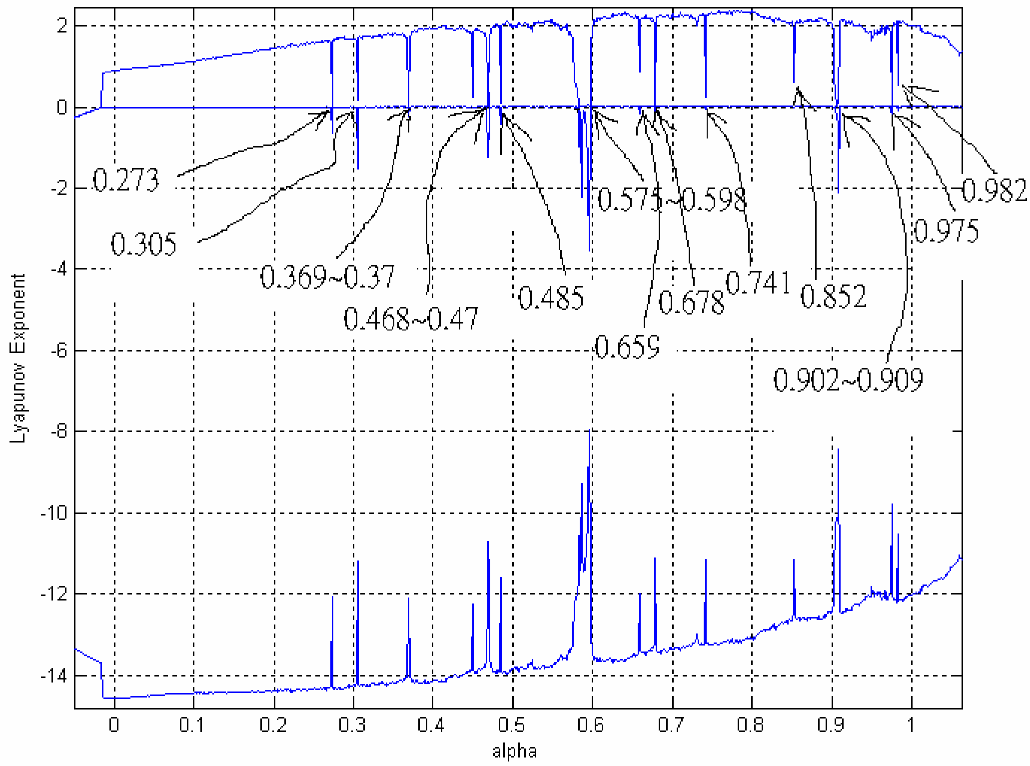

Fig. 4.1.4 Some non-chaotic points of unified chaotic system for $\alpha \in [0,1]$.

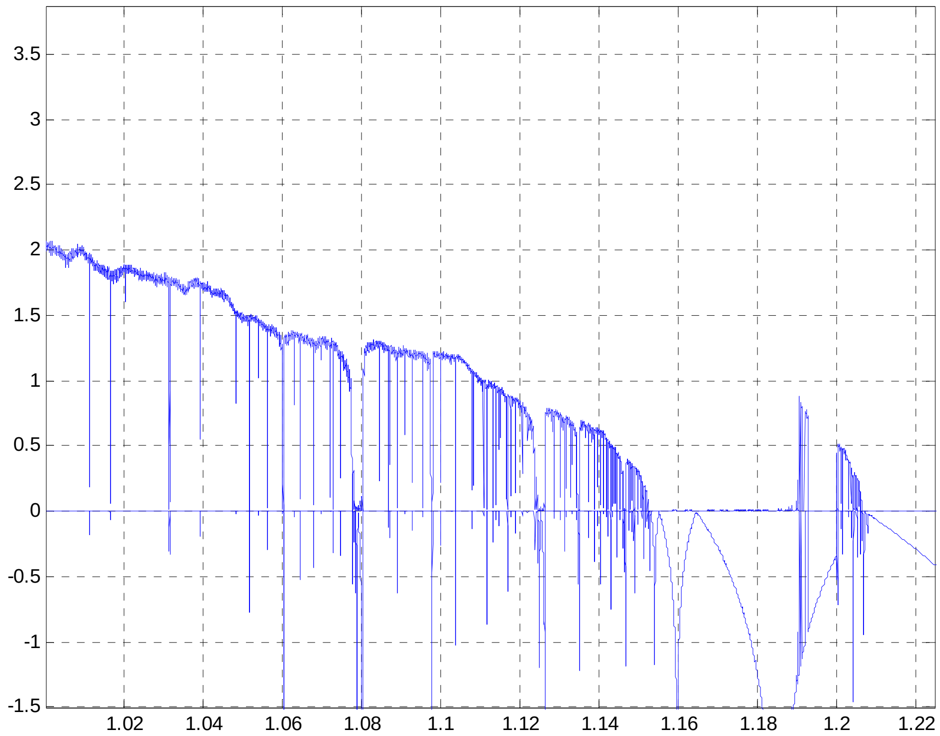

Fig.4.2.1 The magnified part with $\alpha > 1$ of unified chaotic system.

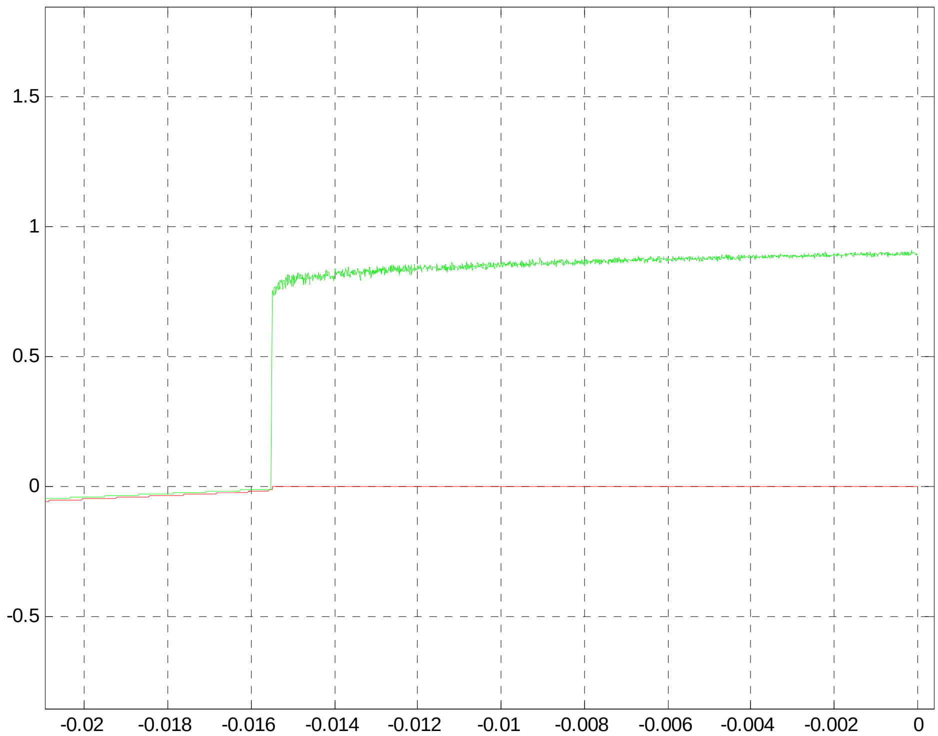

Fig.4.2.2 The magnified part with $\alpha < 0$ of unified chaotic system.

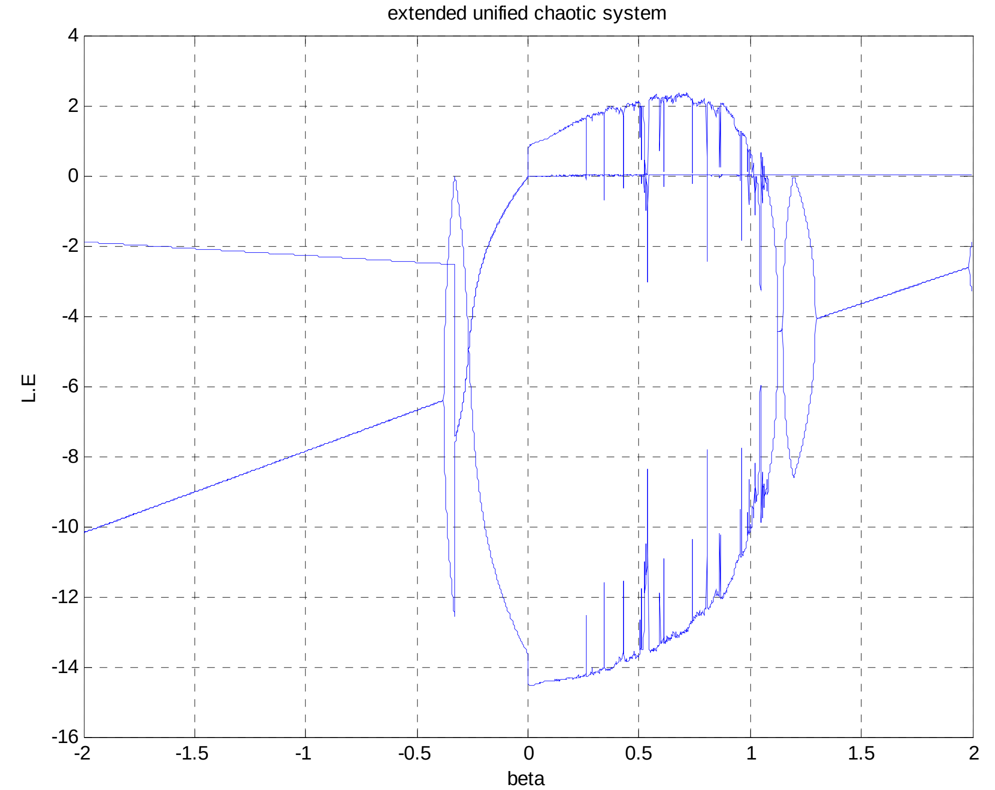

Fig.4.3.1 Lyapunov exponent of extended unified chaotic system.

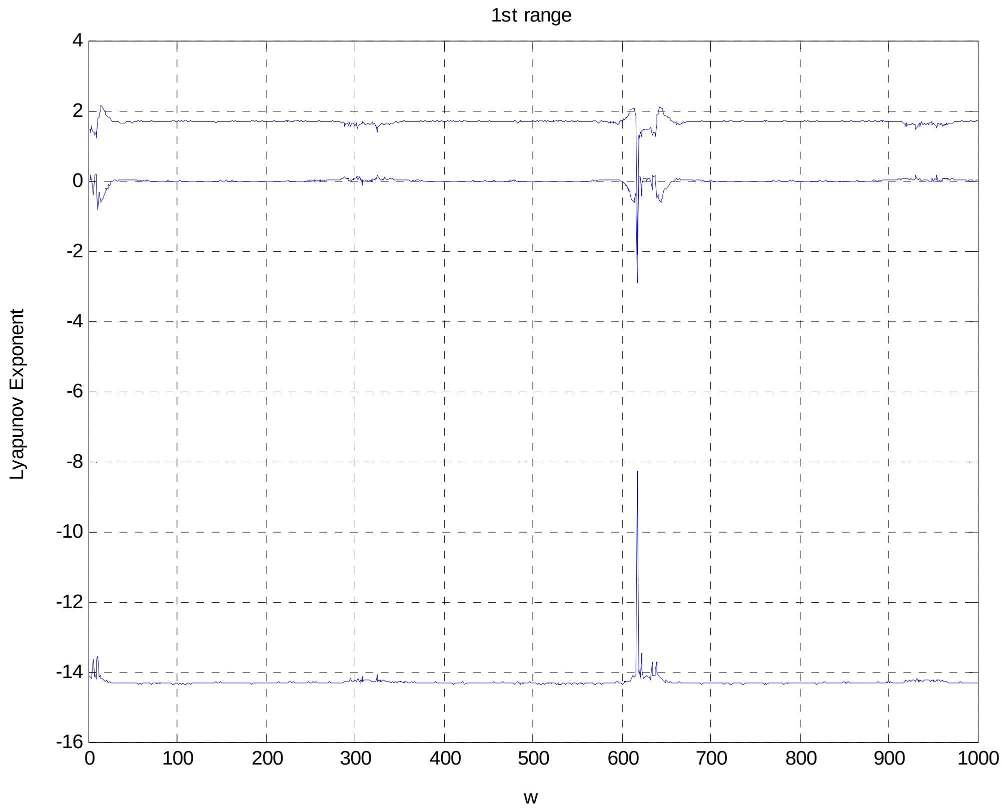

Fig. 4.4.1(a) Lyapunov exponent of extended unified chaotic system($\sin^2 \omega t$).

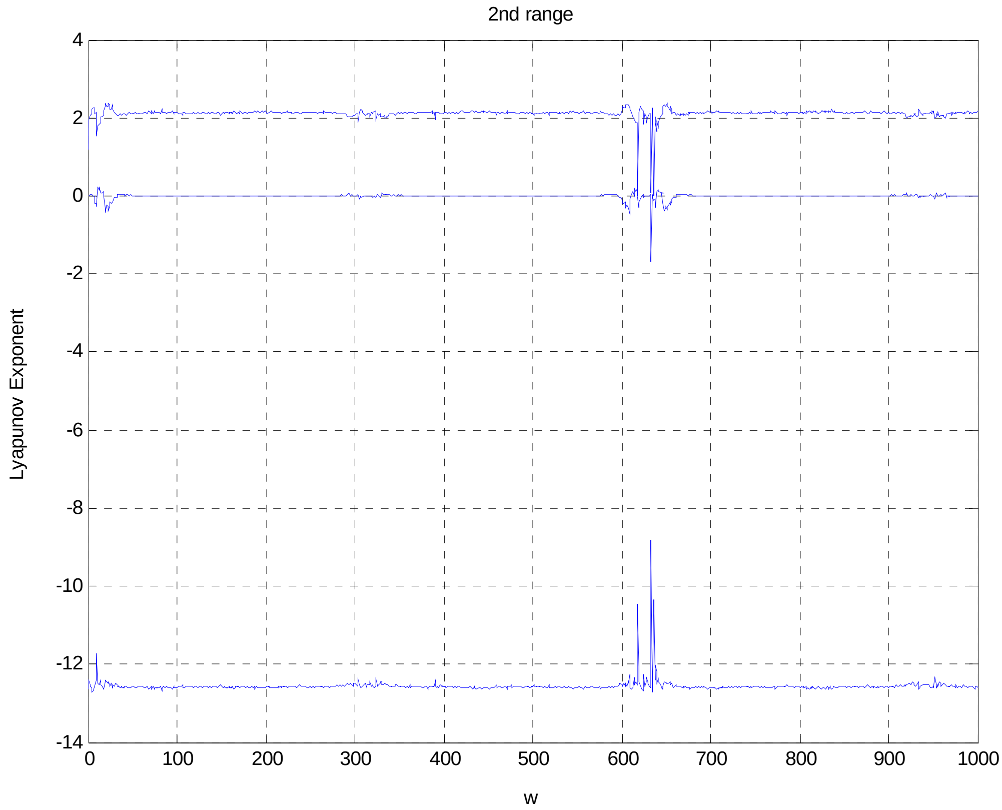

Fig. 4.4.1(b) Lyapunov exponent of extended unified chaotic system($\sin^2 \omega t$).

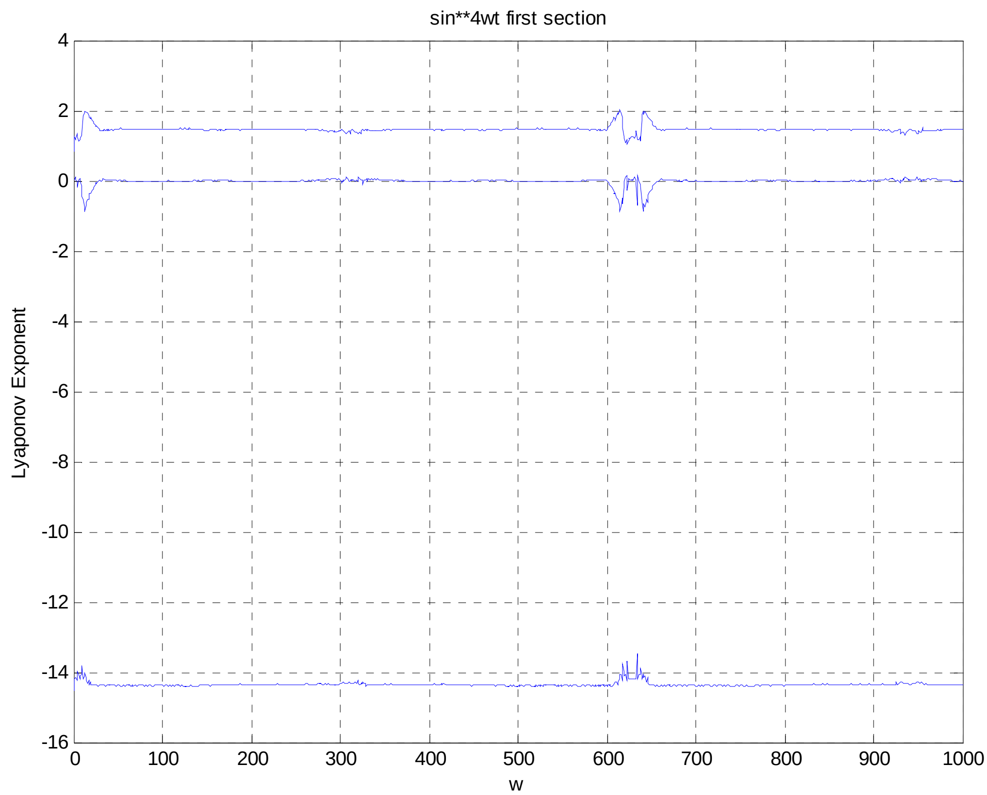

Fig. 4.4.2(a) Lyapunov exponent of extended unified chaotic system($\sin^4 \omega t$).

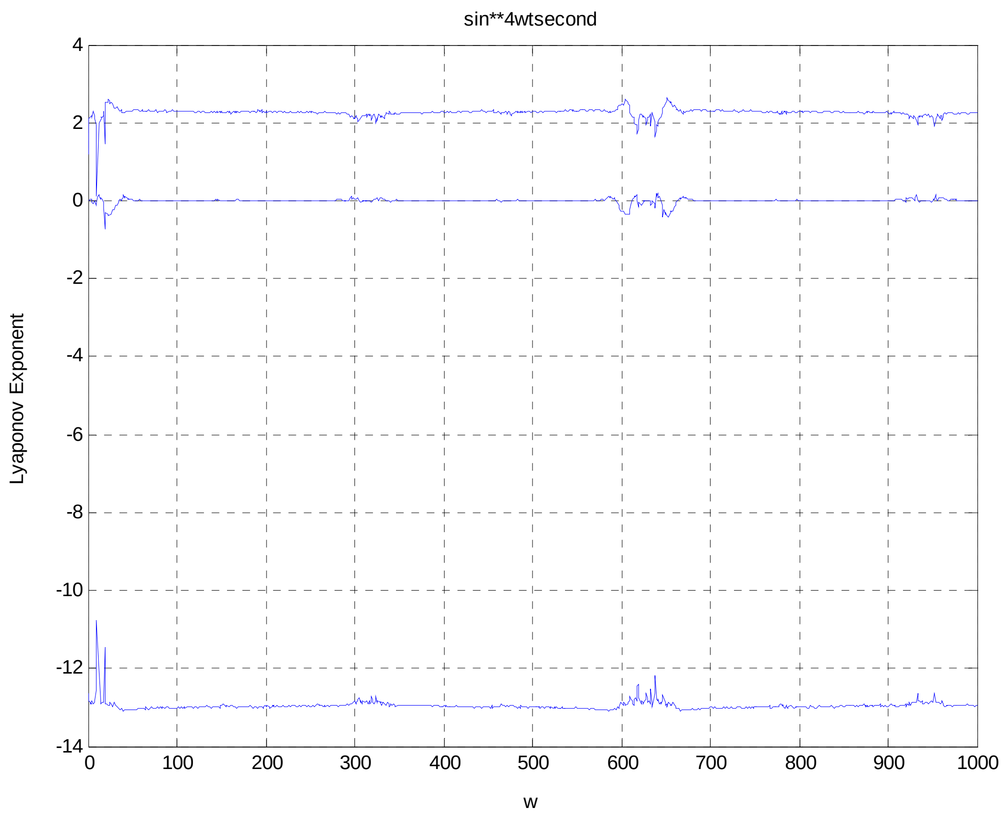

Fig. 4.4.2(b) Lyapunov exponent of extended unified chaotic system($\sin^4 \omega t$).

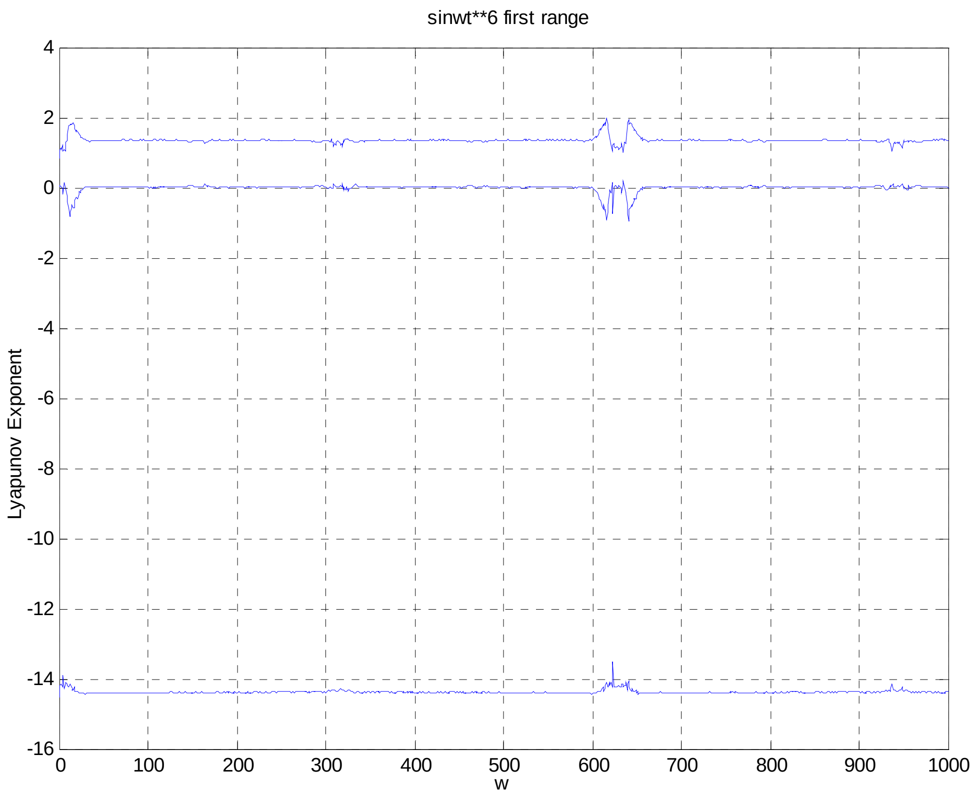

Fig. 4.4.3(a) Lyapunov exponent of extended unified chaotic system($\sin^6 \omega t$).

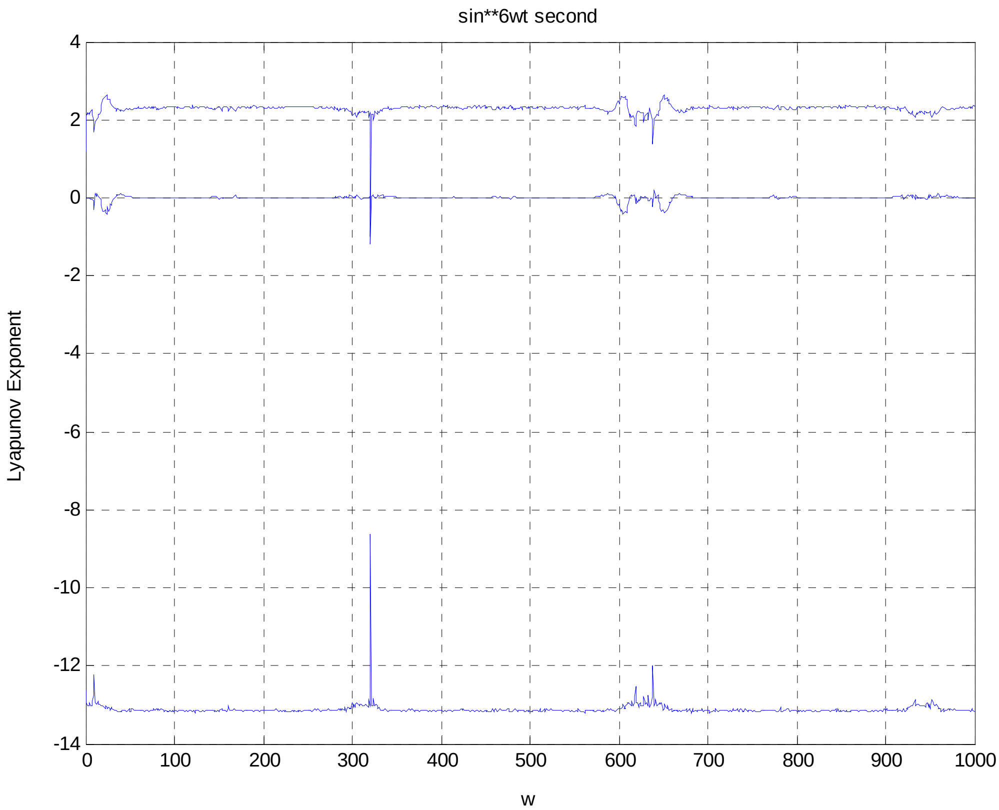

Fig. 4.4.3(b) Lyapunov exponent of extended unified chaotic system($\sin^6 \omega t$).

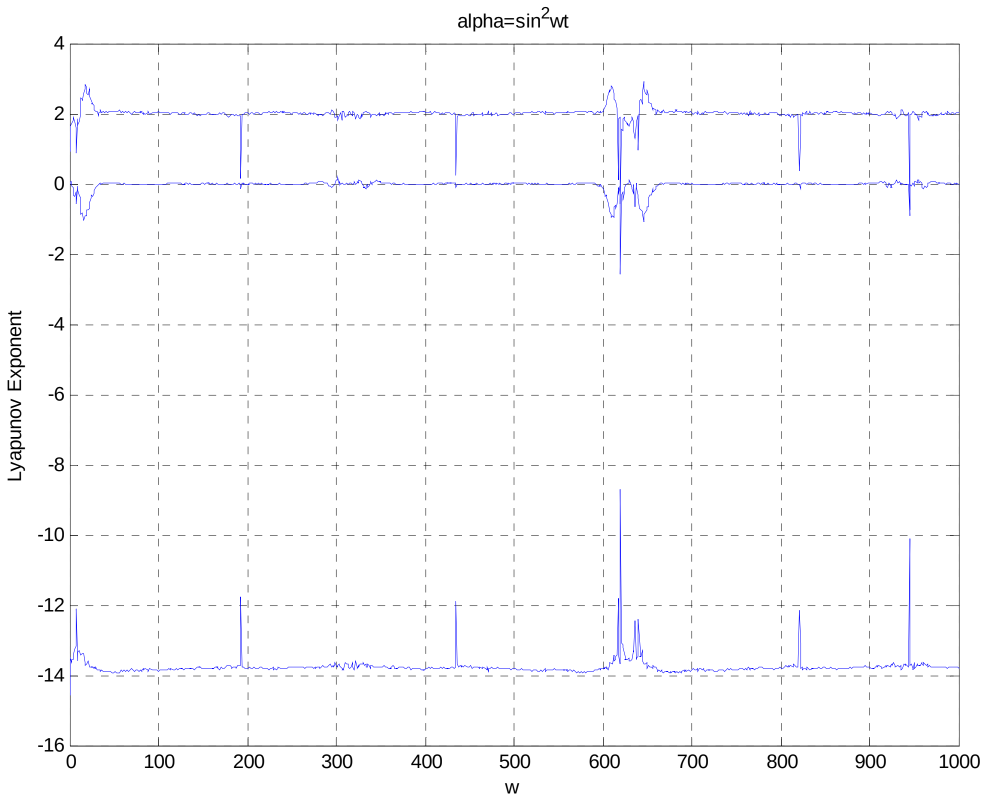

Fig. 5.1.1 Lyapunov exponent of unified chaotic system with $\alpha = \sin^2 \omega t$.

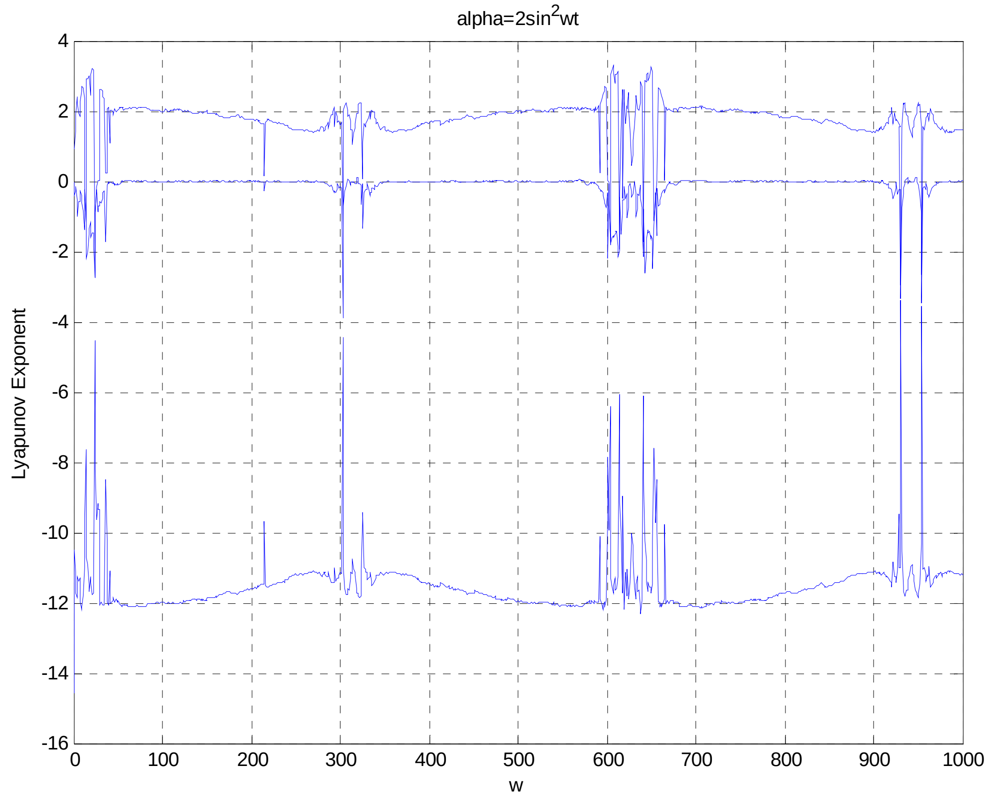

Fig. 5.1.2 Lyapunov exponent of unified chaotic system with $\alpha = 2\sin^2 \omega t$.

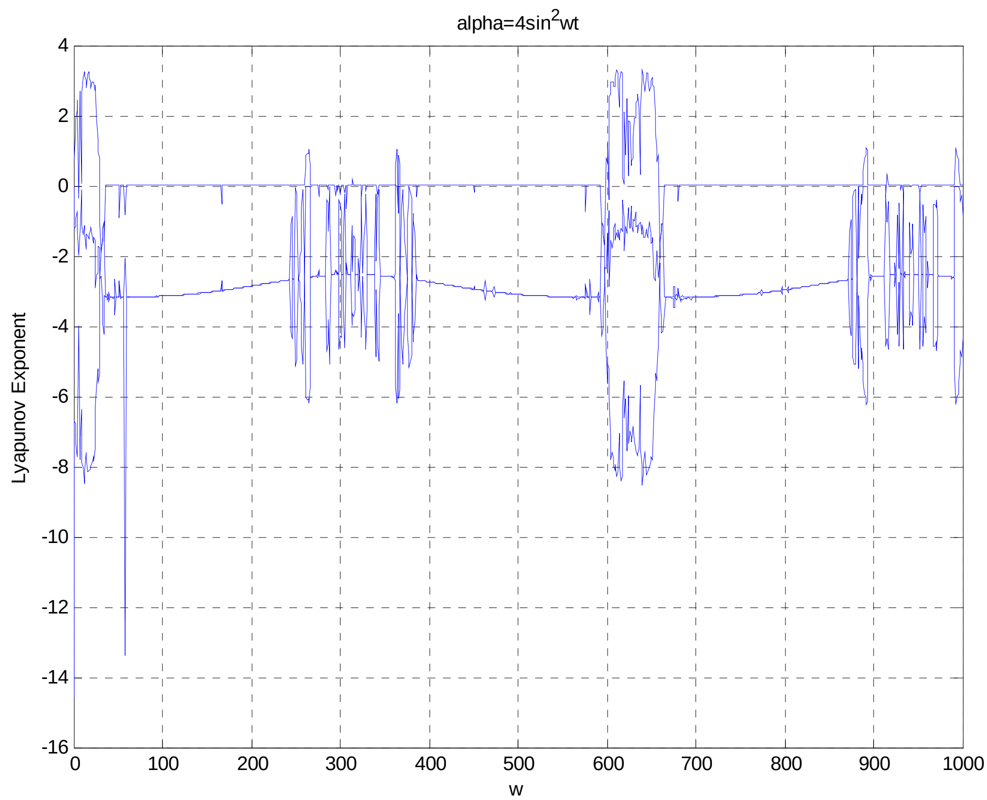

Fig. 5.1.3 Lyapunov exponent of unified chaotic system with $\alpha = 4\sin^2 \omega t$.

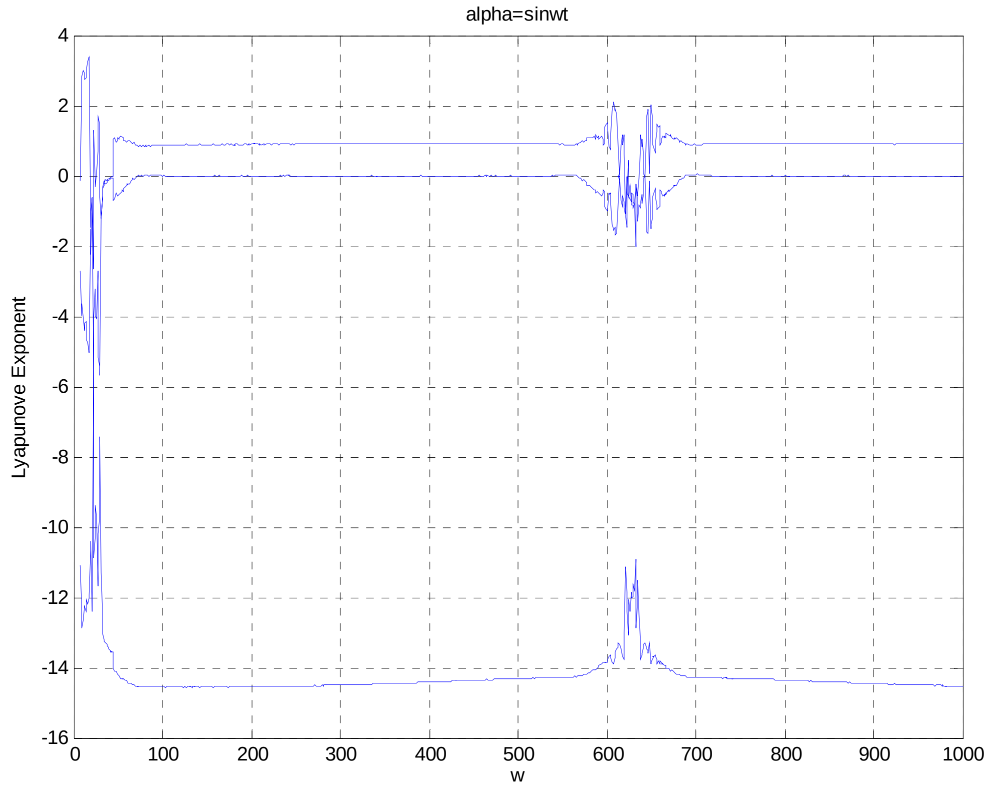

Fig. 5.2.1 Lyapunov exponent of unified chaotic system with $\alpha = \sin \omega t$.

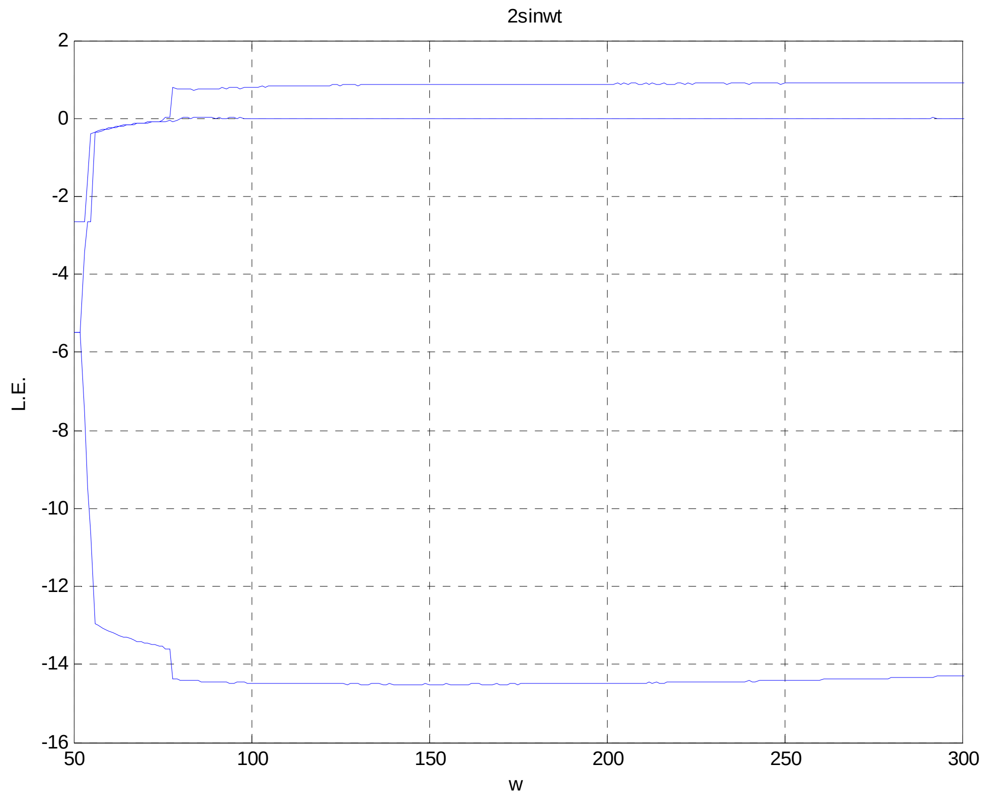

Fig. 5.2.2 Lyapunov exponent of unified chaotic system with $\alpha = 2\sin \omega t$.

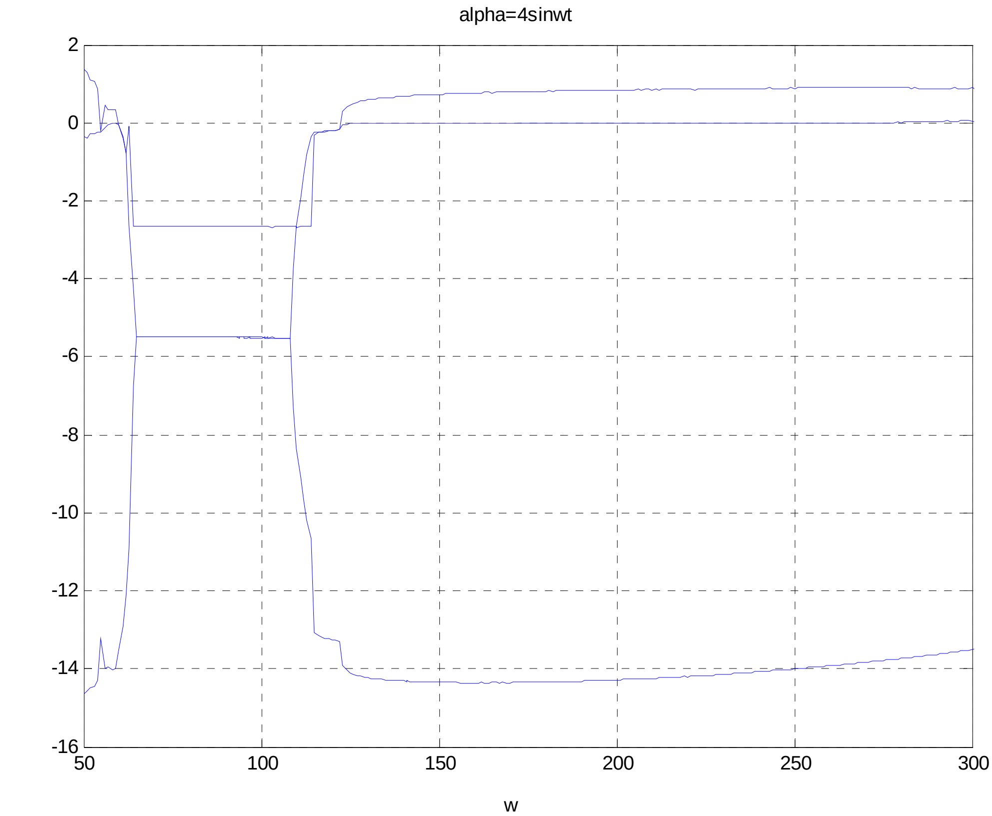

Fig. 5.2.3 Lyapunov exponent of unified chaotic system with $\alpha = 4\sin\omega t$.

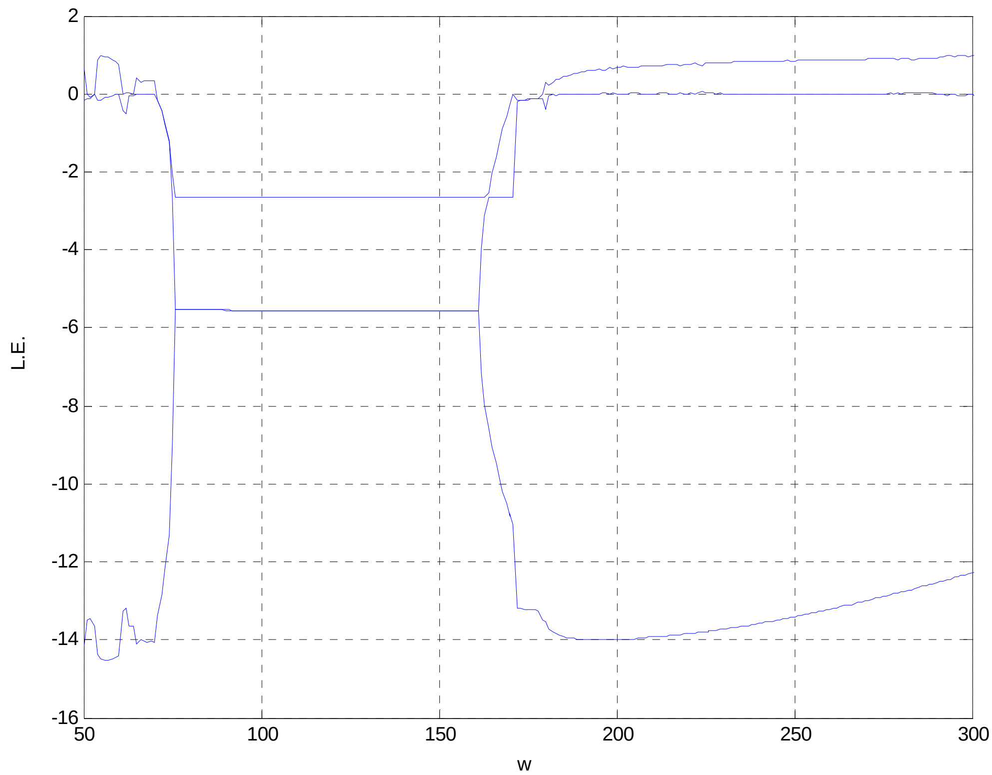

Fig. 5.2.4 Lyapunov exponent of unified chaotic system with $\alpha = 6\sin\omega t$.

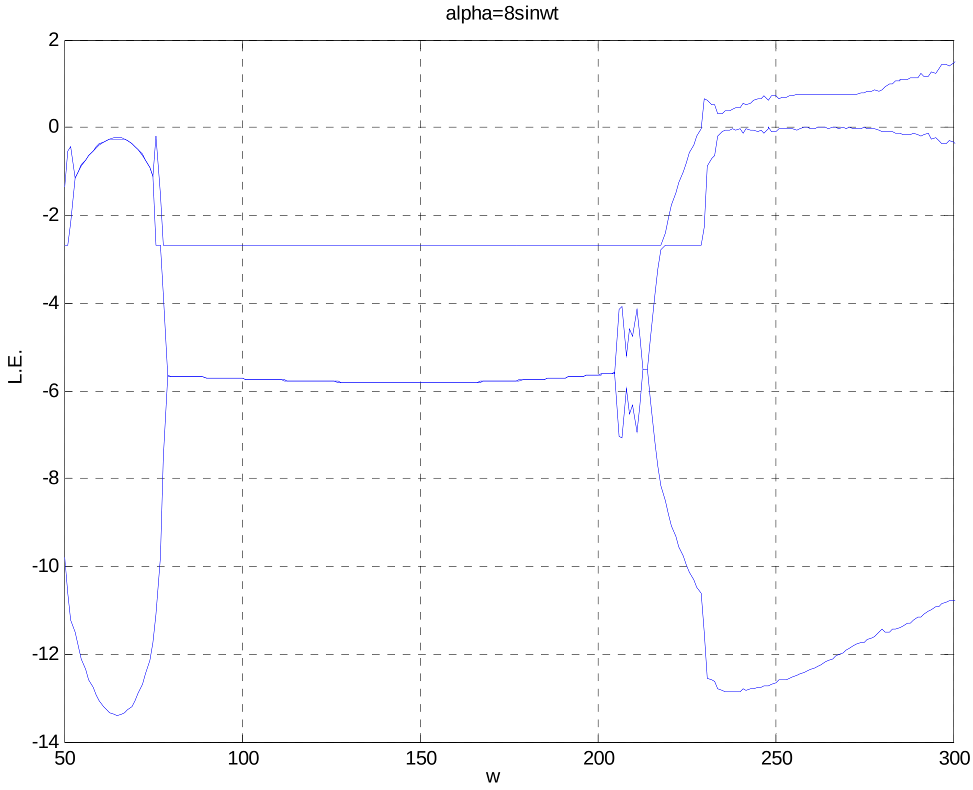

Fig. 5.2.5 Lyapunov exponent of unified chaotic system with $\alpha = 8\sin\omega t$.

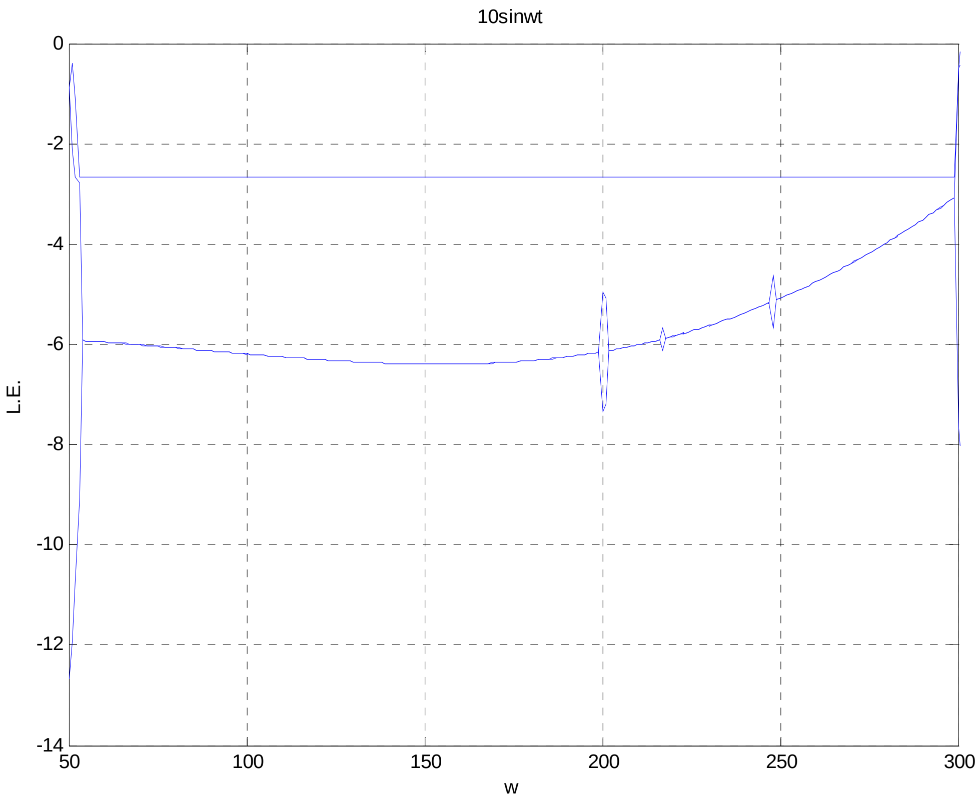

Fig. 5.2.6 Lyapunov exponent of unified chaotic system with $\alpha = 10\sin\omega t$.

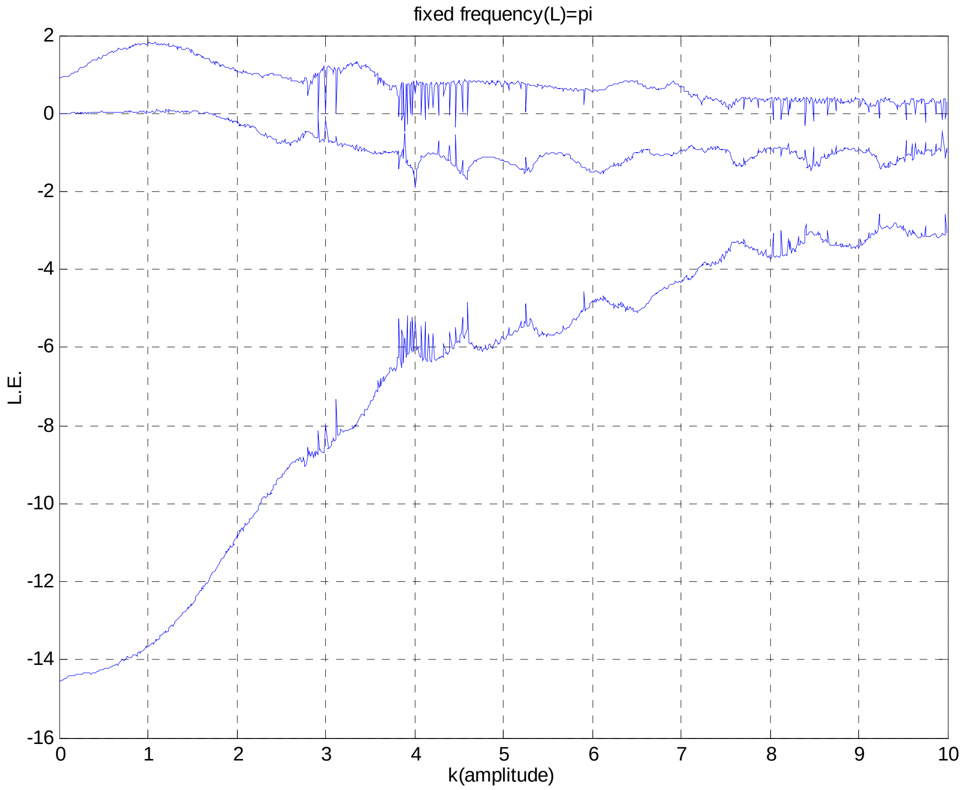

Fig. 5.3.1 Lyapunov exponent of unified chaotic system with $\alpha = f(t)$, $L = \pi$.

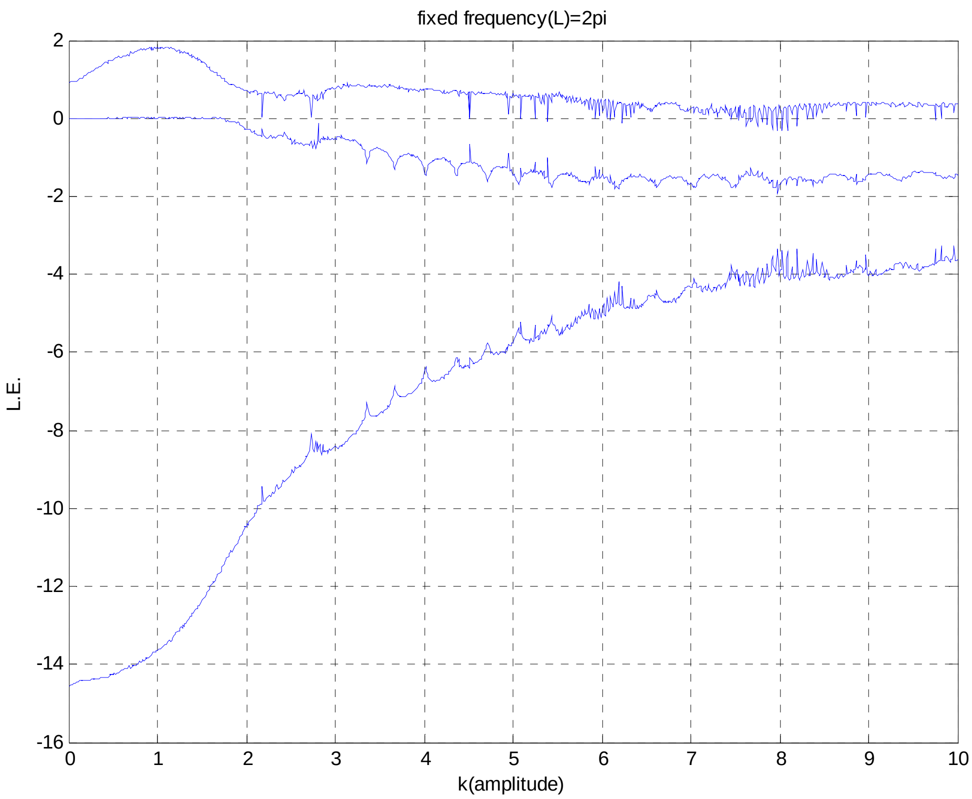

Fig. 5.3.2 Lyapunov exponent of unified chaotic system with $\alpha = f(t)$, $L = 2\pi$.

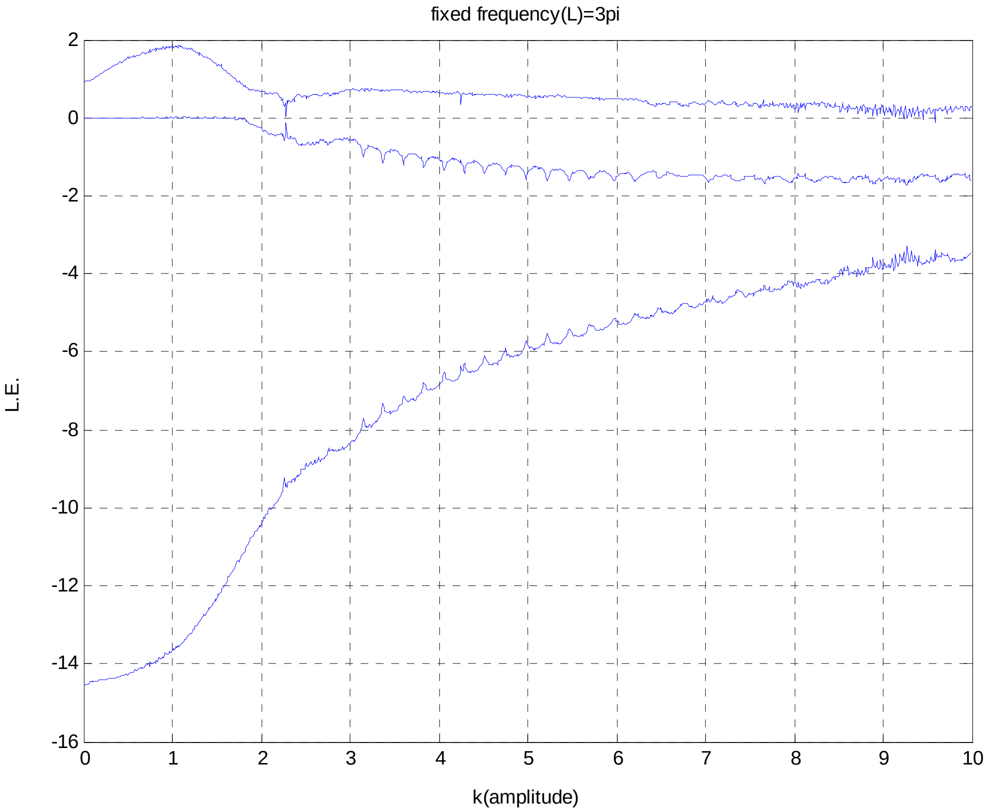

Fig. 5.3.3 Lyapunov exponent of unified chaotic system with $\alpha = f(t)$, $L = 3\pi$.

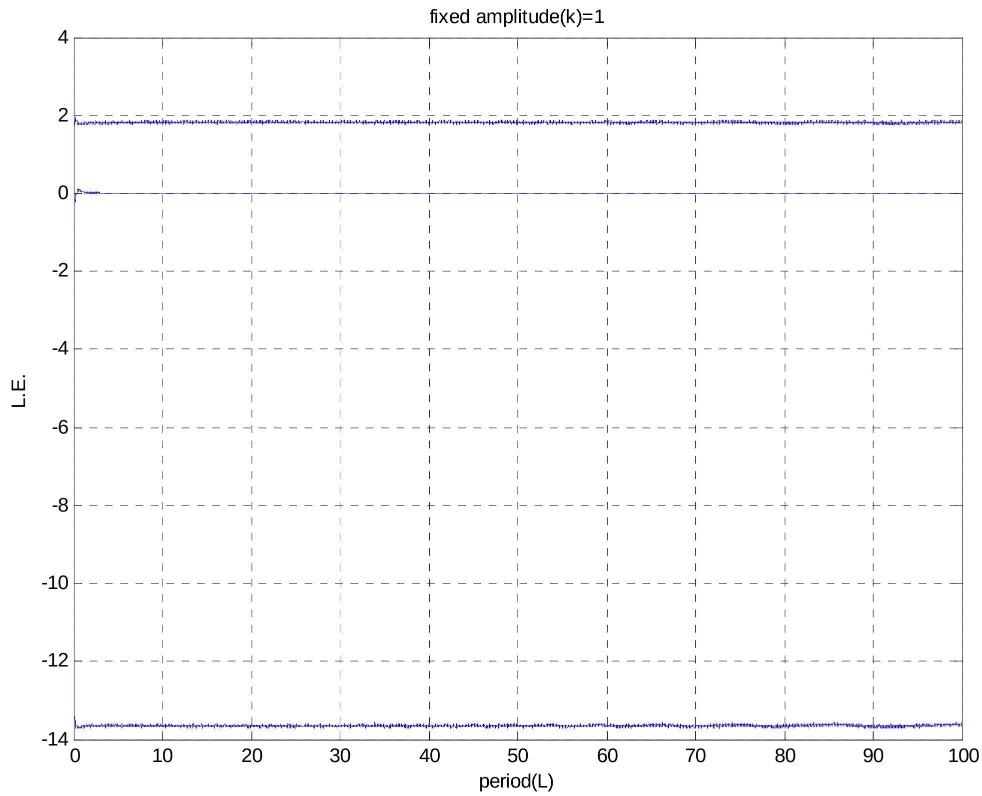

Fig. 5.3.4 Lyapunov exponent of unified chaotic system with $\alpha = f(t)$, $k = 1$.

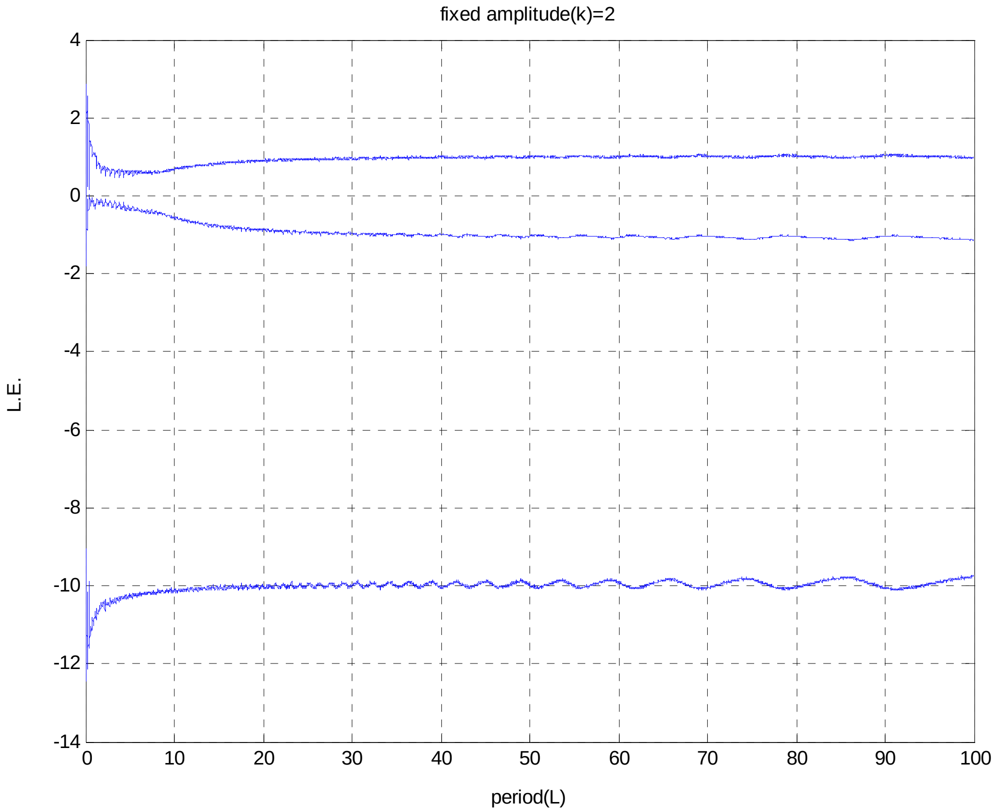

Fig. 5.3.5　Lyapunov exponent of unified chaotic system with $\alpha = f(t),\ k = 2$.

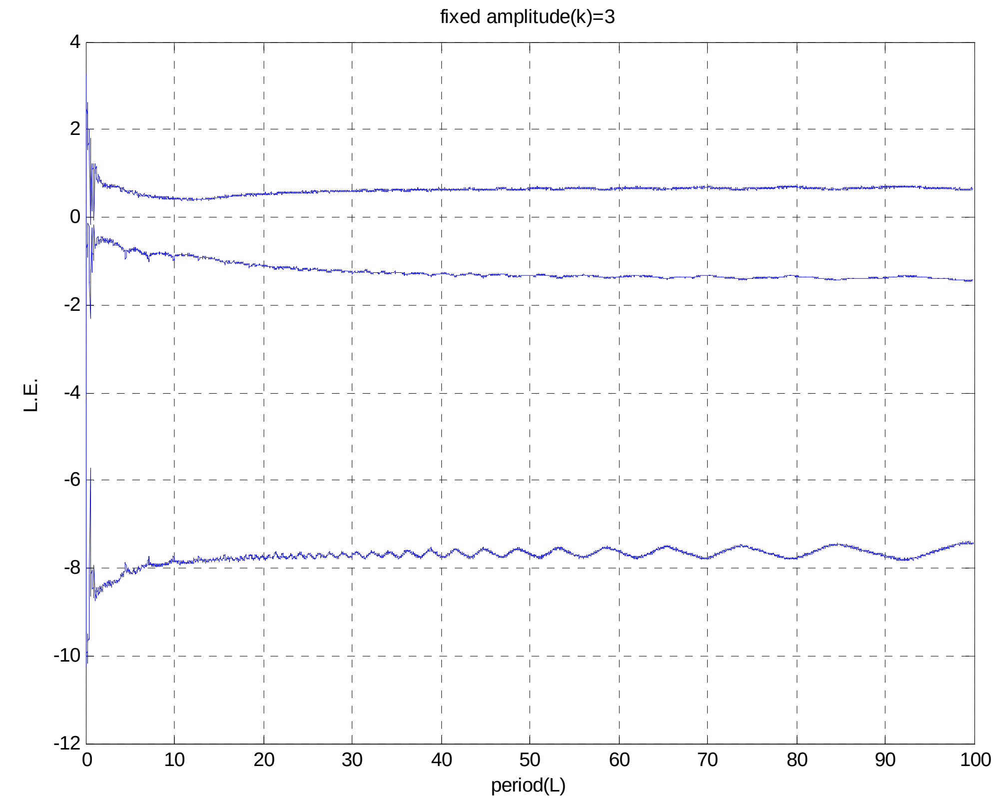

Fig. 5.3.6　Lyapunov exponent of unified chaotic system with $\alpha = f(t),\ k = 3$.

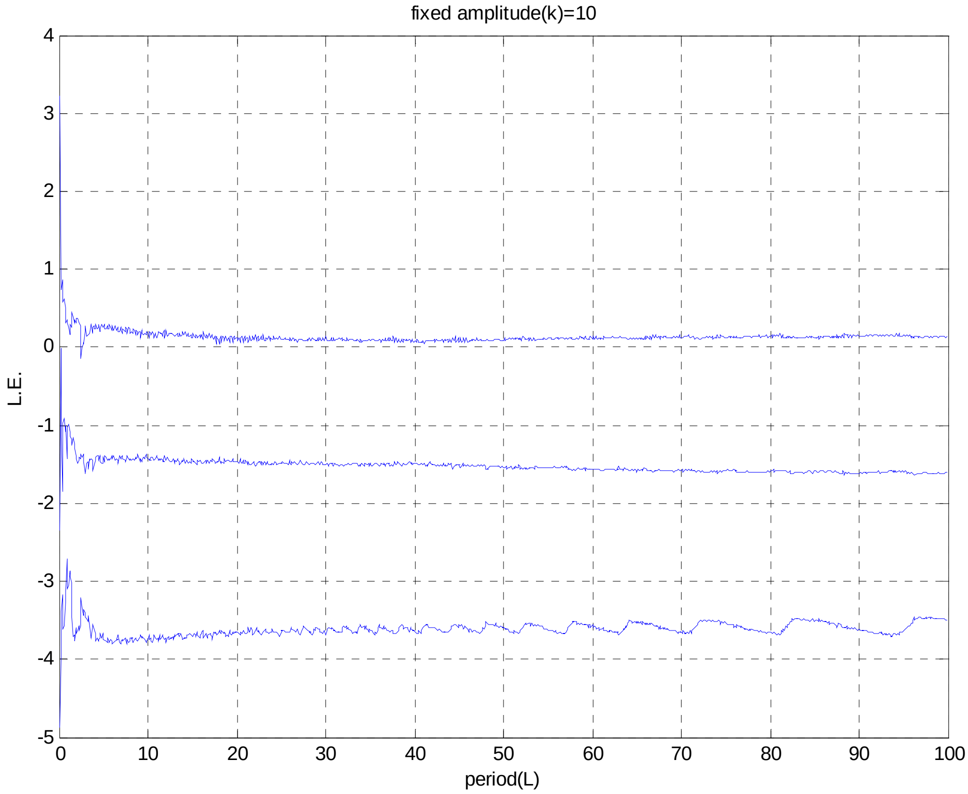

Fig. 5.3.7 Lyapunov exponent of unified chaotic system with $\alpha = f(t),\ k = 10$.

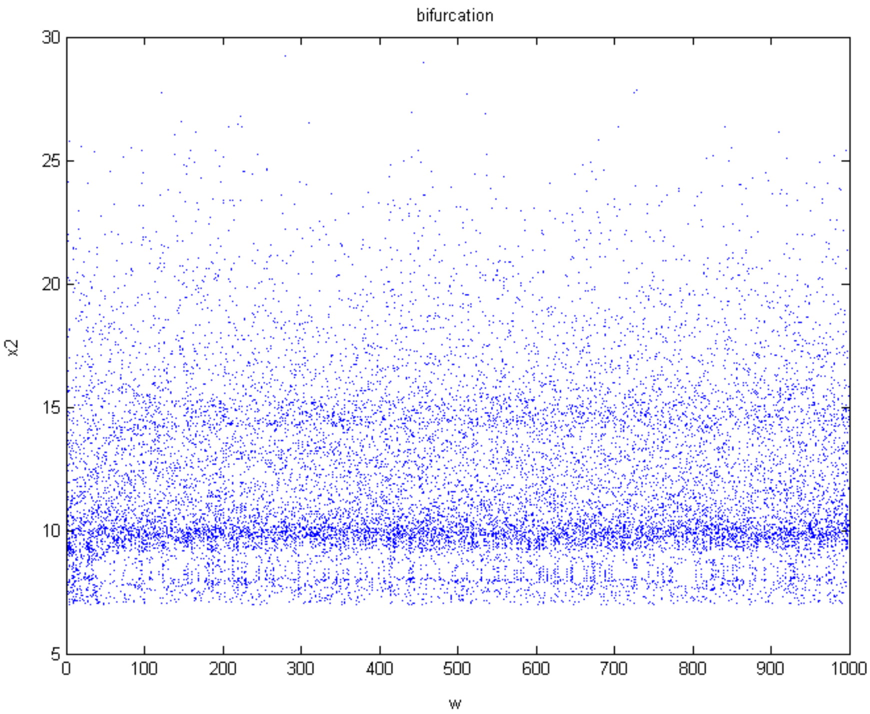

Fig. 5.3.8 Bifurcation diagram of the Lyapunov exponent of unified chaotic system with $\alpha = f(t), k = 1, \omega = 2\pi / L$.

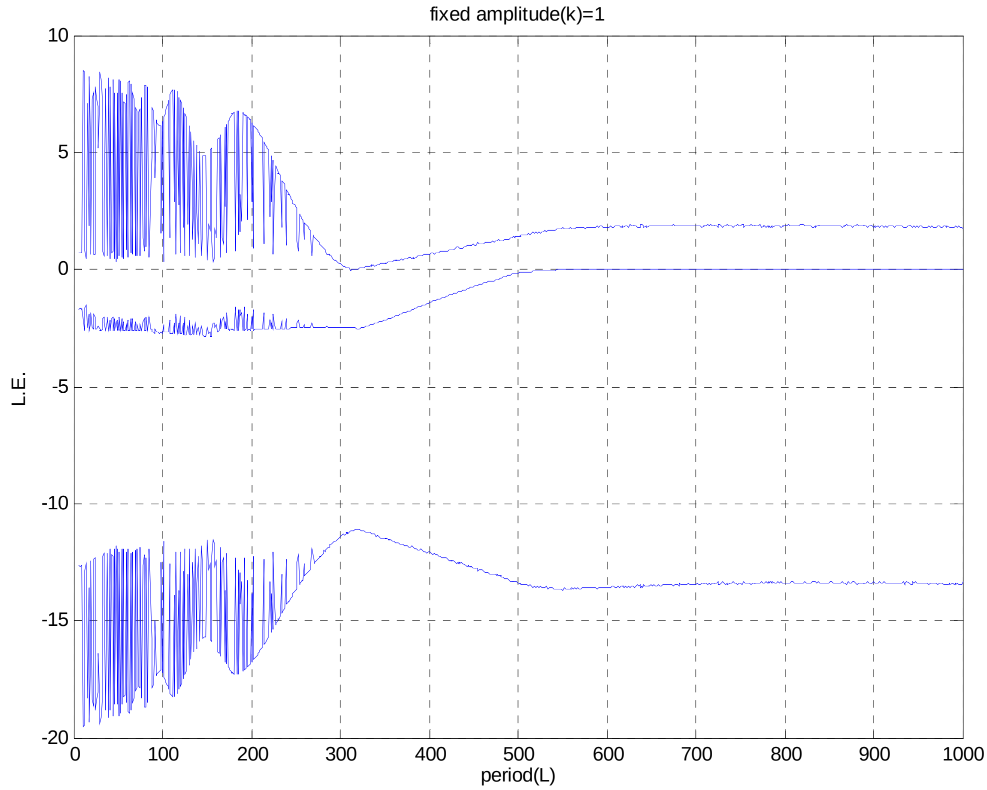

Fig. 5.4.1 Lyapunov exponent of unified chaotic system with $\alpha = g(t)$ $k = 1$.

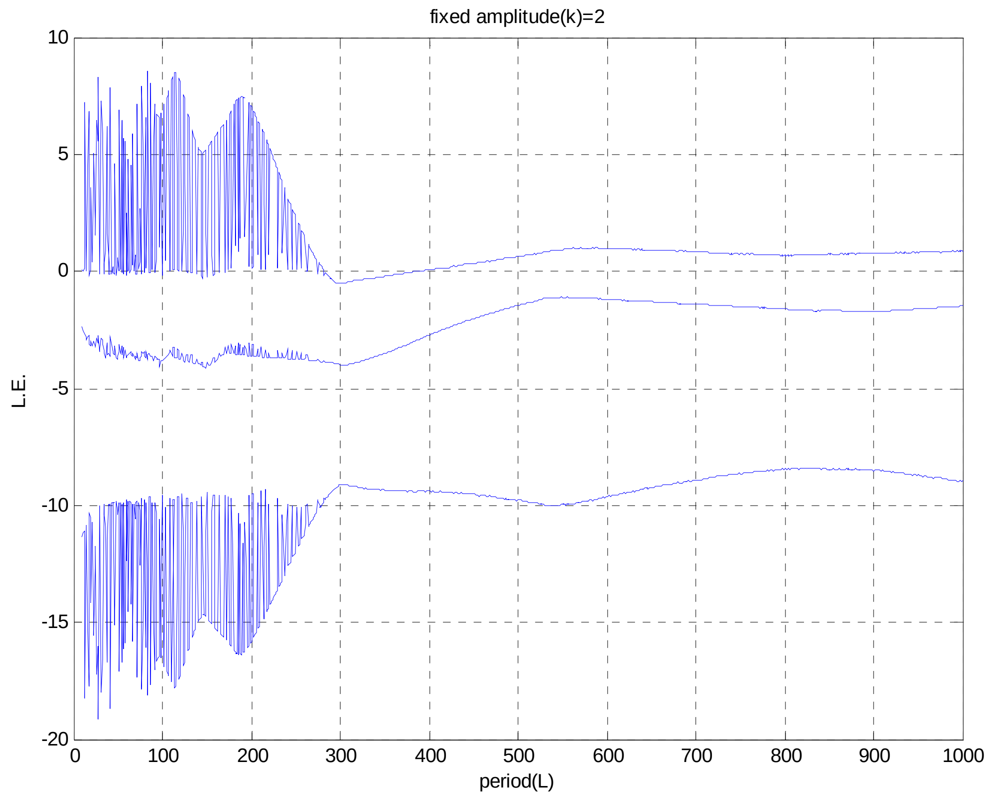

Fig. 5.4.2 Lyapunov exponent of unified chaotic system with $\alpha = g(t)$ $k = 2$.

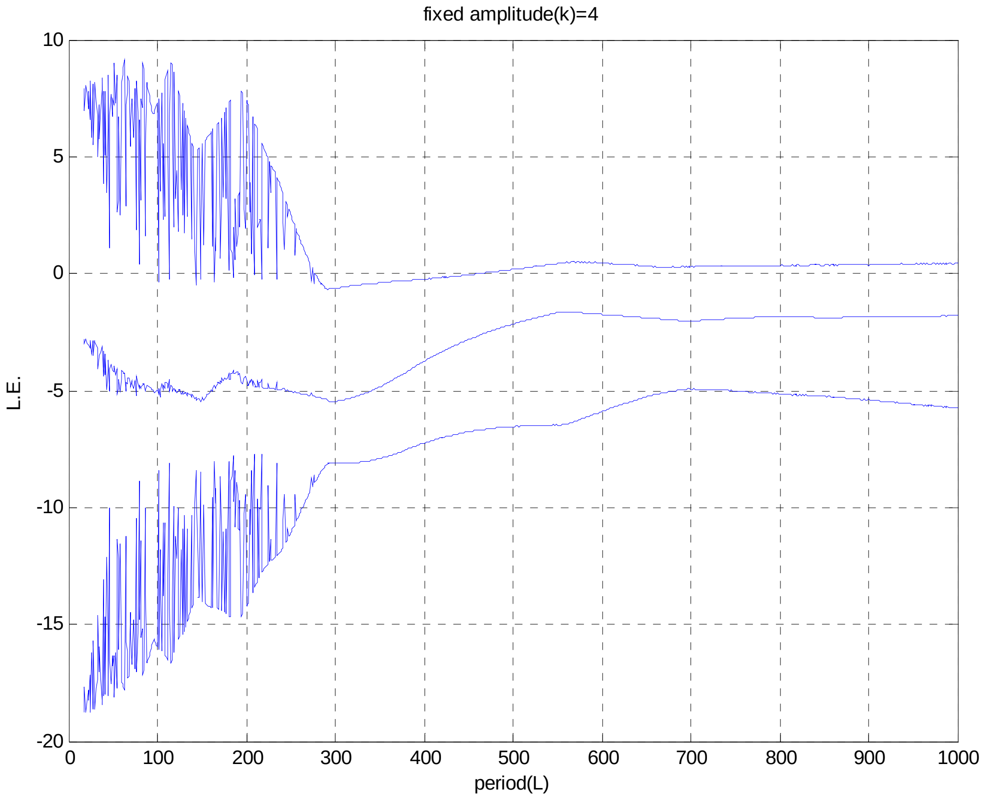

Fig. 5.4.3 Lyapunov exponent of unified chaotic system with $\alpha = g(t)$ $k = 4$.

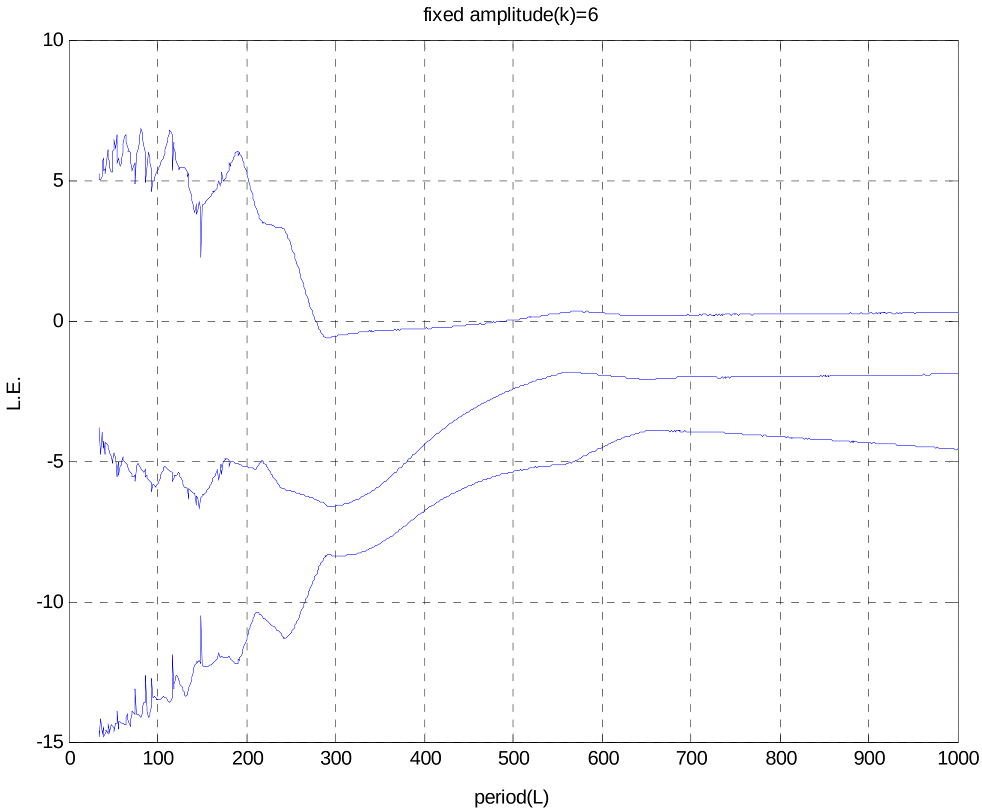

Fig. 5.4.4 Lyapunov exponent of unified chaotic system with $\alpha = g(t)$ $k = 6$.

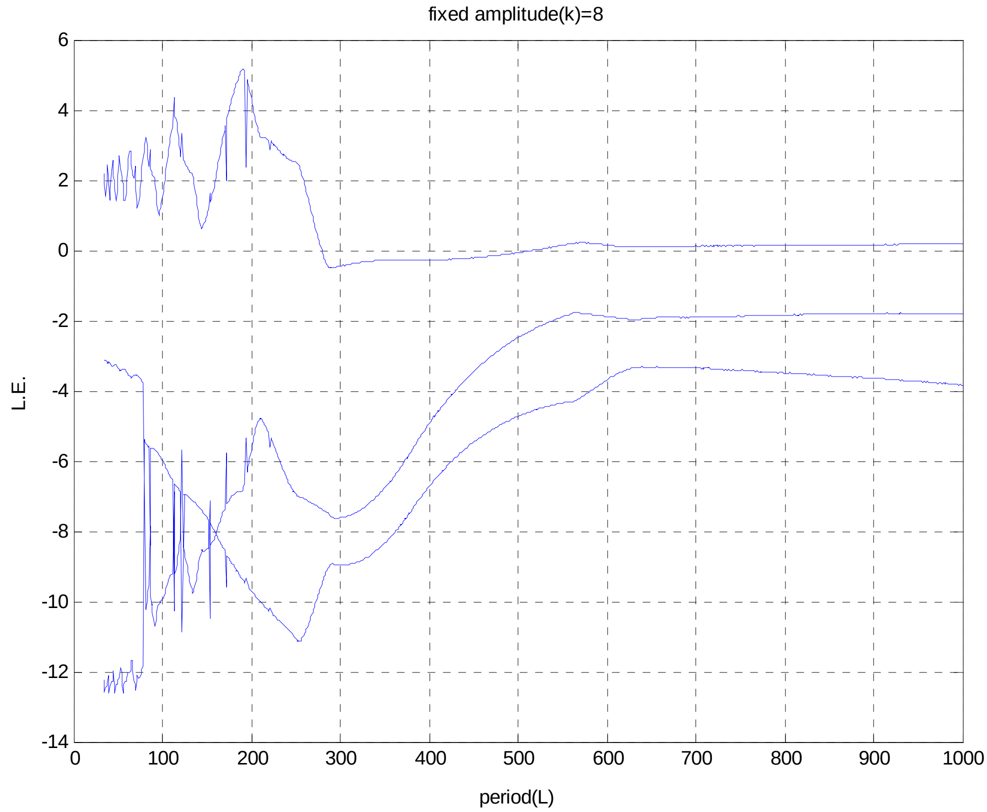

Fig. 5.4.5 Lyapunov exponent of unified chaotic system with $\alpha = g(t)$ $k = 8$.

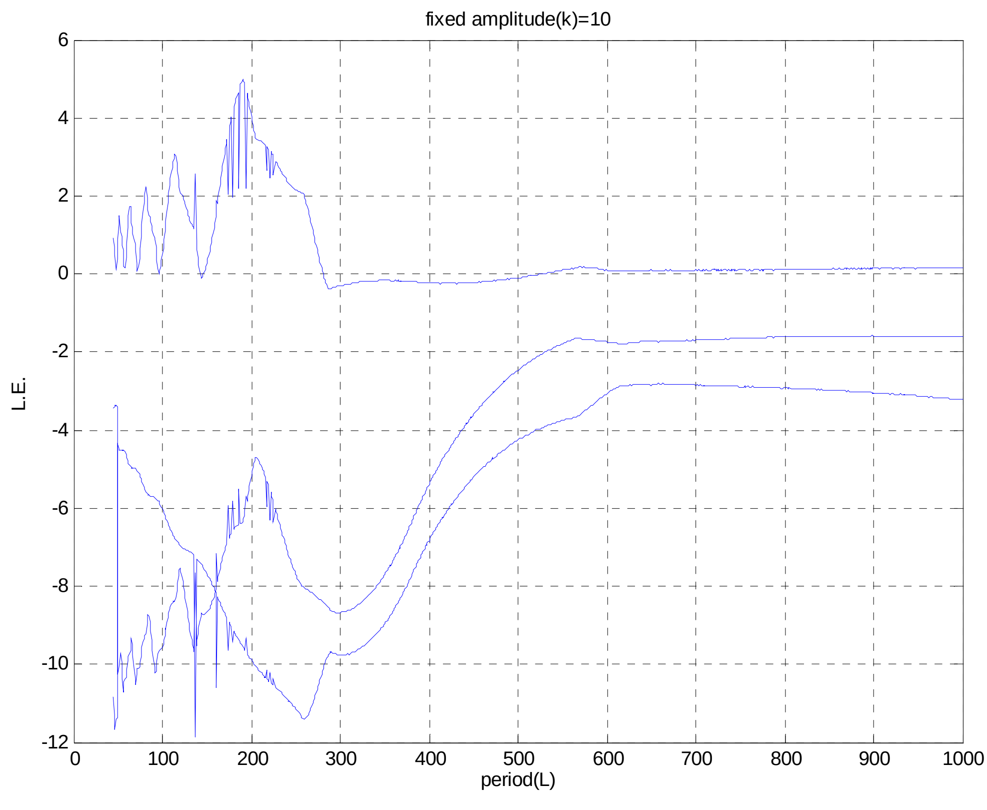

Fig. 5.4.6 Lyapunov exponent of unified chaotic system with $\alpha = g(t)$ $k = 10$.

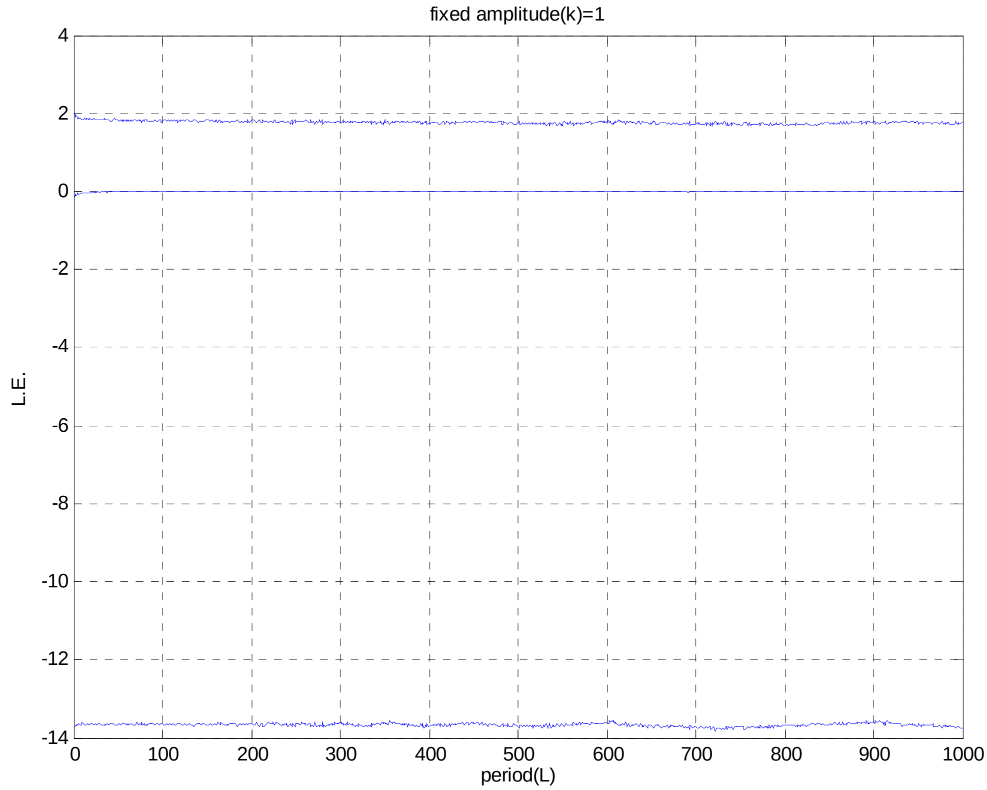

Fig. 5.5.1 Lyapunov exponent of unified chaotic system with $\alpha = q(t)\ k = 1$.

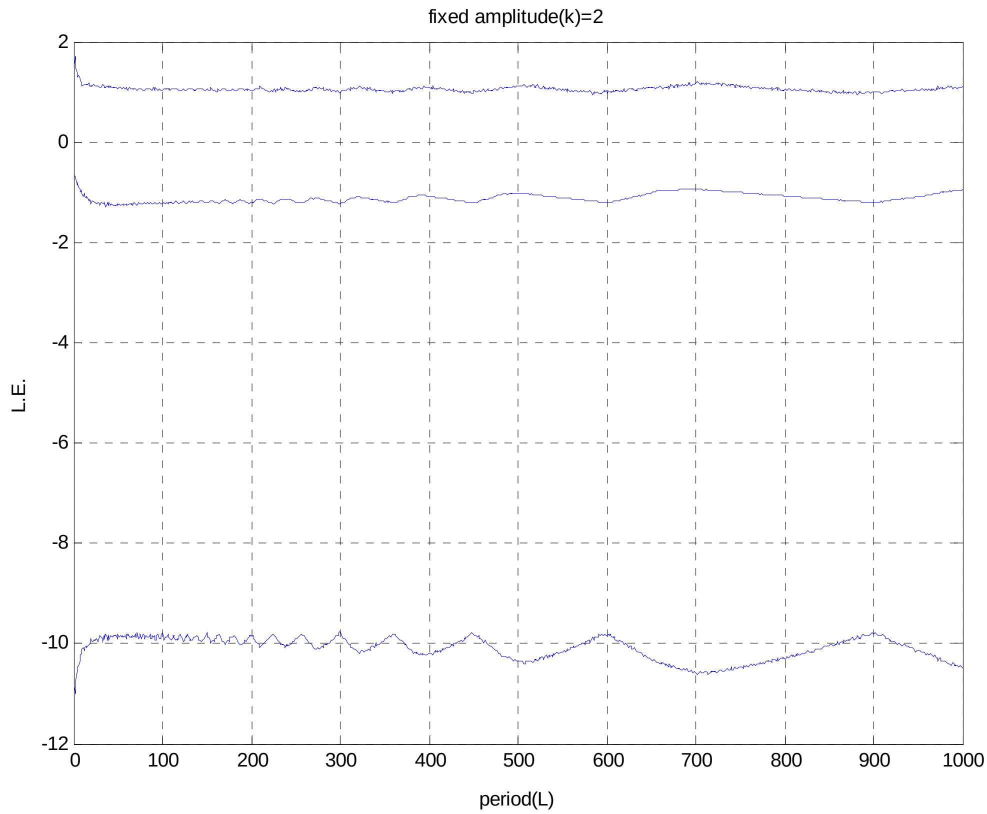

Fig. 5.5.2 Lyapunov exponent of unified chaotic system with $\alpha = q(t)\ k = 2$.

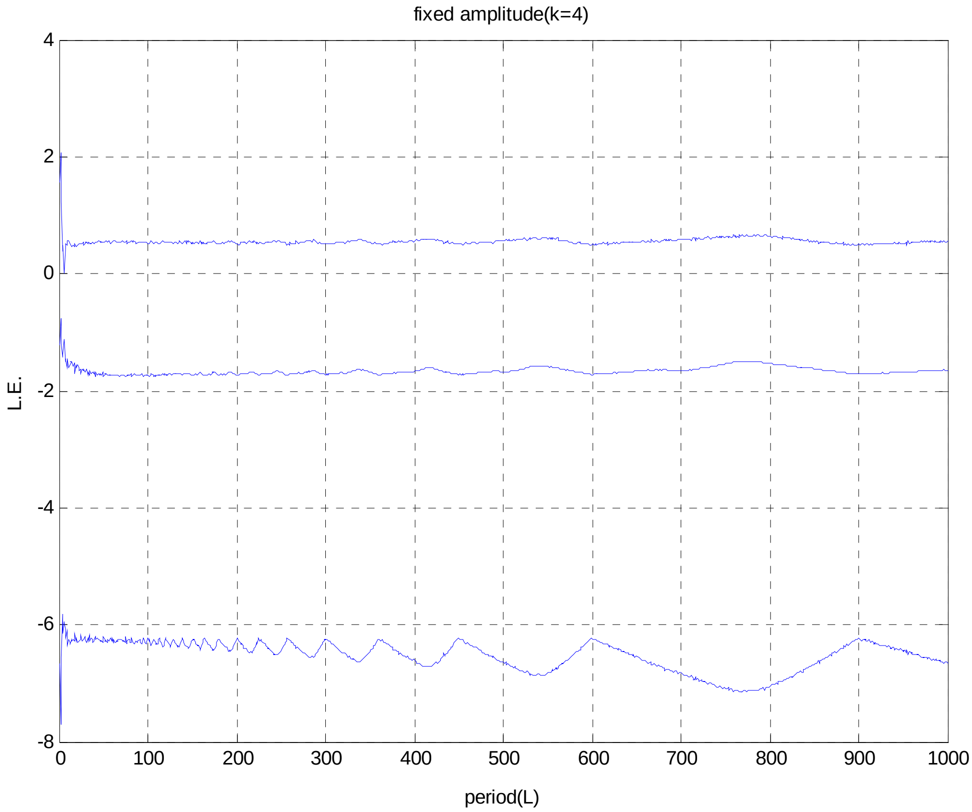

Fig. 5.5.3 Lyapunov exponent of unified chaotic system with $\alpha = q(t)$ $k = 4$.

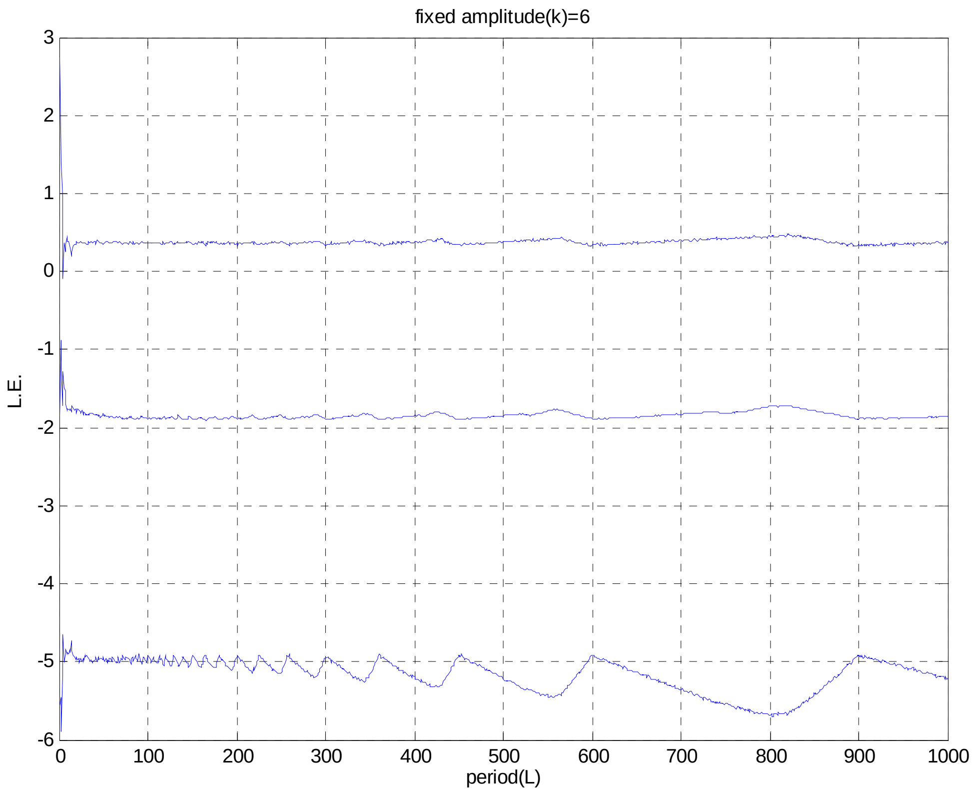

Fig. 5.5.4 Lyapunov exponent of unified chaotic system with $\alpha = q(t)$ $k = 6$.

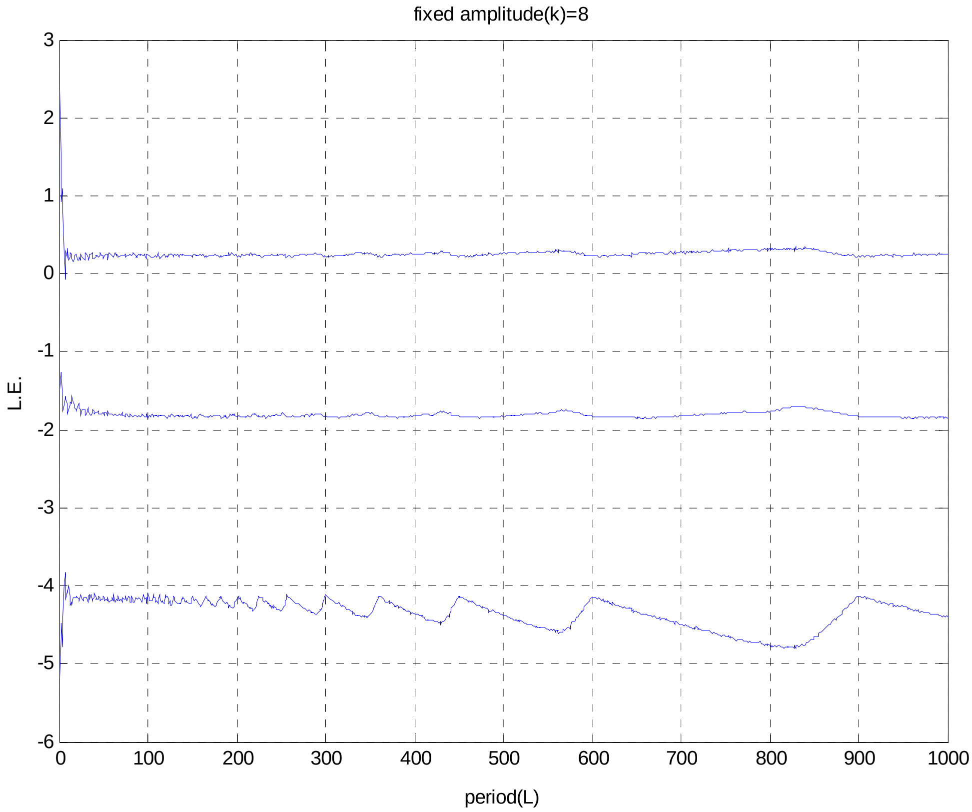

Fig. 5.5.5 Lyapunov exponent of unified chaotic system with $\alpha = q(t)$ $k = 8$.

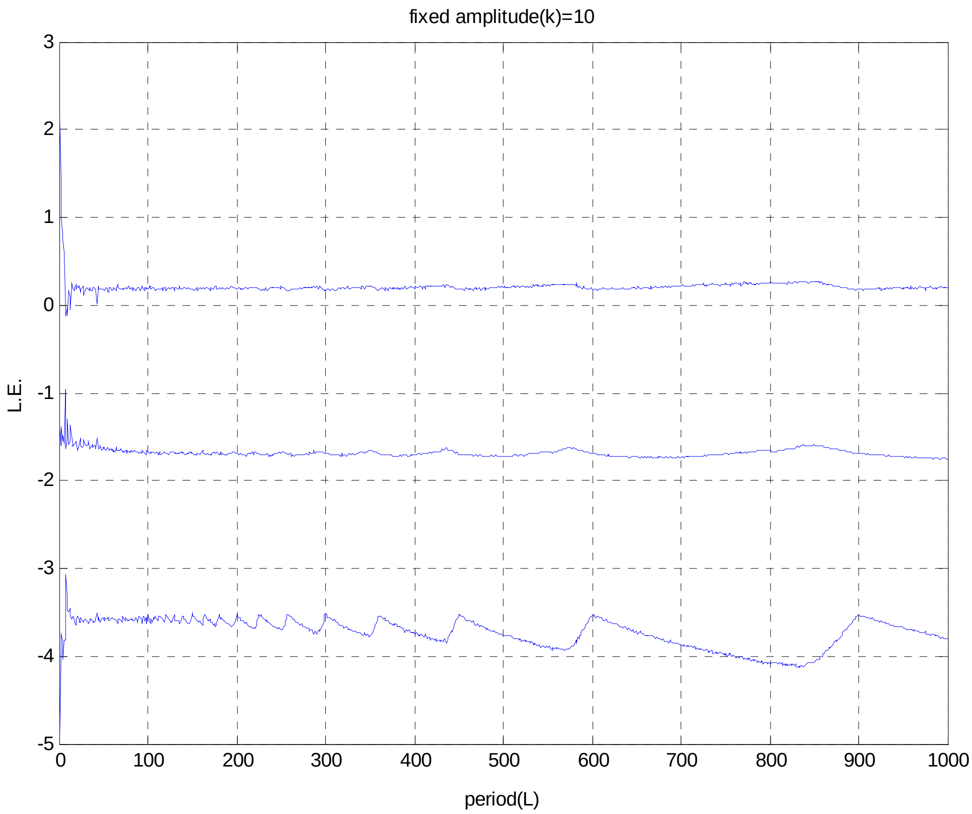

Fig. 5.5.6 Lyapunov exponent of unified chaotic system with $\alpha = q(t)$ $k = 10$.

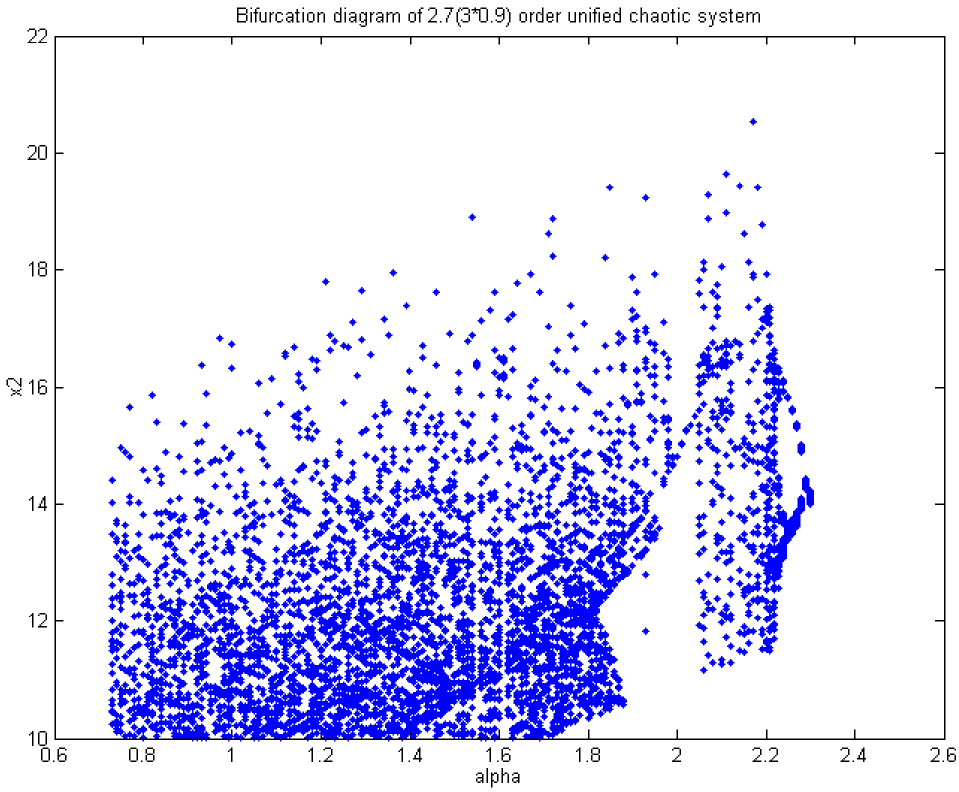

Fig.6.3.1 Bifurcation diagram of 2.7(3×0.9) order unified chaotic system.

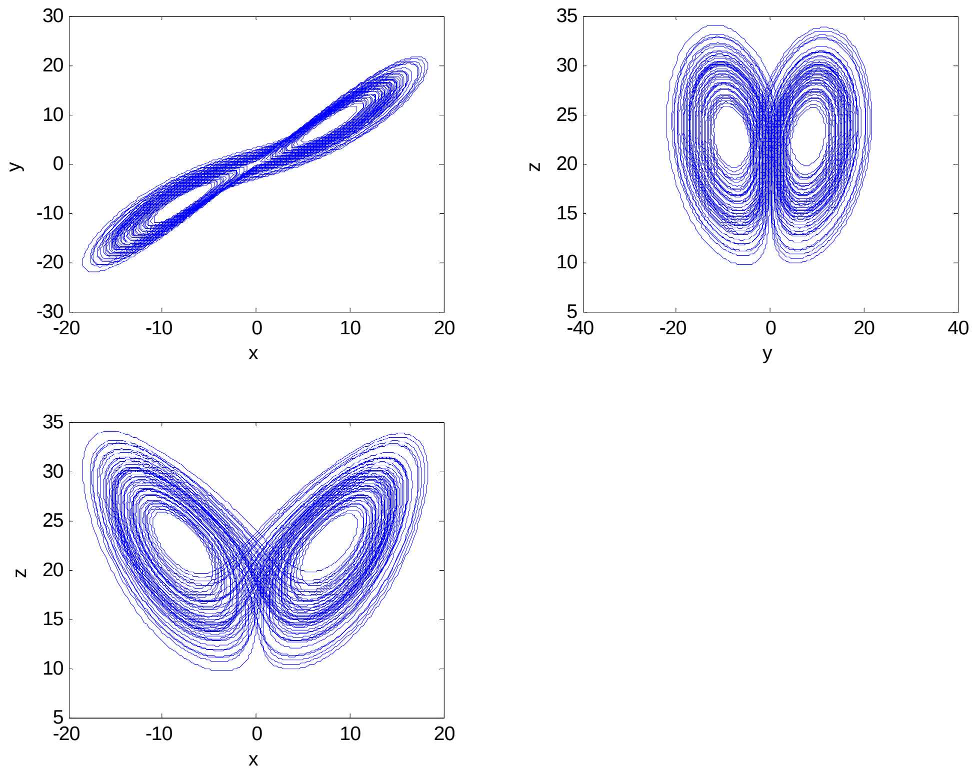

Fig.6.3.2 Phase portrait of 2.7(3×0.9) order unified chaotic system with $\alpha = 0.8$ (Lü).

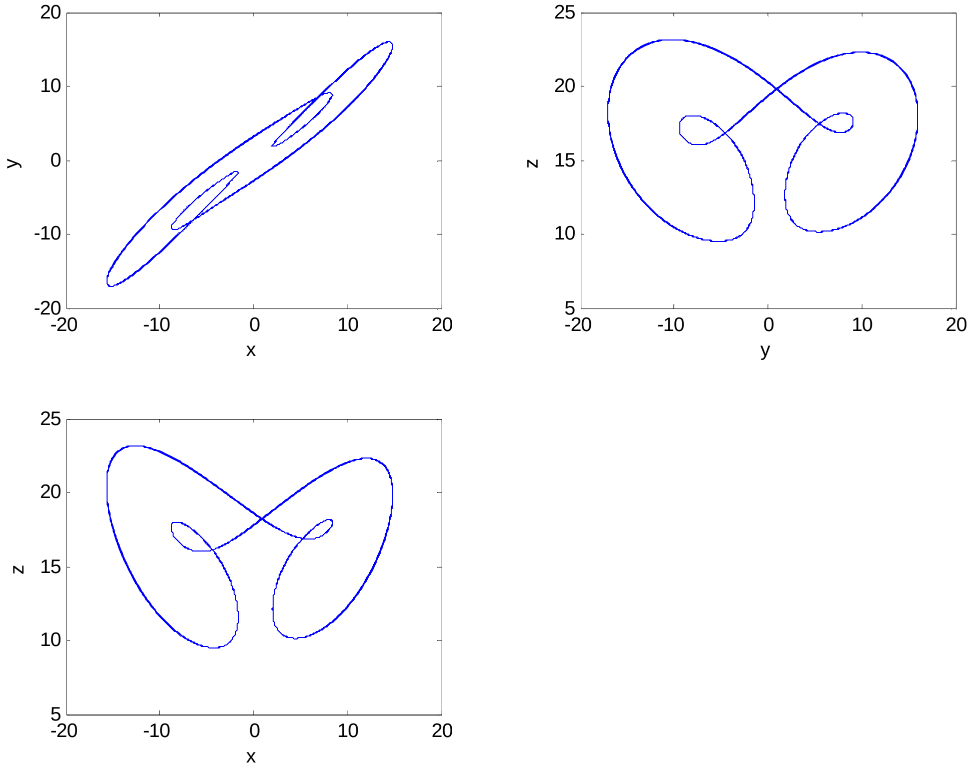

Fig.6.3.3 Phase portrait of 2.7(3×0.9) order unified chaotic system with $\alpha = 2.0$.

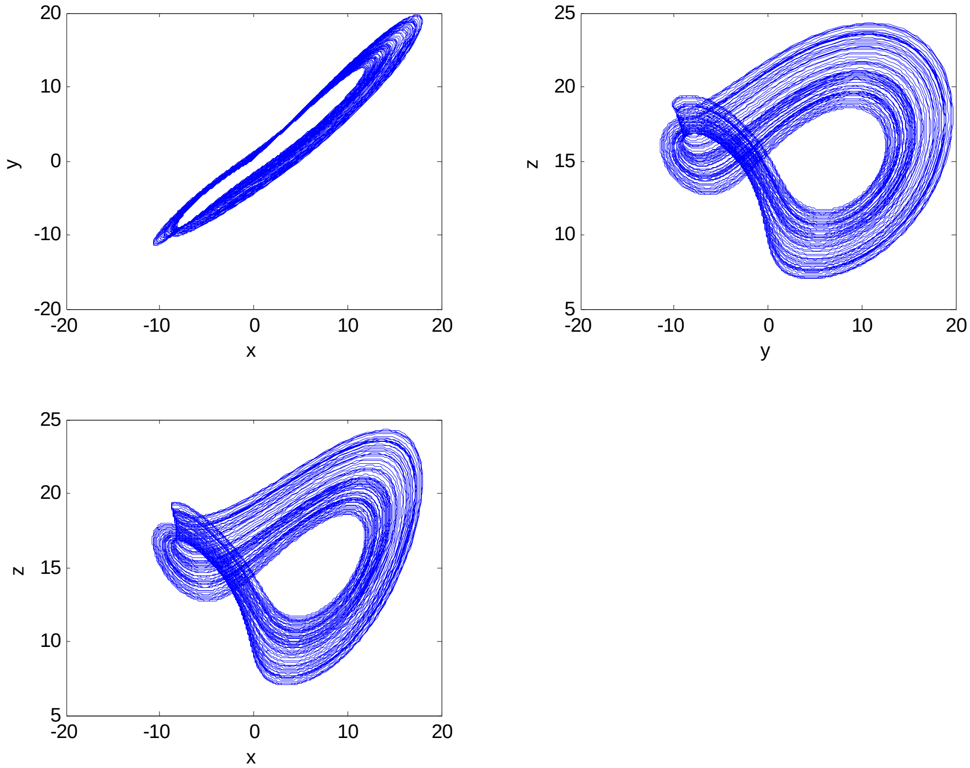

Fig.6.3.4 Phase portrait of 2.7(3×0.9) order unified chaotic system with $\alpha = 2.2$.

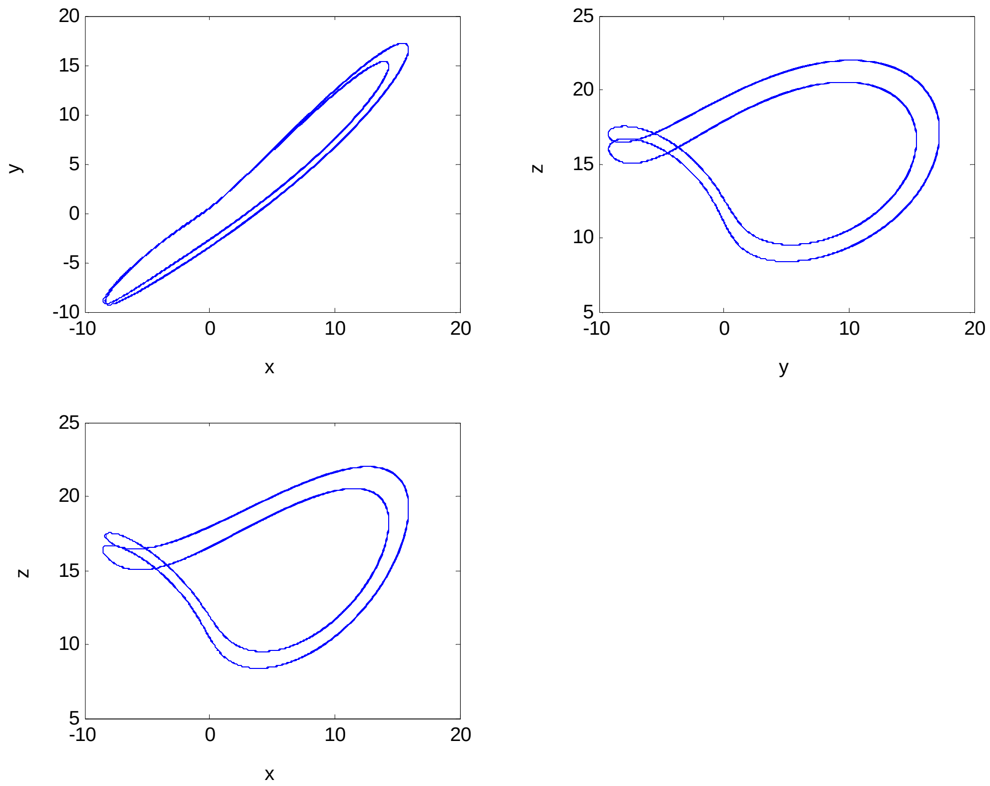

Fig.6.3.5 Phase portrait of 2.7(3×0.9) order unified chaotic system with $\alpha = 2.25$.

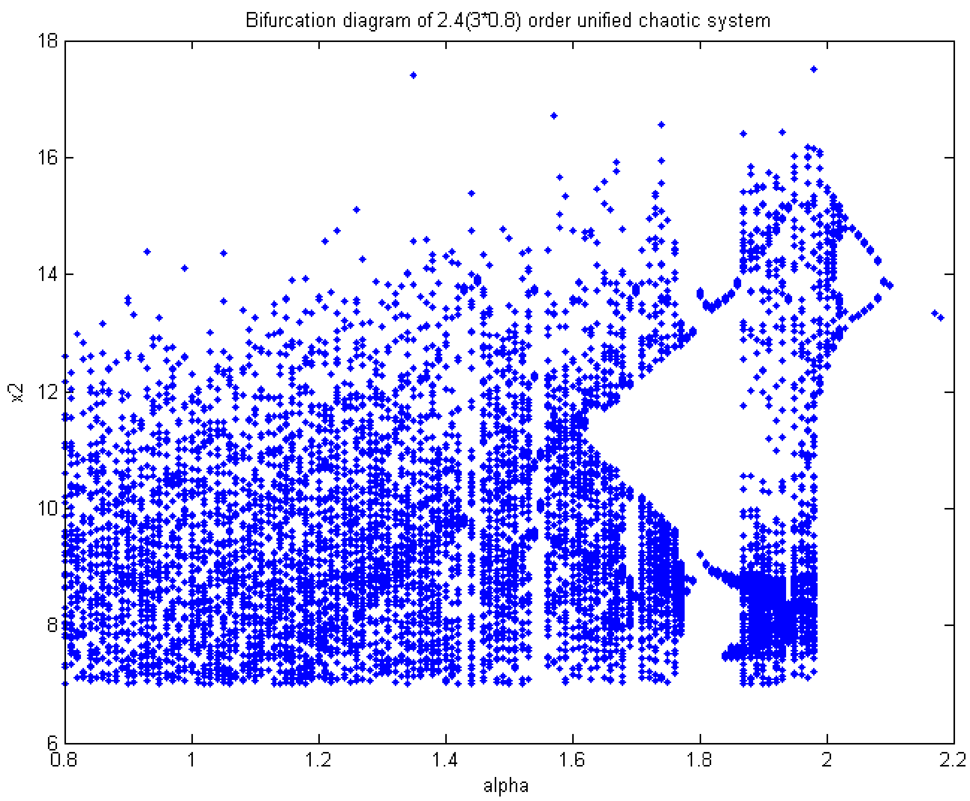

Fig.6.3.6 Bifurcation diagram of 2.4(3×0.8) order unified chaotic system.

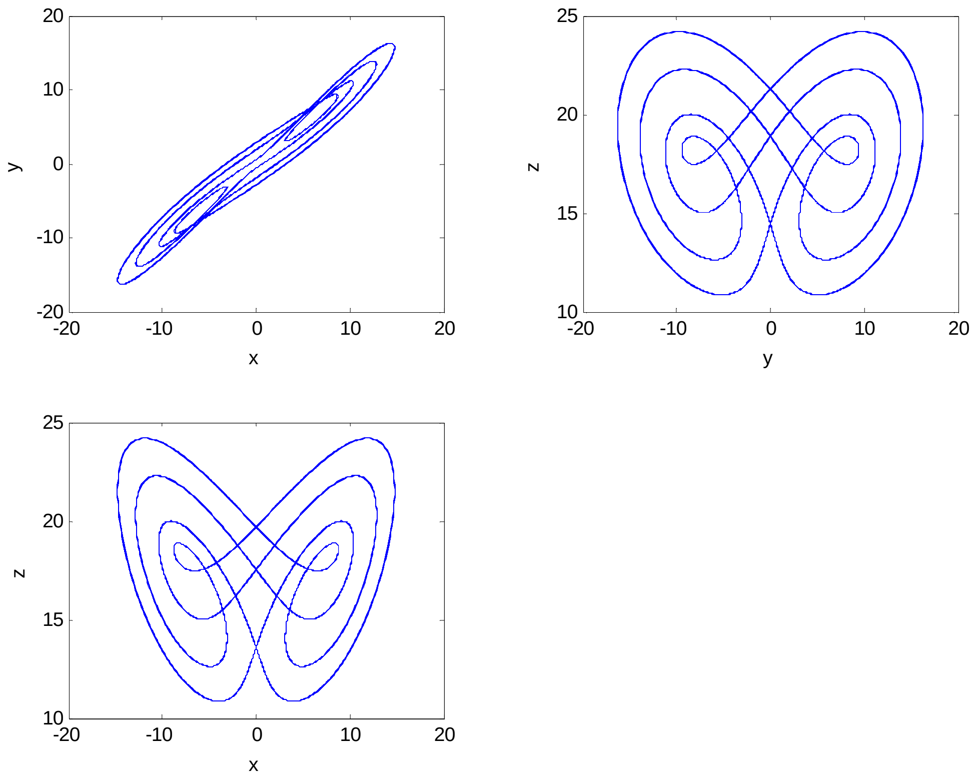

Fig.6.3.7 Phase portrait of 2.4(3×0.8) order unified chaotic system with $\alpha = 1.7$.

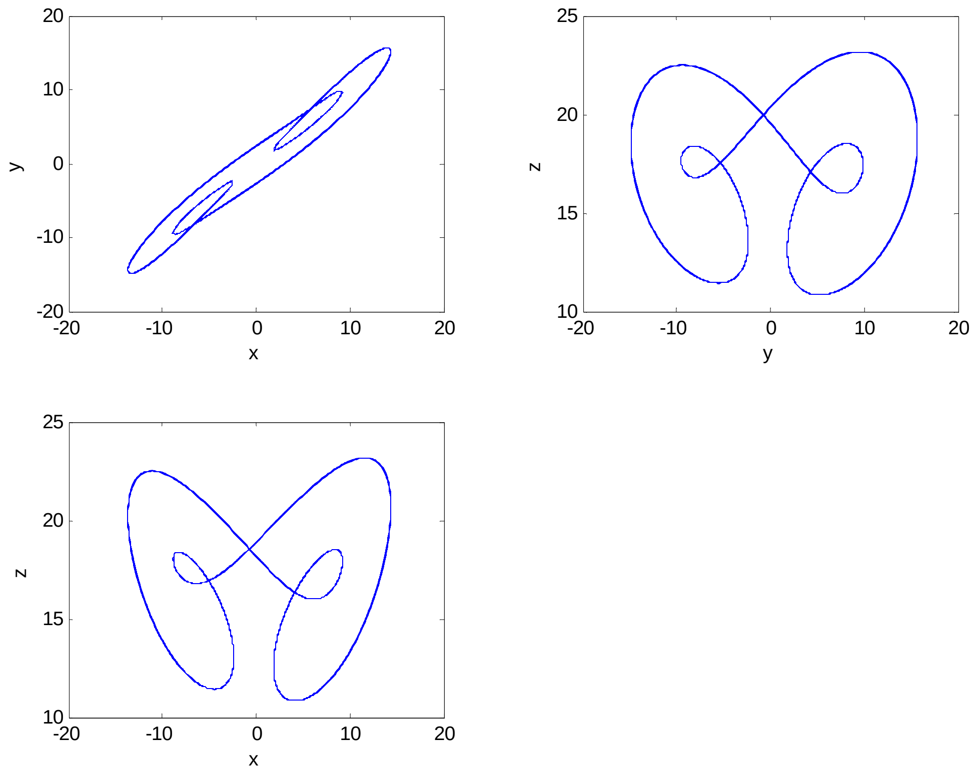

Fig.6.3.8 Phase portrait of 2.4(3×0.8) order unified chaotic system with $\alpha = 1.8$.

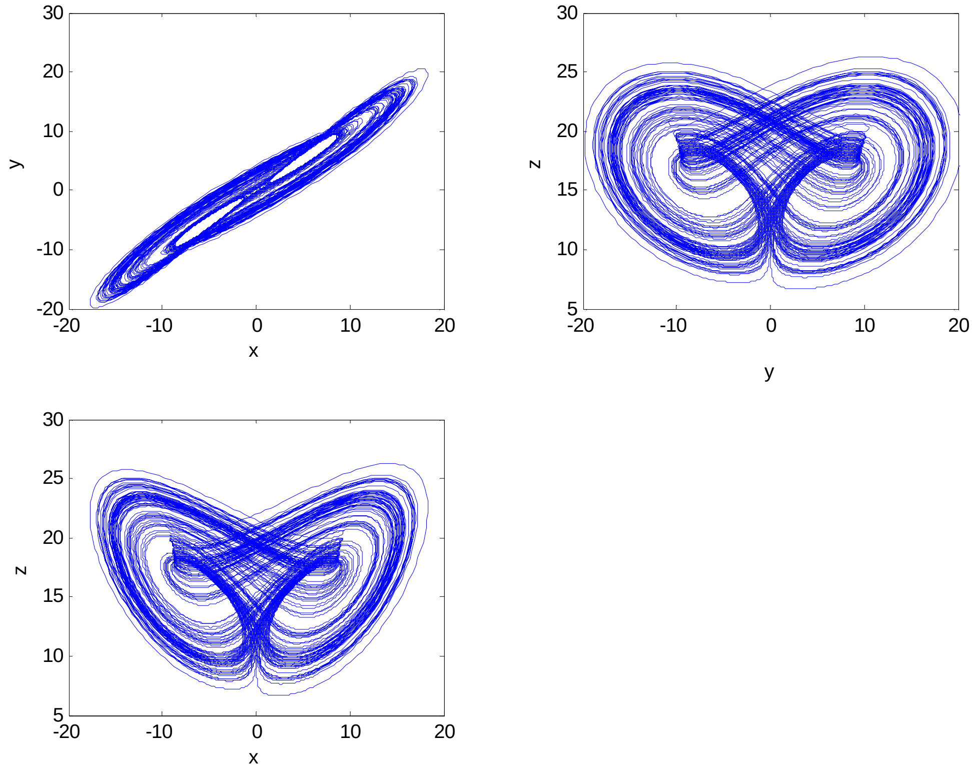

Fig.6.3.9 Phase portrait of 2.4(3×0.8) order unified chaotic system with $\alpha = 1.9$.

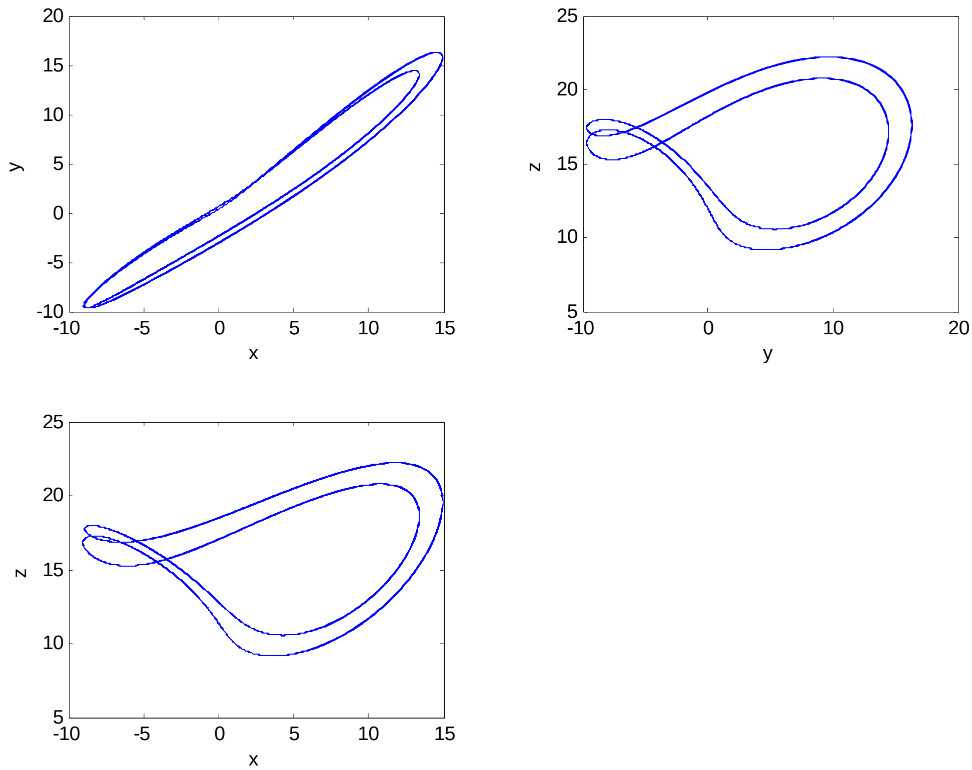

Fig.6.3.10 Phase portrait of 2.4(3×0.8) order unified chaotic system with $\alpha = 2.05$.

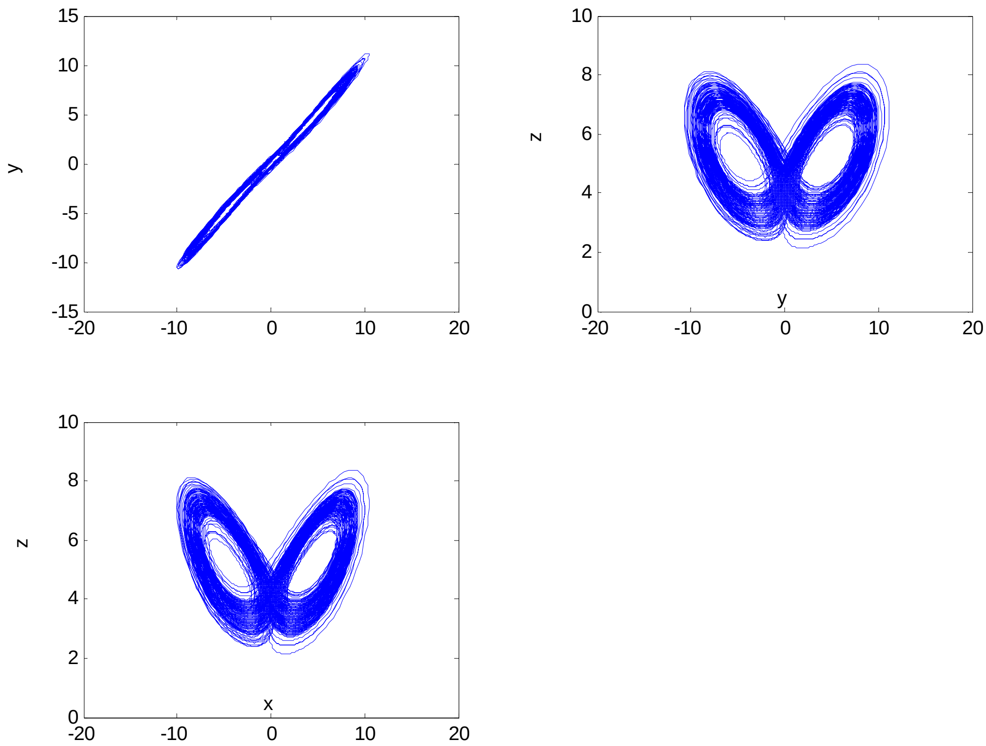

Fig.6.3.11 Phase portrait of 2.1(3×0.7) order unified chaotic system with $\alpha = 3.7$.

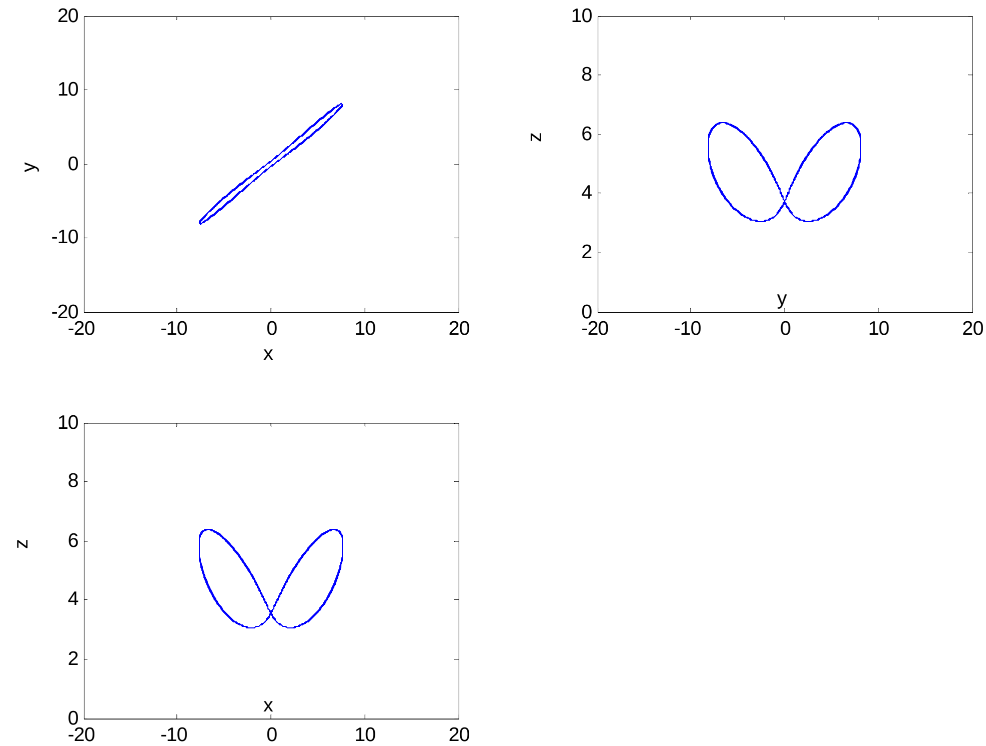

Fig.6.3.12 Phase portrait of 2.1(3×0.7) order unified chaotic system with $\alpha = 3.8$.

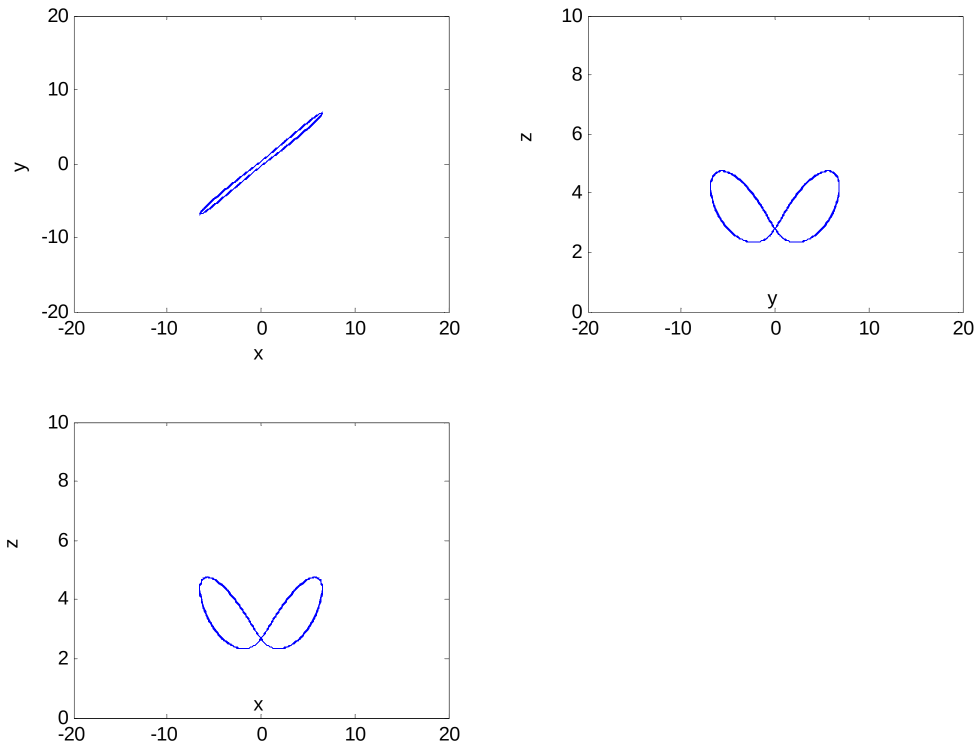

Fig.6.3.13 Phase portrait of 2.1(3×0.7) order unified chaotic system with $\alpha = 4.0$.

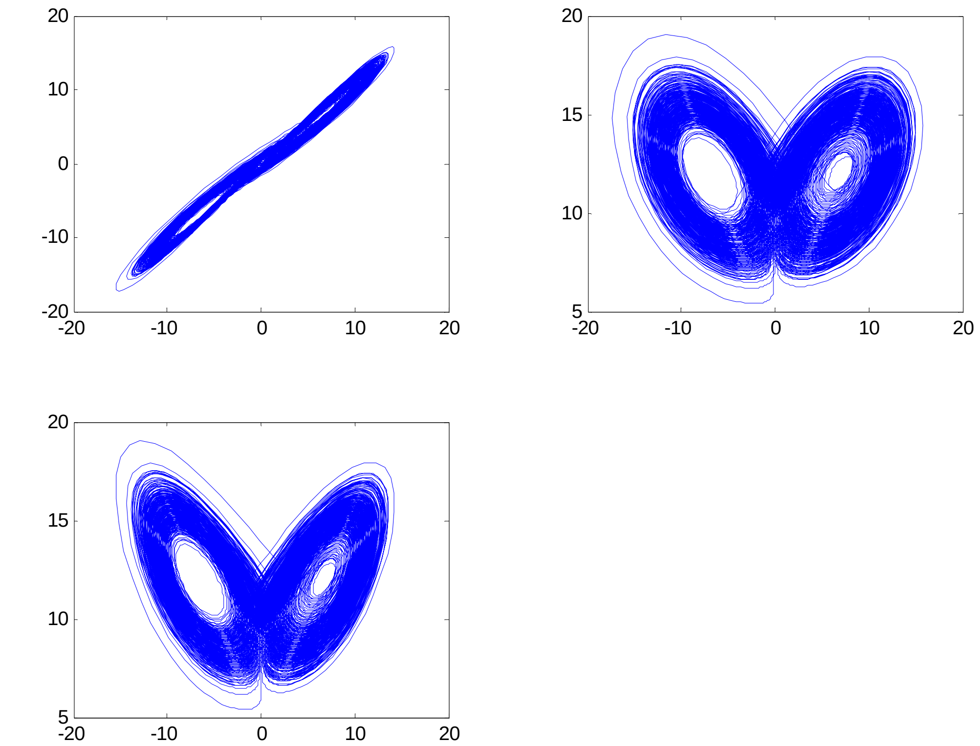

Fig.6.3.14 Phase portrait of 1.8(3×0.6) order unified chaotic system with $\alpha = 2.5$.

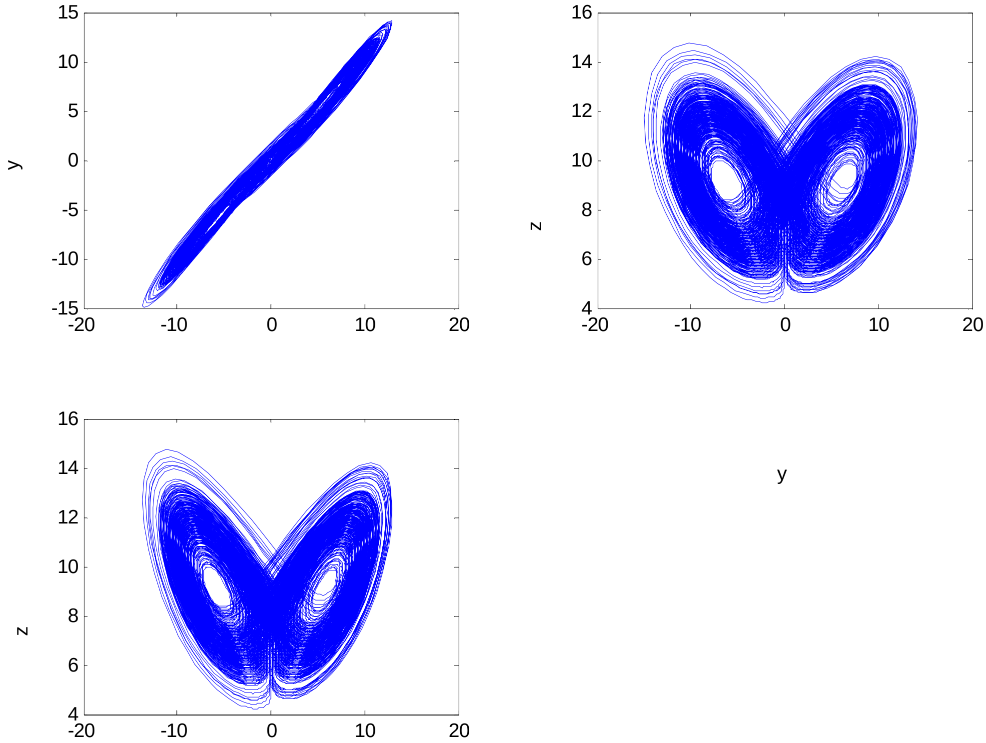

Fig.6.3.15 Phase portrait of 1.8(3×0.6) order unified chaotic system with $\alpha = 3.0$.

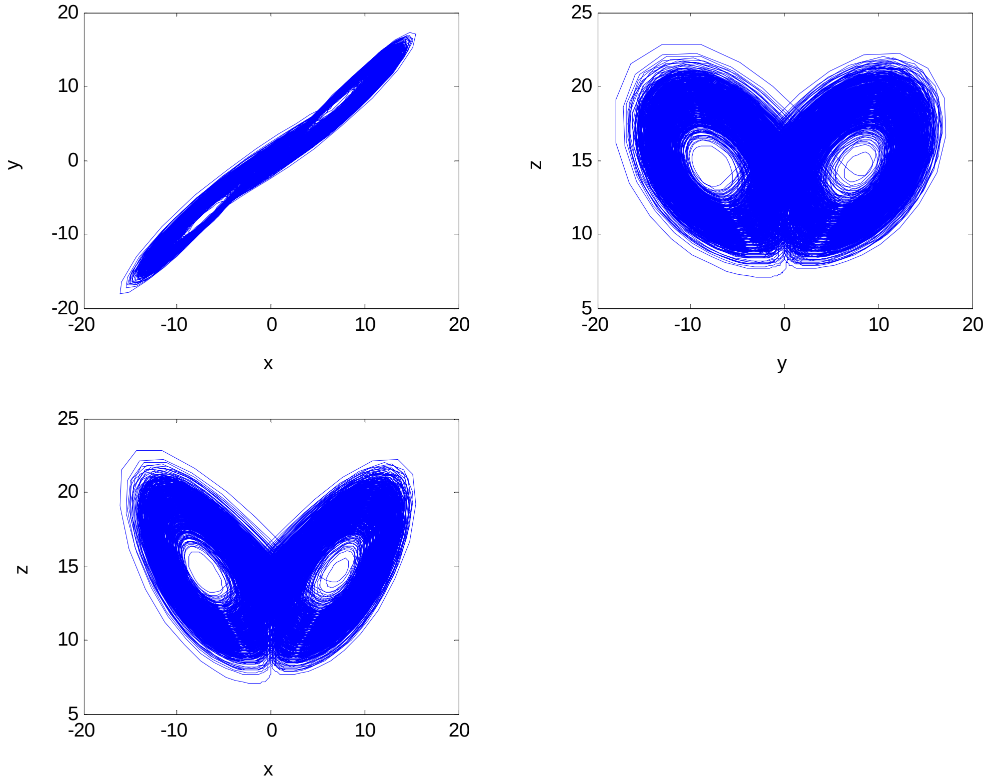

Fig.6.3.16 Phase portrait of 1.5(3×0.5) order unified chaotic system with $\alpha = 2.0$.

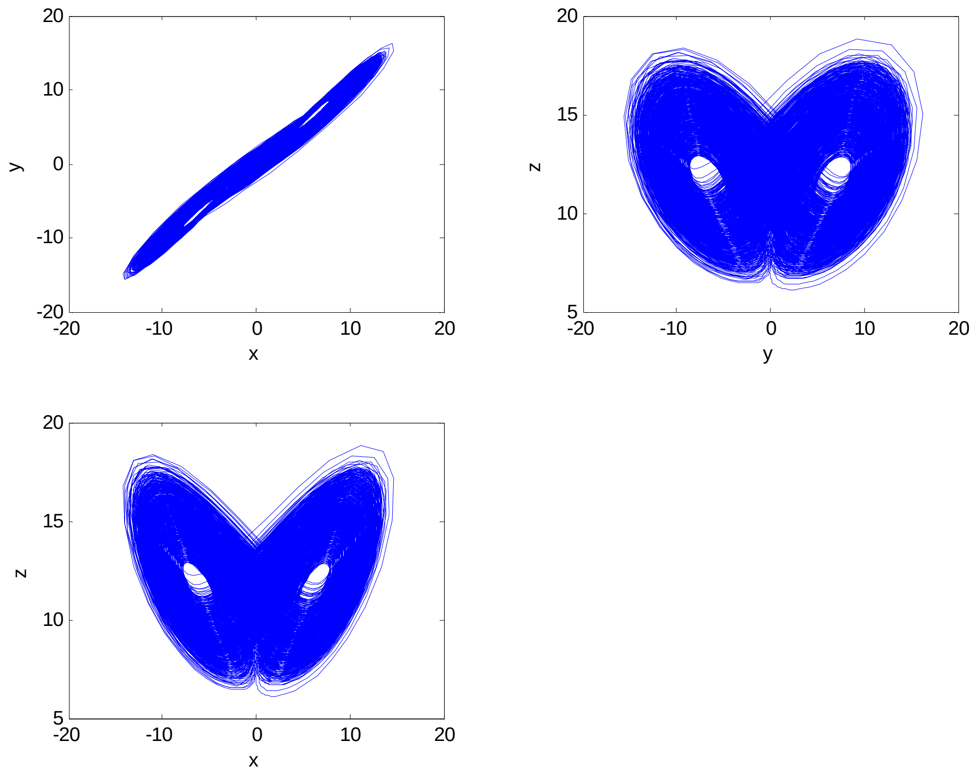

Fig.6.3.17 Phase portrait of 1.5(3×0.5) order unified chaotic system with $\alpha = 2.5$.

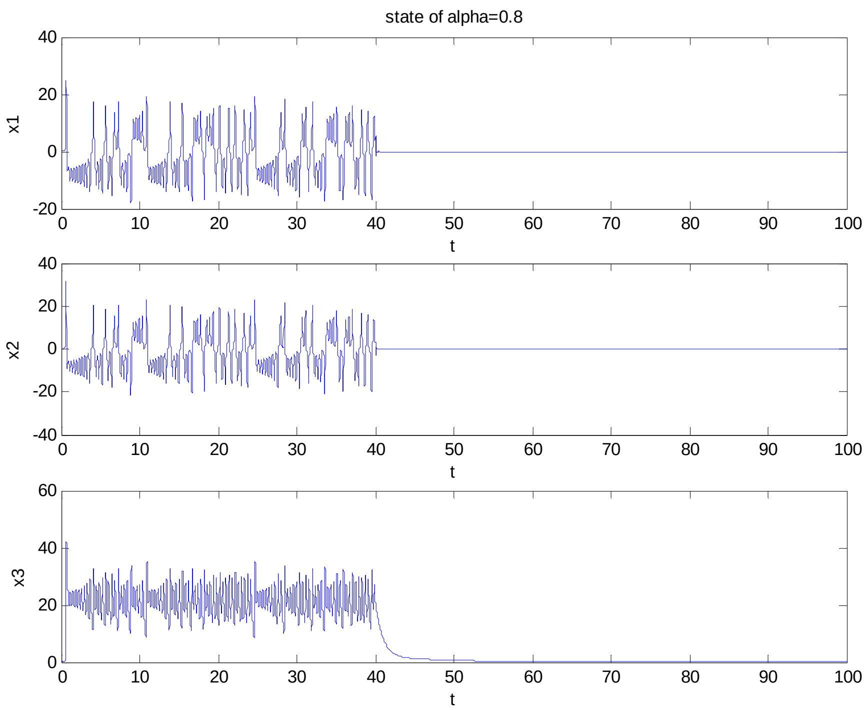

Fig. 6.4.1(a) Time history of the controlled fractional order unified chaotic system with order $a = 0.9$ and system parameter $\alpha = 0.8$.

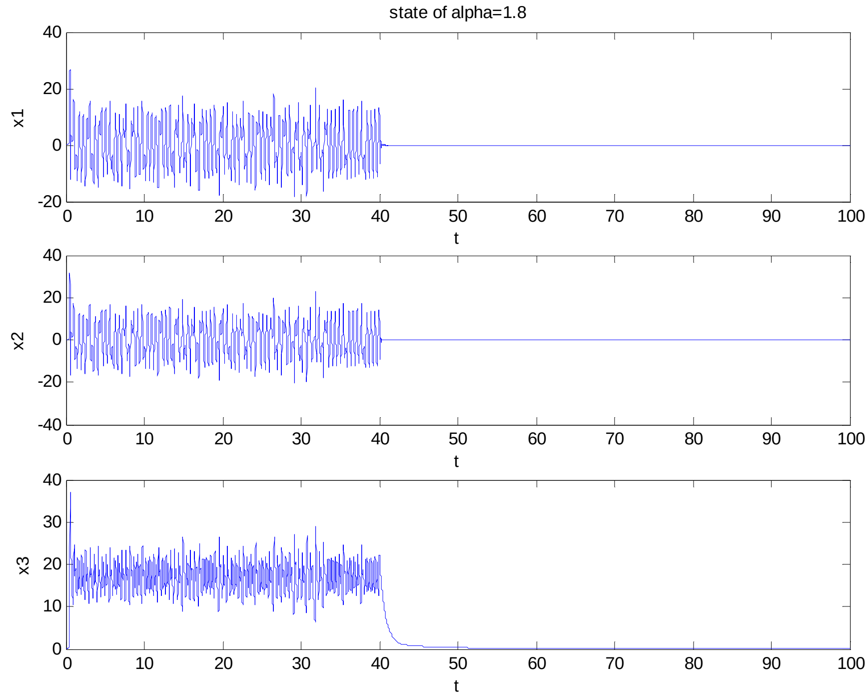

Fig. 6.4.1(b) Time history of the controlled fractional order unified chaotic system with order $a = 0.9$ and system parameter $\alpha = 1.8$.

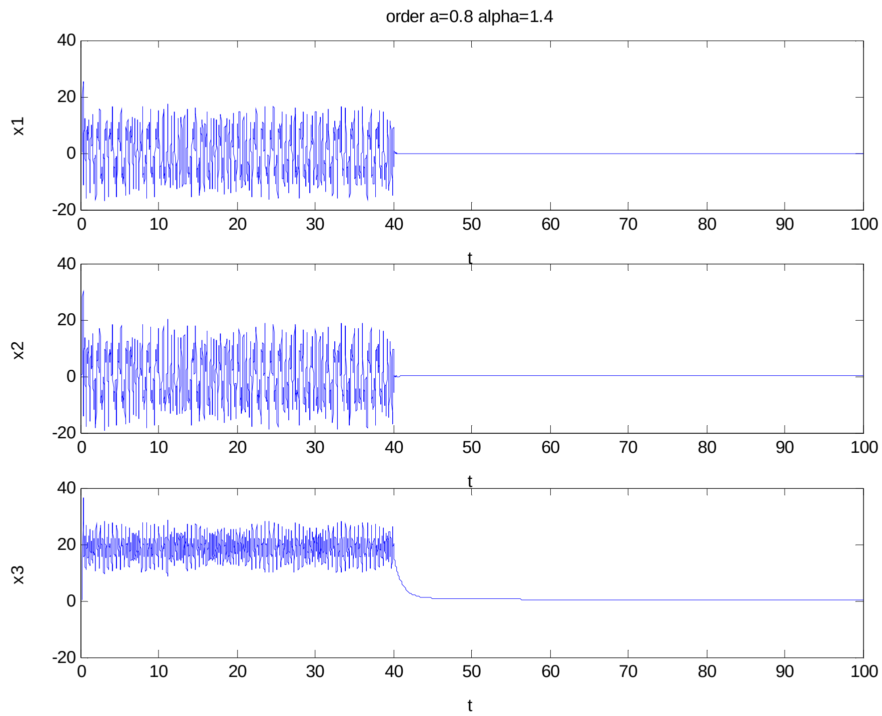

Fig. 6.4.2(a) Time history of the controlled fractional order unified chaotic system with order $a = 0.8$ and system parameter $\alpha = 1.4$.

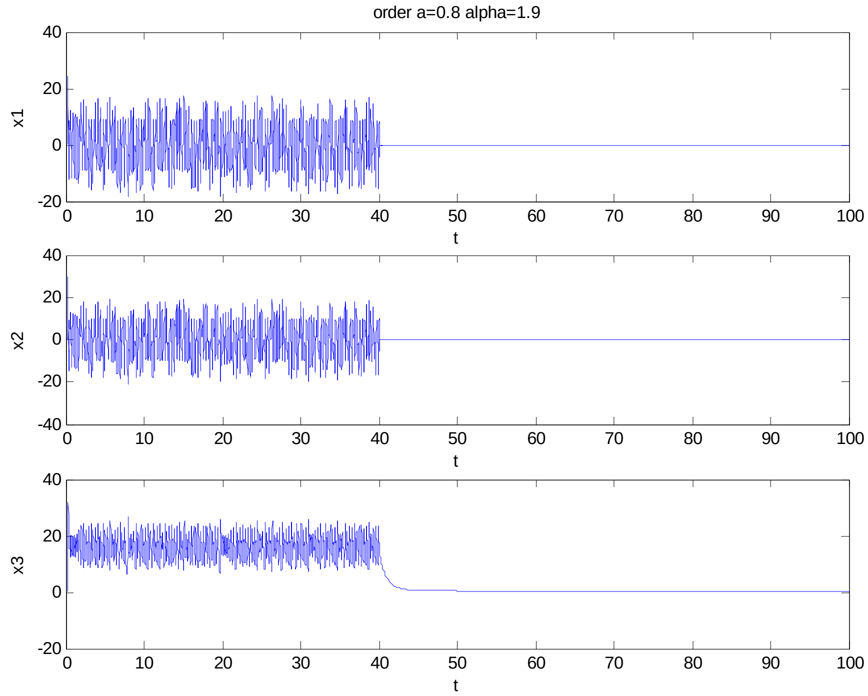

Fig. 6.4.2(b) Time history of the controlled fractional order unified chaotic system with order $a = 0.8$ and system parameter $\alpha = 1.9$.

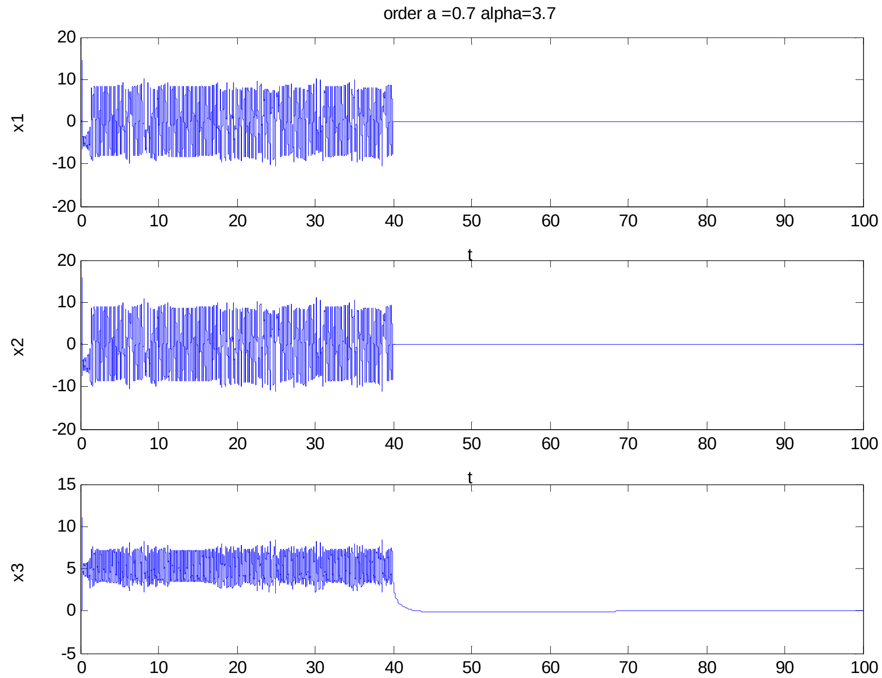

Fig. 6.4.3 Time history of the controlled fractional order unified chaotic system with order $a = 0.7$ and system parameter $\alpha = 3.7$.

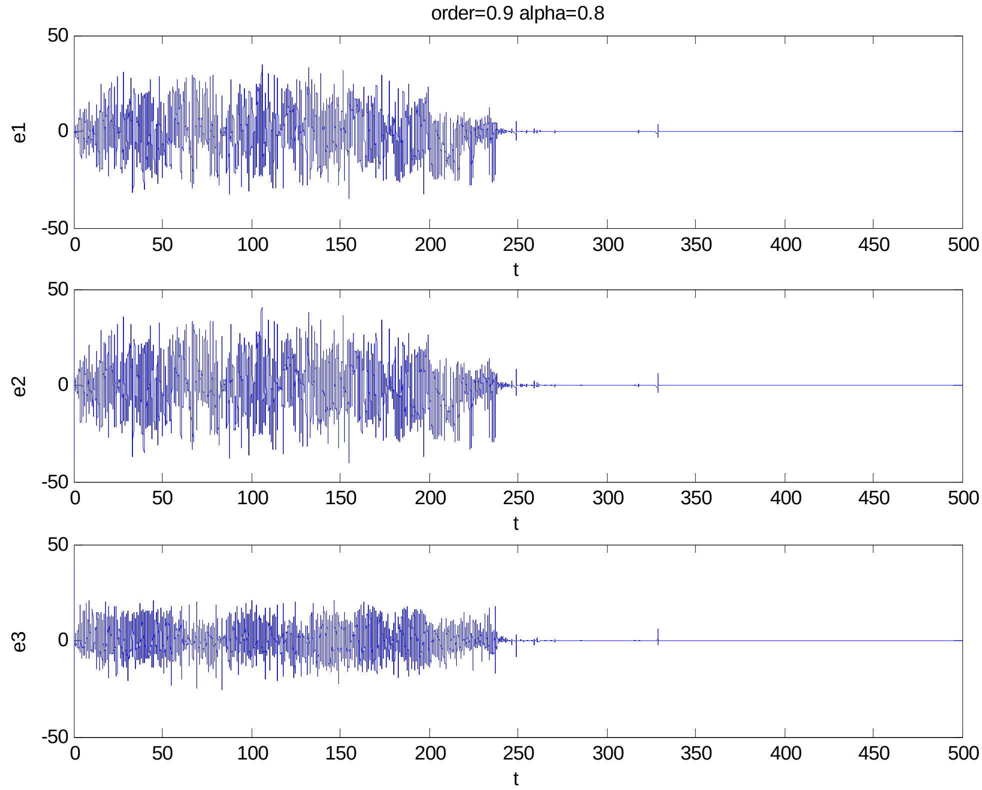

Fig.6.5.1(a) Time history of errors with $\alpha = 0.8$ order=0.9 $k_1 = k_2 = k_3 = 1$.

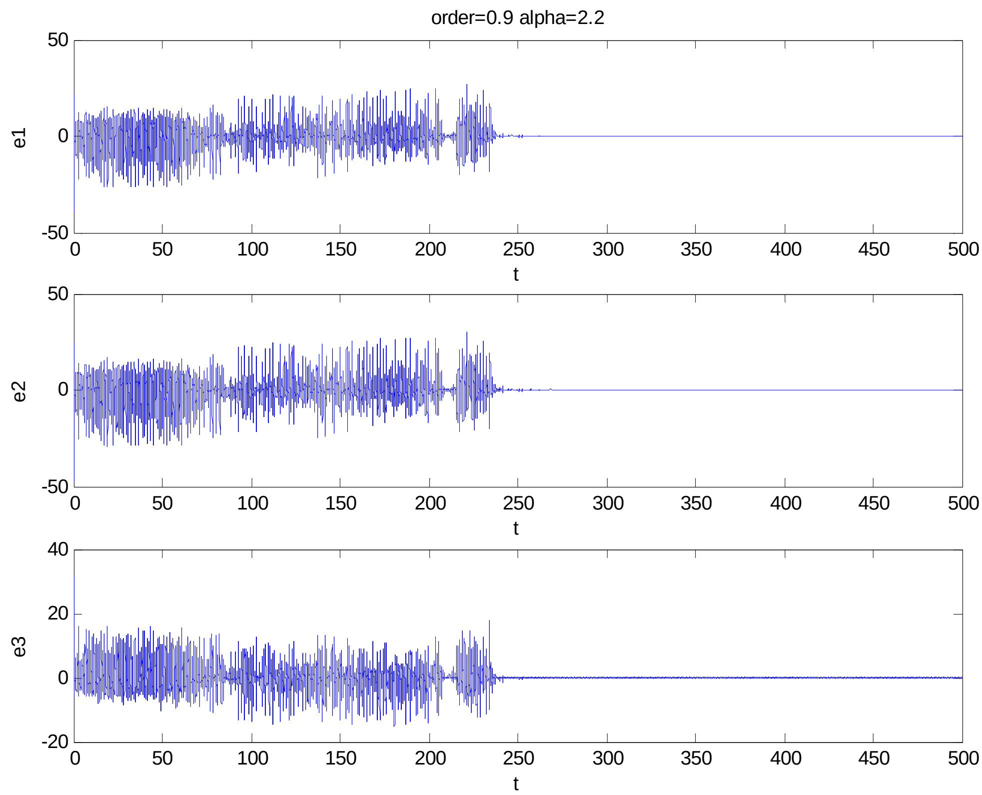

Fig.6.5.1(b) Time history of errors with order=0.9 $\alpha = 2.2$ $k_1 = k_2 = k_3 = 1$.

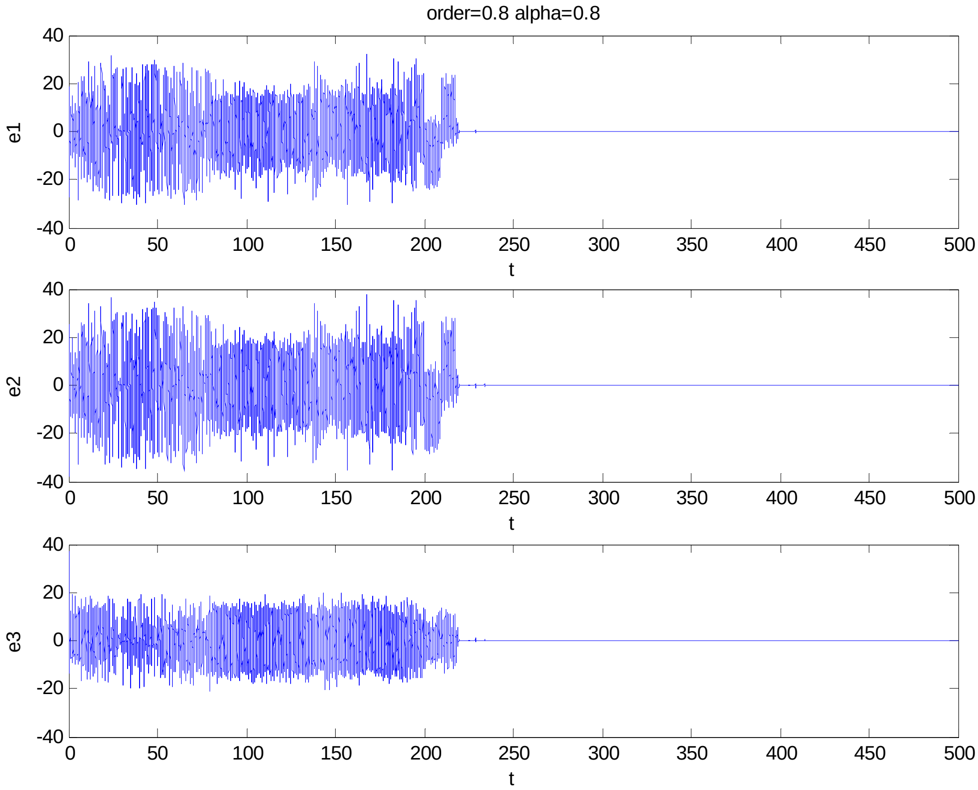

Fig.6.5.2(a) Time history of errors with order=0.8 $\alpha = 0.8$ $k_1 = k_2 = k_3 = 2$.

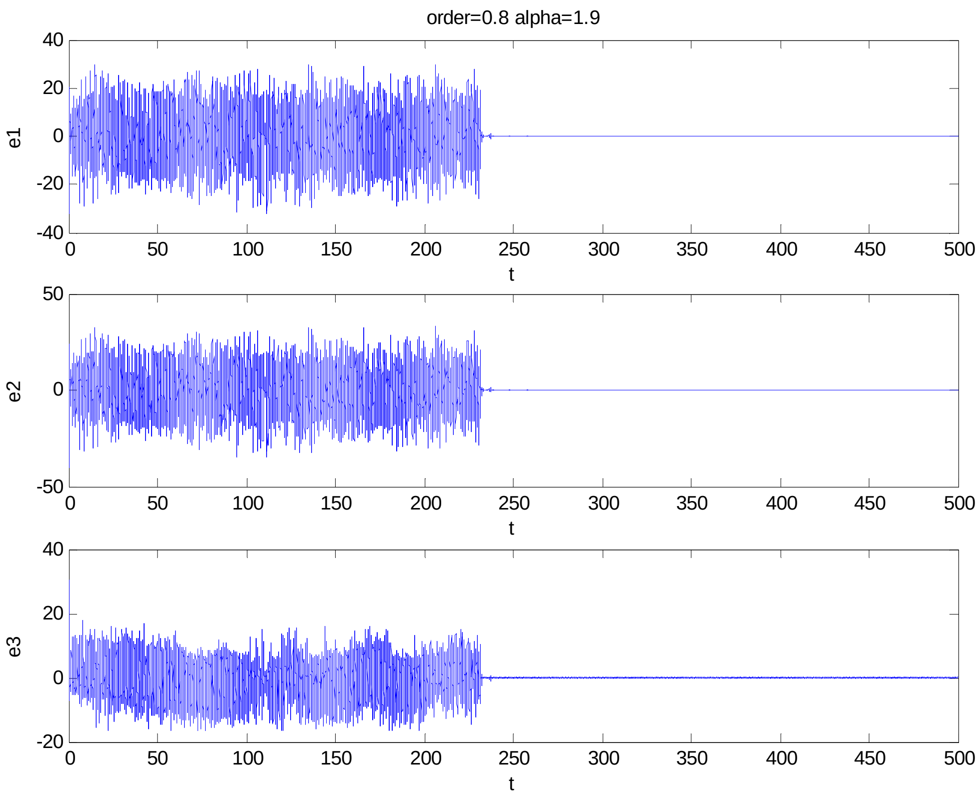

Fig.6.5.2(b) Time history of errors with order=0.8 $\alpha = 1.9$ $k_1 = k_2 = k_3 = 2$.

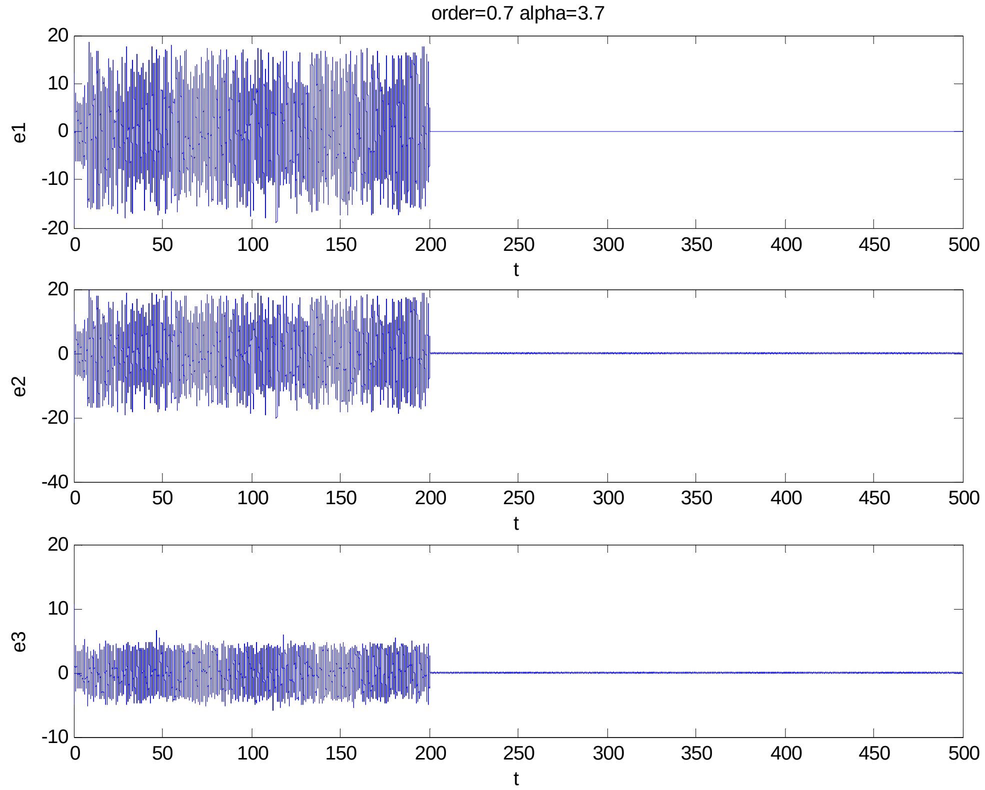

Fig.6.5.3 Time history of errors with order=0.7 $\alpha = 3.7$ $k_1 = k_2 = k_3 = 4$.

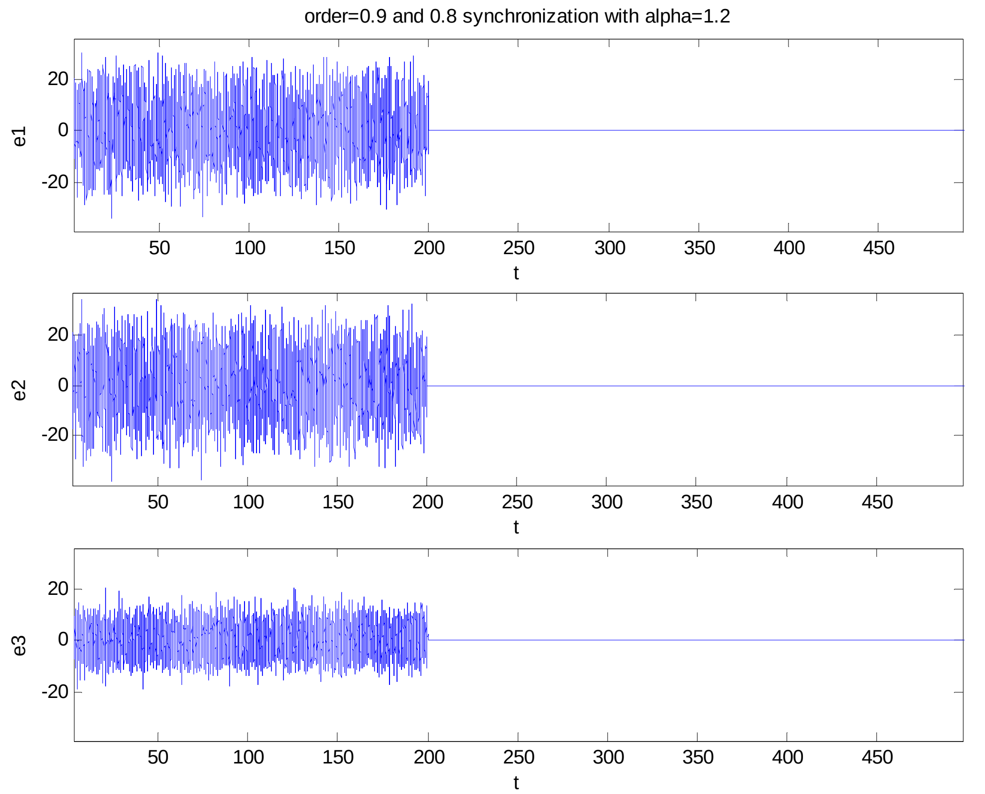

Fig.6.6.1 Time history of errors with $\alpha = 1.2$.

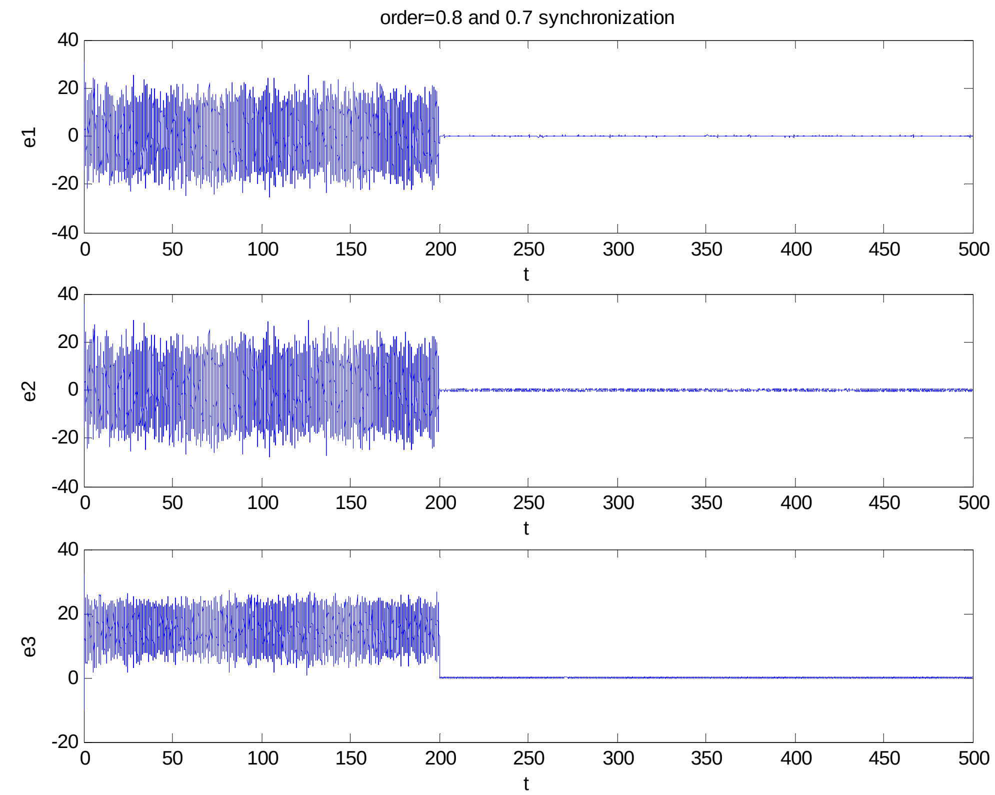

Fig.6.6.2 Time history of errors with master $\alpha = 1.2$ and slave $\alpha = 3.7$.

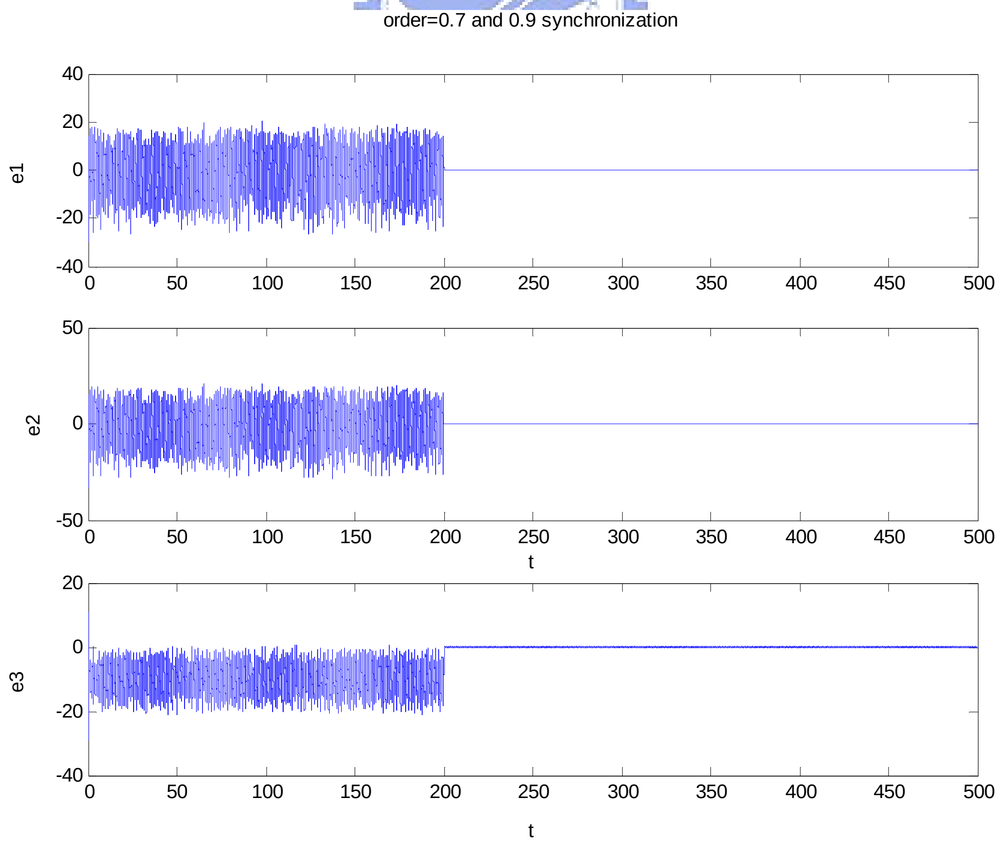

Fig.6.6.3 Time history of errors with master $\alpha = 3.7$ and slave $\alpha = 2.2$.